A CRITICAL ANALYSIS ON THE FIRE SAFETY ASPECTS OF FURNITURE

HAN SHOU SUO

Ph. D.

THE HONG KONG POLYTECHNIC UNIVERSITY

2007

The Hong Kong Polytechnic University

Department of Building Services Engineering

A CRITICAL ANALYSIS ON THE FIRE SAFETY ASPECTS OF FURNITURE

HAN SHOUSUO

A thesis submitted in partial fulfilment of the

requirements for the Degree of Doctor of Philosophy

June 2006

ABSTRACT

Consequent to several big fires in Hong Kong, local citizens are more concerned about furniture fires. Local government has started to review this issue seriously. As furniture plays a prominent role in fatal fire scenarios, a detailed investigation of the probable hazards due to furniture fires is necessary. The objective of this thesis is to carry out an in-depth study on the fire safety aspects of furniture.

General aspects of furniture fires were reviewed first. The relevant regulations, standards and other investigations on the fire safety aspects of furniture were then reported. Key aspects such as thermal properties of materials, smoke production, toxic potency, fire retardant and the effects on and due to the burning environment were considered.

Experiments should be carried out to study the fire behaviour of common furniture and their constituent materials. Local furnitures were studied by bench-scale experiments with a cone calorimeter and full-scale burning tests through a room calorimeter in China. Typical furniture and materials including wood, foam, cloth and plastic materials commonly used were tested under different fire conditions. Key parameters such as the heat release rate, smoke release rate, productions of carbon monoxide and carbon dioxide by burning those samples were measured. The possibility of onsetting flashover in a room fire and smoke toxicity were analyzed.

Heat release rate was identified as the most important parameter in the literature. Available equations with the oxygen consumption method were further reviewed. A general equation for calculating heat release rate with its simplified versions was derived. Corrections for incomplete combustion under different environments and with fire suppression were discussed.

Superposition of the heat release rate curves of individual furniture components was proposed to give the overall results. These were demonstrated by bench-scale and full-scale burning tests. Comparison was made by functional analysis. Predicted curves agree better for tests under higher heat fluxes.

Burning furniture in a room might onset flashover. As observed from full-scale and bench-scale tests in this study, burning furnitures (not yet ignited) under a flashover fire would give very different pictures. Firstly, the heat release rate is much higher than that in burning only part of the combustibles in a small accidental fire before flashover. Secondly, toxicity of smoke will be very different. Therefore, furniture is suggested to be tested in a well-developed fire.

Smoke toxicity of burning furniture is another important aspect in fire safety assessment. The calculation procedure for estimating the lethal toxic potency and fractional effective dose in burning combustibles with a cone calorimeter was clarified. The toxic gases yields other than their concentrations measured in a cone calorimeter should be considered to avoid confusion. Toxic gases are supposed to be dispersed into a specific total air volume. The cone calorimeter is further

demonstrated to be a suitable bench-scale facility to assess the smoke toxicity if a correct calculation method is used under appropriate testing conditions.

A fire risk ranking system with three parameters on flashover propensity, total heat released and smoke toxicity through lethal toxic potency is proposed based on the above study. Potential hazards of different furniture materials can then be specified. The ranking system will be useful for the authorities to set up relevant regulations on controlling the furniture materials.

Lastly, a fire zone model was developed for predicting the fire environment in burning furniture. Thermal radiation of smoke plays a very important role in real room fires and the key properties were reviewed. The zonal method through a non-gray particulate radiation model was applied to upgrade the fire zone model on studying transition to flashover. Effect of vent opening, particulate volume fraction and the external heat transfer coefficient on the transient temperature rise and onsetting flashover were studied. Both the external heat transfer coefficient and the particulate volume fraction are shown to be parameters which can lead to thermal instability, onsetting flashover in a room fire. The size of the vent opening also has a significant effect on the hot layer temperature and wall temperature.

CERTIFICATE OF ORIGINALITY

I hereby declare that this thesis is my own work and that, to the best of my knowledge and belief, it reproduces no material previously published or written nor material which has been accepted for the award of any other degree or diploma, except where due acknowledgement has been made in the text.

_____ (Signed)

HAN Shou Suo (Name of student)

ACKNOWLEDGEMENTS

I wish to express the deepest gratitude to my supervisor, Professor W. K. Chow, who has given me invaluable guidance, supervision and training. His great enthusiasm and devotion to research has inspired me greatly.

Thanks are due to Professor W.W. Yuen of the University of California at Santa Barbara for his guidance on upgrading the fire zone model with thermal radiation while staying at The Hong Kong Polytechnic University as a visiting professor.

Similar thanks are also due to Professor Y. Gao at Harbin Engineering University on supporting the full-scale burning tests in the room calorimeter at Lanxi, Harbin, Heilongjiang, China.

CONTENTS

LIST OF TABLES

LIST OF FIGURES

NOMENCLATURE

A_f	area of fire, m^2
A_w	surface area of the surrounding wall, m^2
b	exponential coefficient of total heat flux $\dot{q}''$
c_p	specific heat capacity at constant pressure, $Jkg^{-1}K^{-1}$
C_0	a soot constant dependent on the fuel, ranging from 2 to 6
C_2	Planck's second radiation constant, 0.014388 mK
C_D	discharge coefficient of the opening
C_S	mass concentration of smoke particles, kgm^{-3}
D	equivalent diameter of the vent, m
e	experimental data used in functional analysis
E	radiative emmisive power, kWm^{-2}
E_b	radiative emmisive power for blackbody, kWm^{-2}
E_{O_2}	generic constant for complete combustion, 13.1 $MJkg^{-1}$ of oxygen consumed
E_{CO}	heat release by oxidizing CO, 17.7 $MJkg^{-1}$ of O_2 consumed
E_S	heat release by oxidizing soot, 12.3 $MJkg^{-1}$ of O_2 consumed
f_v	particulate volume fraction
FED	fractional effective dose
$\dot{G}$	energy gain rate in a room fire, kW
h_c	convection coefficient, $Wm^{-2}K^{-1}$
$\dot{H}$	enthalpy increase of the hot layer, kW

$\dot{H}_o$	net enthalpy flow rate out of the vent, kW
H_R	height of the room, m
H_V	height of the opening vent, m
$I_{b\lambda}$	radiation intensity of monochromatic beam of blackbody, kWm^{-2}
$I_{\lambda L_s}$	radiation intensity of monochromatic beam passing through a smoke layer of thickness L_s, kWm^{-2}
k_s	extinction coefficient of smoke, m^{-1}
k_{co}	correction factor for measuring carbon monoxide only
K_f	flame spread constant
$\dot{L}$	energy loss rate in a room fire, kW
LC_{50}	a parameter for lethal toxic potency, kgm^{-3}
L_R	length of the room, m
L_S	thickness of smoke layer, m
m	sample mass, kg
m_L	mass loss percentage of sample, %
m_s	mass of smoke layer, kg
$\dot{m}$	mass loss rate, kgs^{-1}
$\dot{m}_a$	mass flow rate of intake gas, kgs^{-1}
$\dot{m}_e$	mass flow rate of exhaust gas, kgs^{-1}
$\dot{m}_f$	mass lost rate of fuel, kgs^{-1}
$\dot{m}_{O_2}$	mass flow rate of oxygen in the exhaust gas, kgs^{-1}
$\dot{m}^o_{O_2}$	mass flow rate of oxygen in the incoming gas, kgs^{-1}

M_i	molecular weight of sample i (i is for subscripts O_2, N_2, CO_2, CO, H_2O, soot, a and e) for oxygen, nitrogen, carbon dioxide, carbon monoxide, water vapor, soot, total intake gas and total exhaust gas respectively, $kgkmol^{-1}$
$\dot{n}$	mole flow rate, $mols^{-1}$
N	fraction height of the neutral plane
p	predicted value in functional analysis
PD_q	percentage deviation of heat release rate, %
$\dot{q}$	heat release rate, kW
$\dot{q}_{avg}$	average heat release rate, kW
$\dot{q}_{\max}$	peak heat release rate, kW
$\dot{q}_{net}$	net heat release rate, kW
$\dot{q}_{source}$	heat release rate of fire source, kW
$\dot{q}_w$	heat loss rate from the smoke layer to the wall, kW
$\dot{q}_A$	heat release rate per unit area, kWm^{-2}
$\dot{q}_{A,avg}$	average heat release rate per unit area, kWm^{-2}
$\dot{q}_{A,\max}$	peak heat release rate per unit area, kWm^{-2}
$\dot{q}''$	total heat flux by the free burning fire, kWm^{-2}
$\dot{q}''_b$	heat flux from the smoke layer to the floor, kWm^{-2}
$\dot{q}''_{fa}$	heat flux from the adjacent combustible, kWm^{-2}
$\dot{q}''_{fC}$	heat flux from the cone heater to the fuel surface, kWm^{-2}
$\dot{q}''_{ff}$	heat flux from the fire to the fire base, kWm^{-2}

$\dot{q}''_{f,surr}$	heat flux from the surrounding to the fire base, kWm^{-2}
$\dot{q}''_{max}$	peak heat flux, kWm^{-2}
$\dot{q}''_{w}$	heat flux from the smoke layer to the wall, kWm^{-2}
Q	total heat released, MJ
Q_A	total heat released per unit area, MJm^{-2}
r	stoichiometric ratio
R	radius, m
R_{edge}	edge dependent on the fuel, m
R_{max}	maximum radius of the fire base, m
s	smooth factor used in functional analysis
S_R	smoke release rate for cone test, s^{-1}
t	time, s
t_B	burning time, s
t_{fp}	time to first peak heat release rate, s
t_{ig}	ignition time from starting the test, s
t_{stop}	time for stopping the test, s
T	temperature, ^oC
T_a	temperature of the ambient air, ^oC
T_u	temperature of the upper smoke layer, ^oC
THR	total heat released, MJ
THR_{net}	net total heat released, MJ
TSR	total smoke released for cone test
U_c	adjustable parameter on the wall temperature, 0 to 1

V	volume, m^3
V_c	specified volume for tests with cone calorimeter, 0.01 m^3
$\dot{V}$	volumetric flow rate, m^3s^{-1}
$\dot{V}_{Cone}$	volumetric flow rate set for the cone calorimeter, m^3s^{-1}
V_f	flame spread rate, ms^{-1}
W_R	width of the room, m
W_v	width of the vent, m
x	flashover propensity, $kJm^{-2}s^{-2}$
X_i	mole fraction of the i^{th} species (i is O_2, N_2, CO_2, CO, soot and H_2O) of the total exhaust gas, %
X_i^o	mole fraction of the i^{th} species (i is O_2, N_2, CO_2, CO, soot and H_2O) of the total incoming gas, %
X_i^A	mole fraction of the i^{th} species (i is O_2, N_2, CO_2 and CO) of the exhaust gas with soot and H_2O removed, %
$X_i^{A^o}$	mole fraction of the i^{th} species (i is O_2, N_2, CO_2 and CO) of the intake gas with soot and H_2O removed, %
y	total heat released per unit area for fire risk parameter, MJm^{-2}
z	fire risk parameter to quantify the smoke toxicity, m^3kg^{-1}
Z_d	discontinuity height of the smoke, m
Δh_c	net heat of combustion, $MJkg^{-1}$
$\Delta h_{c,eff}$	effective heat of combustion, $MJkg^{-1}$
Δh_g	heat of gasification, $MJkg^{-1}$
Δm	mass loss, kg

$\Delta \dot{m}_{O_2}$	rate of oxygen consumed, kgs^{-1}
$\Delta \dot{m}_{O_2}^{CO}$	mass consumption rate of oxygen to oxidize carbon monoxide, kgs^{-1}
$\Delta \dot{m}_{O_2}^{S}$	mass consumption rate of oxygen to oxidize soot, kgs^{-1}
$\Delta \dot{m}_{CO}$	net production rate of carbon monoxide, kgs^{-1}
$\Delta \dot{m}_{S}$	net production rate of soot, kgs^{-1}
α	expansion factor
α_g	absorption coefficient of gas
α_s	absorption coefficient of soot
α_T	absorption coefficient of total smoke
α_λ	absorptivity for the monochromatic beam
β	mole ratio of products generated to oxygen consumed
λ	spectral wavelength
σ	Stefan-Boltzman constant, 5.67×10^{-11} $kWm^{-2}K^{-4}$
σ_S	specific extinction area on soot mass basis, m^2kg^{-1}
ρ_a	density of ambient air, kgm^{-3}
ε	emissivity
ε_g	emissivity of gas
ε_s	emissivity of soot
κ	equivalent absorption coefficient
χ	combustion efficiency
ϕ	oxygen depletion factor

CHAPTER 1 INTRODUCTION

1.1 Background

The number of big building fires started from burning furniture in the Far East appears to be increasing. In Hong Kong, the big fires in the Garley building [SCMP 1996] and Mei Foo Sun Chuen [SCMP 1997] had led to significant revisions of the building fire safety codes [BD codes 1996a, 1996b and 2004; FSD 2005]. Consequently, foam sofa furniture has to be treated with fire retardants [Consumer Protection Circular 1999; FSD 2000]. There is no excuse to have such a big fire during the refurbishment of the building such as the Garley building fire without adequate fire protection.

Although there had been numerous studies on furniture fires in the literature [Babrauskas and Grayson 1992] including the Combustion Behaviour of Upholstered Furniture (CBUF) project [Sundstöm 1996] in Europe; and others in USA [Babrauskas et al. 1982; Fowell 1994; Krasny et al. 2001; UL1056 2000; ASTM1537-02a 2002], not many works [Au Yeung and Chow 2002] were on local furniture samples. Design, technology and materials used in different places would change the fire behaviour of furniture. Very little information on burning local furniture is available. It is necessary to carry out an in-depth study on fire safety aspects of local furniture.

1.2 Objectives and Methodology

The main objective of this thesis is to study the fire safety aspects of furniture and thereby apply the results for studying fire safety protection of furniture and the design of fire safe furniture.

Fire hazards are mainly the result of a combination of different factors including ignitability, flammability of the generated volatiles, heat release rate, total heat released, flame spread, smoke obscuration and smoke toxicity. Heat release rate is the most important parameter in fire hazard assessment. Smoke toxicity is the major reason for fire deaths in building fires. An in-depth study focusing on these two aspects for furniture fires was carried out in this study.

Basic concepts of furniture fires were reviewed first. Full-scale and bench-scale burning tests were carried out to set up a basic database on burning local furniture. The burning behaviours were then summarized for in-depth studies. A general equation for accurate calculation of heat release rate based on the oxygen consumption method was derived and the superposition principle for using heat release rate results was investigated. Thermal radiation and flashover were studied with a zone fire model developed. Smoke toxicity of burning furniture is another important aspect to be considered. The calculation procedure for estimating the lethal toxic potency LC_{50} on burning combustibles with a cone calorimeter was clarified. Finally, a ranking system on the fire safety aspects of furniture was summarized to give an overview of the fire safety aspects of furniture.

1.3 Outline of the Thesis

In addition to the introduction, there are ten chapters in this thesis. Fire safety aspects of furniture to be considered are discussed in Chapter 2 with key points summarized.

The importance of heat release rate is summarized in Chapter 3. The fire data of furniture materials and furniture from full-scale and bench-scale burning tests were reported.

Heat release rate in burning combustibles is the most important parameter in fire hazard assessment. A general equation for calculating heat release rate by the oxygen consumption method was derived in Chapter 4. Key parameters were corrected under different conditions. Key points to be watched were clarified.

There are many standard tests on studying furniture materials and components starting from a small fire. The burning behaviours of furniture under a well-developed fire were studied and discussed in Chapter 5. It is proposed that furniture should be tested under a flashover fire, not just only a small fire source.

Thermal radiation plays a very important role in real room fires by contributing significantly to ignition, flame spread and flashover. In Chapter 6, radiation related to furniture fires was reviewed with the relations between thermal radiation and flashover discussed.

A furniture fire in a small room with a low ventilation factor is very easy to develop to flashover with great damages. Flashover is a very important scenario to be considered in fire hazard assessment. A new zone fire model for studying flashover was developed with an accurate radiation model. This was illustrated in detail in Chapter 7. Factors affecting the flashover were demonstrated.

The heat release rate has to be understood in fire hazard assessment. Most likely, only the heat release rates of individual items are available. The rate of heat release in burning multiple combustibles together should be estimated. How the curves can be combined to estimate the resultant heat release rate curve by the principle of superposition was demonstrated in Chapter 8 with bench-scale and full-scale tests. Comparison was made by functional analysis.

Smoke toxicity of burning furniture is another important aspect to be considered in fire safety assessment. The calculation procedure for estimating the lethal toxic potency LC_{50} on testing materials with a cone calorimeter was clarified in Chapter 9. This point demonstrated that the cone calorimeter is a good bench-scale facility to assess the smoke toxicity of burning combustibles, not only capable of testing thermal hazard.

Fire safety ranking system for furniture fire was summarized in Chapter 10. The thesis ends in Chapter 11 with conclusions.

CHAPTER 2 FIRE SAFETY ASPECTS OF FURNITURE

2.1 Introduction

Apart from those big local fires, there were other fires started from burning furniture elsewhere as recorded [Sundstöm 1996; Krasny et al. 2001]. Upholstered item is identified to be a key factor to give fire risks in buildings. Burning upholstered furniture is likely to cause deaths in home fires than other categories. Upholstered furniture's major contribution may be as the source of fuel for fires originating from other items. Furniture always plays a major role in the growth and propagation of the fires that could lead to great life and property losses.

Consumer products in developed countries are required to pass a series of assessments by following the codes and standards [e.g. UL1056 2000], though such requirement should be verified to be feasible. Most of the furnitures commonly used in the Far East including Hong Kong were not assessed so rigorously. Consequent to several big fires in burning lots of furniture or starting from igniting furniture foam, some more fire safety standards on materials are specified by the Hong Kong government [BD codes 1996a, 1996b and 2004; Consumer protection circular 1999; FSD 2000 and 2005]. However, there is no demonstration that such requirements were set up following an extensive research. More importantly, there is no database on fire testing results of local furniture.

Without knowing the fire behaviour of common furniture and their constituent materials, it is difficult to establish scientific standards to assess the fire safety of furniture and convince the citizens that the furniture can really give fire safety. Systematic fire tests on assessing local furniture should be carried out to get a more reliable database before setting up new regulations.

2.2 Furniture Samples to be Assessed

Furniture is a complicated product comprising many different materials and assemblies. Furniture includes all movable items such as cupboards, wardrobes, chests, tables, desks, beddings, chairs, sofas, and so on. Typical combustible components of furniture include:

- Padding such as fire-rated cotton batting; polyurethane foam (fire-rated FR or non fire-rated NFR); foam, cotton, polyester.
- Fabrics covering such as wool, leather; cotton/linen/rayon; and blend.
- Frame made of wood product or plastic materials.

Furniture components might be different for different furniture, but there are similarities in the furniture materials. Wood and plastics are widely used as furniture materials. Most cover fabrics are cellulosic or thermoplastic. Cellulosic fabrics include cotton and cotton derivatives like rayon. Thermoplastics are synthetic fibers such as nylon, polyester and acrylic.

In this study, materials commonly used in the local furniture and typical furniture were selected as testing samples. Fire behaviours of fabric and foam treated with and without fire retardant, wood, plywood and plastic materials such as polycarbonate (PC) were assessed with a cone calorimeter. Typical wood desk and table, foam sofa and foam cushions were tested in a standard room calorimeter [Chow et al. 2003; Chow and Han 2004]. These furniture are commonly used in local offices and residential buildings in China. Compared to the furniture used in other tests, there might be slight differences in the material composition or surface treatment, giving some changes in their fire behaviours.

2.3 Experimental Facilities used for Furniture Fire Tests

There are many instruments used for fire tests. Bunsen burner is used in testing the ignitibility or flammability of building materials [BS476 1979]. Critical oxygen index apparatus is used to measure the minimum oxygen concentration that just supports flame combustion of a material [BS EN ISO4589:2 1999]. There are now many multifunctional apparatuses widely used in bench-scale experiments such as cone calorimeter [Babrauskas 1984; ISO5660 2002, ASTM1354 2004], medium-scale rigs such as furniture calorimeter [Babrauskas et al. 1982] and single-burning item test [BS EN 13823: 2002], and full-scale burning tests such as the room calorimeter [ISO9705 1993] and large exhaust hoods [Newman 2005].

In this study, bench-scale burning tests were undertaken using a cone calorimeter, and full-scale burning tests were conducted in a room calorimeter.

The cone calorimeter first developed by Babrauskas at NBS in the early 1980s is now the most widely used apparatus to measure bench-scale combustion characteristics of various materials or combinations of materials. A fan-duct system is used to collect the flue gas. It operates by using radiation feedback from a conical heater above the samples. The apparatus and testing procedure have been standardized internationally. A cone calorimeter equipped with relevant analyzers can be used to measure many important parameters including the ignition time, heat release rate, effective heat of combustion, mass loss rate, smoke and soot production, and toxic gases production.

A room calorimeter is used to measure the combustion characteristics of objects such as sofa, table and other full-scale burning items. The specimen is burnt in the same way as in cone calorimeter tests, but simply on a larger scale. One major difference between the calorimeter apparatuses is that a constant radiant heat flux from a heated element throughout an entire combustion test is used for the cone calorimeter, which causes the sample to burn almost completely away. However, an ignition fire source is used in the room calorimeter for the initial stages of fire growth and then the item is allowed to burn under its own radiation feedback.

Both full-scale and small-scale burning tests are important [Au Yeung and Chow 2002]. However, it is impossible to carry out full-scale tests regularly due to the complexity and cost. Relevant information can be deduced from smaller scale testing results.

2.4 Fire Safety to be Considered

Furnitures are the key combustibles in a building in terms of fire load. Fire hazard from the furniture is much greater than the fire hazard from other items in a building. Decisive factors affecting the fire hazards are the materials used in furniture, furniture type, size and the amounts of the combustible furniture.

On the other hand, furniture poses different fire hazards depending on the surroundings in which they are used. The fire behaviours of furniture depend on the burning environment such as the location of furniture, ignition source and ventilation conditions.

Both thermal effect and smoke aspect including smoke obscurity and smoke toxicity in burning furniture should be considered. Flashover caused by burning furniture and furniture fire behaviour under flashover conditions should be clarified and further studied.

2.4.1 Thermal hazard

A piece of burning furniture, particularly sofa or cushion foam, was observed to be a common starting point of a fire. Heat released might then be strong enough to ignite adjacent items such as wood partition walls, floor coverings and some other furniture which are not easy to ignite by electrical faults or cigarettes. The effect of this starting fire on adjacent combustibles is obvious. Furniture fire in a small room with a low ventilation factor is very easy to develop to flashover with great damages.

Analysis of thermal effects includes the threshold value and the exposure time required to reach the threshold for the scenario should be considered. Injury can result from exposure to thermal radiation from either flames or hot gas. Properties of furniture materials, such as ignitability, flame spread and heat release rate are important [Chow 2002].

Protection against ignition of the upholstered furniture would change the possible scenario. As heat flux from a flaming heat source is critical to ignite them, ignitibility for all items can be classified into three classes: easy, normal and hard to ignite with the benchmark values of 10, 20 and 40 kWm^{-2} respectively [Babrauskas 1981].

2.4.2 Smoke hazard

Smoke is best defined as the gaseous products of combustion in which small solid and liquid particles are dispersed. It contains burnt and partially burnt products formed in the flame, as well as some products that are given off by the chemical degradation of the fuel.

Among those potential danger factors of fires, smoke toxicity has been claimed as the dominant cause of residential fire deaths [Birky et al. 1979]. About half of the accidental fire fatalities were due to the inhalation of smoke and toxic gases, not due to burns. Therefore, toxicity is a very important topic of fire science and should not be overlooked in designing fire safe furniture. Toxic effects result from inhalation exposure to products of combustion. The general effects on humans include reduced

decision-making ability and impaired mobility, leading to incapacitation or death. Carbon monoxide and hydrogen cyanide are the predominant toxicants found among over a hundred gaseous combustion products [Purser 2002].

Burning furniture may produce a great amount of highly toxic gases. The quantity of toxic gases produced depends on the processes of ignition, oxygen available, flame spread, heat release rate, and the chemical composition of the burning materials. Natural materials commonly used in furniture include wood, cotton, and wool. With the rapid development of material science, more synthetic materials are used as structural components and decorative panels of furniture. Nylons and polyurethane foams are good examples. As two major toxicants, carbon monoxide is always present in fires, while hydrogen cyanide will be present in high concentration when nitrogen-containing materials such as acrylics, nylons, polyurethane foams, or wool are burnt. One of the main reasons that more people die from smoke inhalation than heat is because smoke moves faster through the building than fire. This explains why more smoke-related casualties were reported.

Smoldering fires may yield a substantially higher conversion of a fuel to toxic compounds than flaming fires. Because of the complex structure and diversified materials used, upholstered furniture may give smoldering fires easily. Experiences show that smoldering transfers easily from cigarettes to medium and heavy weight cellulosic and acrylic fabrics, and then to many commercial padding materials, especially cotton and polyurethane foams.

Further, with so many fire retardants being used, their toxicity upon burning should be tested. The toxicity hazard of fire retardant has been recognized in recent years. Non-commercial fire retarded rigid polyurethane foams produce an unusual toxic combustion product [Levin 1987]. The trend of fire safe furniture should be focused on design materials which would produce less toxicants upon burning but can stand significant temperature changes.

2.5 Factors Affecting Furniture Fires

2.5.1 Fire load

Fire load is defined [BS7974 2001] as "the sum of the calorific energies which could be released by the complete combustion and all the combustible materials in a space, including the facing of the walls, partitions, floors and ceilings".

Fire duration and the severity of damage are affected by fire load. Building fires occur in enclosed spaces and at the early stage, the fire size is small with little amount of combustibles burning. The fire is therefore fuel-controlled and depends on the fire temperature. When the heat flux and room air temperature increase to higher values, flashover might occur due to thermal radiation feedback. The fire then grows bigger and becomes ventilation-controlled.

Decreasing fire load of upholstered furniture may lead to reduction in fire load for a room, such that it is insufficient to lead to flashover [Bukowski et al. 1990]. The fuel

elements affecting the fire behaviour of upholstered furniture are the cover fabric, the seat cushion material, and the padding material. The interaction of these fuels during combustion is a function of the material composition, thickness, and density. Furniture made by materials with less fuel load should be designed. Effort should be put to minimize the amount of furniture or maximize the room space to reduce the proportion of fuel load to room space. Materials with less fuel load should be designed to substitute or partially substitute the existing components of furniture. For example, some parts of the furniture can be made with metal instead of wood.

2.5.2 Furniture geometry and configuration

Geometry and configuration of the furniture would affect its fire behaviour. Certain design may slow down the fire development, while certain design can produce more rapid fire development. There are many design styles and features in the market. However, some similarities exist in the construction of chairs and sofas, which are far more significant in determining their fire behaviours. For any composite of fabric and padding materials, cigarette ignition resistance is better in flat areas than in crevices. The seats, backs and arms are perpendicular to each other, enhancing radiant heat transfer, which promotes flaming ignition and accelerates burning rates. Similarly, the crevices formed at the intersection of backs, seats, and arms promote smoldering ignition. It has been reported that chairs without armrests show lower peak heat release rates and slower fire development rates.

Further, the air space between the back padding and the rear fabric panel, and the air space within the decking would affect fire development by providing preferential

pathways for flame spread within an item of furniture. Because melting seat materials may form a pool fire under the chair soon after ignition, it is also recommended to use panel-mounting rather than webbing to support chair cushioning, which may reduce the tendency to pool burning and cause a major reduction of fire hazard.

2.5.3 Fire retardants

To minimize the damage of a fire, it is necessary to increase the fire endurance of furniture materials. Commonly used materials such as wood, polyurethane foams, fabrics and other products should be treated with fire retardants. Fire retardants, primarily for protecting cellulose-based products, have been widely used in furnishings. Coating or impregnating can be used for the fire retardant treatment to reduce the flammability of a combustible material. Coatings may suppress flame spread or create a non-combustible surface. Other advantages are cost-saving, and easy to apply without weakening the substrate. Whether a fire-retardant coating is effective or not depends upon a number of factors such as the coating thickness and durability under fire exposure. A coating may delay ignition of the substrate for just a few minutes. Because of its vulnerability to damage, the life expectancy of coating might be short. Coating solely cannot solve all the problems. The amount of coating applied and whether it can cover up the whole surface are important. Impregnation is another important method to treat furniture materials such as fabrics and foams with fire retardants.

Fire retardants delay ignition and have proven to save lives. While benefits achieved through enhanced fire safety are critical, they should be achieved in a manner that minimizes risk to human health and the environment. In some cases, the use of fire retardants may increase the amount of smoke and toxic gases produced by combustion. In UK, a compulsory effort has been made to reduce the flammability of furniture and fire retardant foams since 1992 [Paabo and Levin 1998]. Therefore, new fire-retardant materials for furniture should be developed and tested properly to protect materials which ignite easily.

2.6 Summary

Changes in fire properties of furniture materials might result in changes in the fire risk and hazard. Thermal properties of materials, fire retardant, total combustible mass, smoke production and toxic potency, geometry and configuration are all important aspects that need to be considered for assessing the fire safety of furniture.

Studying the material properties only is not good enough to improve the fire behaviours of furniture. The burning environment such as the ignition source and ventilation condition should be considered as well. There might be great differences between furniture fires started from a small fire source and those started from a flashover fire. High peak heat release rate but short burning duration might cause little damage. Heat release rate, fire load or total heat released of furniture fires are all important for assessing the hazard of furniture fires. As furniture fires would

produce toxic smoke, the toxicity effect of furniture materials should also be considered.

CHAPTER 3 HEAT RELEASE RATE

3.1 Importance of Heat Release Rate

The heat release rate (HRR) [e.g. Babrauskas and Grayson 1992] in a room fire has to be understood in hazard assessment. This will give key information on the size of the fire; the rate of fire growth, and consequently the release of smoke and toxic gases; the time available for escape or fire suppression; and the type of suppressive action that is likely to be effective [Chow 2002]. The temperature in a room, transportation and concentrations of smoke and toxic gases, heat flux and flame spread, pyrolysis and ignition of fuels can be predicted by HRR. Other attributes that define the fire hazard such as the possibility of having a flashover fire can be estimated. HRR has been recognized as one of the most important fire properties of a material [Sundstöm 1996; Krasny et al. 2001].

With compartment fire hazard assessment as the primary application, there is a need for high quality HRR data, and consequently, for devices and methods to measure it accurately. HRR depends on the material combination [Cox 1995], the configuration of the item, its total mass and the ventilation conditions. The ignition source and other adjacent items can also have an effect on the value of HRR. In principle, the HRR could be computed by multiplying the calculated mass loss rates in the pyrolysis and evaporation by its effective heat of combustion. However, that in fact gives only a semi-quantitative estimation. The reason is that the value of effective heat of combustion for most materials during the burning process is not constant. If

HRR is not computed directly by effective heat of combustion, it might be calculated by indirect method such as measuring the rate of oxygen consumed in the combustion with oxygen consumption principle. The oxygen consumption principle is now widely used in the heat release measurement. A general equation on accurate calculating the heat release rate based on oxygen consumption method will be derived in the following chapter.

There are two basic approaches to estimate the HRR of a material. The first approach is to carry out full-scale burning test with a room calorimeter [ISO9705 1993]. The second approach is to use bench-scale burning test with a cone calorimeter [Au Yeung and Chow 2002; ISO5660 2002]. It is important to ensure repeatability and reliability of the experimental results. According to ISO standards [ISO3534-1:1993], reproducibility is the precision under conditions where the test results are obtained with the same method on identical test items in different laboratories with different operators using different equipments. Repeatability is the precision under the conditions where independent test results are obtained with the same method on identical test items in the same laboratory by the same operator using the same equipment within short intervals of time. The standard calorimeter and room calorimeter with their accessories used in this study were calibrated following the standard technical manual before each test. Three samples were tested for each bench-scale test and average values were shown in the tables. Because of the vast volume of data generated, one set of the measured data was plotted to illustrate the results in the following figures. Only one sample was tested for each full-scale burning test due to funding limitation.

3.2 Tests with a Cone Calorimeter

The testing sample is placed under a conical electric furnace emitting thermal radiation. The surface of the specimen is exposed to a constant radiative heat flux up to 100 kWm^{-2}. Volatile gases from the heated specimen are ignited by an electrical spark igniter. Combustion gases are collected by an exhaust hood for further analysis. This gas analysis makes it possible to calculate the heat release rate through the oxygen consumption method; and to assess the production of toxic gases from the specimen.

Smoke production can be assessed by measuring the attenuation of a laser beam by smoke in the exhaust duct. The attenuation is related to the volume flow, resulting in a measure of smoke extinction area. Some gases including toxic gases such as carbon monoxide CO are usually measured.

Results measured from a cone calorimeter are useful in understanding the fire behaviour, both heat and smoke aspect, of burning materials. Results from the cone calorimeter might be taken as a 'yardstick' for assessing whether the furniture is safe in a fire and to complement full-scale burning tests. Therefore, the fire behaviour of materials is suggested to be assessed at least by a cone calorimeter. A ranking system can be worked out for 'grading' the materials concerned in the later section.

3.2.1 Tests on fabric materials used in furniture

3.2.1.1 Testing arrangements of fabric materials

Cloth with and without fire retardant additives were tested by a cone calorimeter under incident heat fluxes of 10 kWm^{-2}, 20 kWm^{-2}, 30 kWm^{-2}, 50 kWm^{-2} and 70 kWm^{-2}. The samples were cut into squares of surface area 10 cm by 10 cm. Each kind of sample was tested three times in three different testing groups. These tests by a cone calorimeter in Chapter 3 are labeled as:

C3A1: Cloth without fire retardant tested under 70 kWm^{-2};

C3A2: Cloth without fire retardant tested under 50 kWm^{-2};

C3A3: Cloth without fire retardant tested under 30 kWm^{-2};

C3A4: Cloth without fire retardant tested under 20 kWm^{-2};

C3A5: Cloth without fire retardant tested under 10 kWm^{-2};

C3B1: Cloth treated with fire retardant tested under 70 kWm^{-2};

C3B2: Cloth treated with fire retardant tested under 50 kWm^{-2};

C3B3: Cloth treated with fire retardant tested under 30 kWm^{-2};

C3B4: Cloth treated with fire retardant tested under 20 kWm^{-2};

C3B5: Cloth treated with fire retardant tested under 10 kWm^{-2}.

3.2.1.2 Results analysis on burning fabric materials

The average values of testing results are shown in Table 3.1. Results on the heat release rate are shown in Figure 3.1.

The cloth in tests C3A5 and C3B5 did not burn under the heat flux of 10 kWm^{-2}.

Under a flashover heat flux of 20 kWm^{-2}, the sample treated with fire retardant for test C3B4 was not ignited. But there was much smoke released for test C3B4. The sample without fire retardant for test C3A4 was ignited at 66 s and the peak heat release rate reached 55 kWm^{-2}.

Under a heat flux of 30 kWm^{-2}, the sample treated with fire retardant even ignited faster within 5 s for test C3B3, comparing with 26 s for C3A3. However, the peak heat release rate for C3B3 (29 kWm^{-2}) is much lower than that for C3A3 (78 kWm^{-2}).

When tested under a high radiative heat flux of 50 kWm^{-2}, i.e. much higher than the flashover heat flux of 20 kWm^{-2} at floor level, but encountered at ceiling, samples with and without fire retardants (tests C3A2 and C3B2) were ignited quickly. Samples treated with fire retardants ignited faster in test C3B2. Values of pkHRR are slightly different, about 83 kWm^{-2} for C3B2 and 90 kWm^{-2} for C3A2.

There are no significant differences for samples with and without fire retardant while exposed to 70 kWm^{-2} in tests C3A1 and C3B1, both ignited rapidly with higher peak heat release rates of 117 kWm^{-2} for C3A1 and 116 kWm^{-2} for C3B1. This is a good demonstration that exposing the fabric materials even with fire retardants to high heat fluxes might not be safe.

3.2.2 Tests on Plywood

3.2.2.1 Testing arrangements of plywood

Three groups of plywood widely used for furniture in the Far East were selected. Those were 5 mm thick samples of three veneer layers labeled as plywood A; 7.5 mm thick samples of six veneer layers labeled as plywood B; and 18 mm thick samples of three veneer layers labeled as plywood C. All were cut into squares of 100 mm by 100 mm.

The testing arrangements for the three sets of testing samples are:

Plywood A: Tested under 20 kWm^{-2}.

C3C1: Bare plywood;

C3C2: Plywood coated with a shiny paint without fire retardancy;

C3C3: Plywood treated with a sticky and white fire-retardant paint FR1;

C3C4: Plywood treated with a thin colourless fire-retardant paint FR2.

Plywood B: Tested under 50 kWm^{-2}.

C3D1: Bare plywood;

C3D2: Plywood coated with a shiny paint without fire retardancy;

C3D3: Plywood treated with a sticky and white fire-retardant paint FR1;

C3D4: Plywood treated with a thin colourless fire-retardant paint FR2.

Plywood C: Bare plywood only.

C3E1: Plywood under a heat flux of 20 kWm^{-2};

C3E2: Plywood under a heat flux of 50 kWm^{-2};

C3E3: Plywood under a heat flux of 70 kWm^{-2}.

3.2.2.2 Results analysis on burning plywood

The testing results are shown in Table 3.2. The heat release rate curves are shown in Figure 3.2.

All the plywood samples were ignited under the above heat fluxes and observed to burn steadily. The bottom part of the samples bent up with more vigorous burning. Two peaks appeared in the heat release rate curves. About half of the combustibles were burnt out after having the first peak of the heat release rate.

The ignition times were delayed for the plywood samples treated with fire retardant coatings under lower radiative heat fluxes at 20 kWm^{-2}. Delay in ignition was not so long when the heat flux increased to 50 kWm^{-2}. The protective coating applied to the samples expanded and separated from the plywood surface. More oxygen was drawn to give more vigorous burning. Once ignited under a high heat flux, the plywood samples burnt in a similar way with roughly the same thermal parameters as shown in Table 3.2. Thermal aspects were not different for samples treated or not treated with fire retardants. However, the peak values of smoke release rate and carbon monoxide concentrations increased greatly for samples treated with shiny paints and fire retardant coatings. Tests on bare plywood C without any coatings under high

heat flux of 70 kWm^{-2} generated less volume of smoke and lower concentration of carbon monoxide. A possible reason is due to complete combustion of the bare plywood without any protective coating under higher external heat fluxes.

3.2.3 Tests on other materials with a cone calorimeter

Bench-scale burning tests on furniture materials including sofa foam, wood used in the desk and plastic materials will be separately reported in Chapter 5, Chapter 8 and Chapter 9 to study the furniture tested under flashover fire, superposition of heat release rates and smoke toxicity measured with a cone calorimeter.

3.3 Full-scale Burning Tests

Very little information is available on heat release rates in burning local furniture. Such information has to be measured for fire hazard assessment. Fire behaviour of furniture was investigated by Babrauskas years ago [Babrauskas 1979; Babrauskas et al. 1982]. The heat release rate and other parameters on burning furnitures were measured in furniture calorimeter or room calorimeter. Furniture fires developed up to flashover were studied. However, most of the tests started from a smaller ignition source. There were not many studies on burning furniture in a flashover fire. Note that burning furniture might lead to flashover in a small enclosure. Therefore, the first stage is to study the fire behaviour of furniture ignited by a small fire source. Moreover, studies on furniture exposed to a flashover fire should be carried out. The

importance of furniture tested under flashover will be demonstrated in the later chapter.

The testing procedure was basically following standard procedures as in ISO9705 [1993] and ASTM1537 [2002]. The procedures were changed slightly to suit local constraints and for setting up flashover fires. The smaller gasoline ignition source gave an average heat release rate of 20 kW with a duration of 3 min. This was different from the standard ignition source of 100 kW in 10 min and 300 kW for another 10 min in ISO9705; and a constant 19.3 kW standard ignition source with a duration of 80 s in ASTM1537. This smaller ignition source was used to understand igniting furniture under an accidental fire. Another bigger ignition source with a peak heat release rate of 2.4 MW was used to set on flashover. The fire behaviour of furniture was then assessed under flashover.

Full-scale burning tests on studying the heat release rates of selected furniture samples under accidental and flashover fires were carried out in a room calorimeter [ISO9705 1993].

3.3.1 Tests on foam cushion and wood table

Plywood table and square cushions made with foam and a fabric covering were selected and tested with different arrangements as shown in Figures 3.3 and 3.4. A steel frame was used to support the cushions.

3.3.1.1 Testing arrangements of cushion and table

Samples of cushion and table tested in a room calorimeter in Chapter 3 are labeled as:

R3A1: Testing one cushion horizontally placed on the floor

R3A2: Testing one cushion vertically placed

R3A3: Testing one cushion treated with fire retardant horizontally placed

R3A4: Testing two cushions

R3A5: Testing three cushions

R3A6: Testing six cushions

R3A7: Testing one table

R3A8: Testing one table and four cushions

R3B1: Testing four cushions with igniter 1

R3B2: Testing four cushions treated with fire retardant with igniter 1

R3B3: Testing four cushions with igniter 1 at different place to test R3B1

R3B4: Testing four cushions same to R3B2, but with igniter 2

R3B5: Testing four cushions same to R3B4, but with different position of igniter

R3C1: Testing a pool fire of 0.5 litre gasoline in a round pan with a diameter of 0.2 m, used as a small starting fire (igniter 1) for tests R3A1 to R3A6 and R3B1 to R3B3

R3C2: Testing a pool fire of 0.5 litre gasoline in a 0.25m × 0.25m square pan, used as a small starting fire (igniter 2) for tests R3B4 and R3B5

R3C3: Testing with a pool fire of 3.0 litre gasoline in a 0.35m × 0.35m square pan, used as a small starting fire (igniter 3) for tests R3A7 and R3A8

The size of table is shown in Figure 3.3. The testing arrangements for cushions are also shown in Figure 3.4.

3.3.1.2 Results analysis on burning cushions and table

The testing results are shown in Table 3.3. Results on the heat release rate are shown in Figure 3.5. The following points are observed:

- There are obvious differences in the heat release rate in burning cushions under different arrangements. Both the positions of cushion and igniters [Cleary et al. 1994] have effects on the burning behaviours.
- The times to ignition and peak heat release rate were delayed a short time for samples treated with fire retardants.
- Samples were burning more vigorously under a higher heat flux of ignition source or more combustibles were involved in the combustion which can be illustrated by the superposition of several combustibles.

The total heat released in burning a table with four cushions in test R3A8 was 435 MJ. This value is much higher than 257 MJ by adding up the values of 60 MJ for testing four cushions in test R3B4 and 197 MJ for testing one table only in test R3A7. There would be more thermal feedback on the combustibles and give a more complete combustion for burning several items together than burning them separately.

3.3.2 Full-scale burning tests on wood desk and sofa

Nine tests on three sets of four-seater sofa and two wood desks will be illustrated in Chapter 5 to demonstrate the importance of furniture tested under flashover fire.

3.4 Summary

The importance of the heat release rate was pointed out in this chapter. Experimental studies on local furniture materials with a cone calorimeter were carried out. The furniture arrangements were tested also in a room calorimeter.

On the cone tests, almost all the samples for fabric and plywood were ignited and kept steady burning under a heat flux higher than 20 kWm^{-2}. The ignition time was shorter for fabric than that for plywood. Higher heat release rate was measured in burning plywood. Anyway, burning fabric is easy to start a fire. Igniting the plywood afterward would be dangerous. Therefore, ignition time, heat release rate including total heat released and peak heat release rate under an agreed heat flux should be considered together for thermal fire hazard assessment.

Burning a large furniture item with more combustibles might give a bigger post-flashover fire. From the above full-scale and bench-scale tests, burning furniture under a higher external heat flux will give a higher heat release rate and total heat released. Furniture treated with common protective coating samples used in this study would be safe only under small accidental fires. Such protective coating would

burn vigorously under a flashover fire. Smoke aspects should also be watched. Therefore, it is necessary to test furniture under a well-developed fire.

CHAPTER 4 HEAT RELEASE RATE CALCULATION IN OXYGEN CONSUMPTION CALORIMETRY

4.1 Introduction

As discussed in Chapter 3, heat release rate in burning combustibles is the most important parameter in fire hazard assessment [Babrauskas and Grayson 1992; Babrauskas 2003]. This is very important in performance-based design of many big construction projects in the Far East [Chow 2005]. There had been many arguments on selecting a design fire while implementing the fire engineering approach for those projects failed to comply with the prescriptive codes in Hong Kong [Chow 2003]. Therefore, heat release rate should be estimated with updated theory and new instruments. Methods for calculating the heat release rate [Babrauskas and Grayson 1992; Babrauskas 2002] include sensible enthalpy rise method, substitution method, compensation method and oxygen consumption method. The oxygen consumption method [Thornton 1917; Huggett 1980; Krause and Gann 1980; Sensenig 1980] is now widely used in bench-scale experiments such as cone calorimeter [Babrauskas 1984], medium-scale rigs such as furniture calorimeter [Babrauskas et al. 1982] and single-burning item test [BS EN 13823: 2002], and full-scale burning tests such as the room calorimeter [Enright 1995] and large exhaust hoods [Newman 2005].

The concept of oxygen consumption was proposed by Thornton [1917], and then widely applied later [Huggett 1980; Krause and Gann 1980] with rapid development

of accurate gas sensors. The mass lost rate of oxygen for burning is measured first, and then multiplied by the heat generated per unit mass of oxygen consumed for that fuel (similar to calorific value for heat generated per unit mass of fuel burnt) to get the heat release rate. As burning common fuels in a building fire would involve breaking similar chemical bondings of hydrogen-hydrogen, hydrogen-carbon, and carbon-oxygen, the heat generated per unit mass of oxygen consumed appears to be a constant E_{O_2} (roughly equal to 13.1 $MJkg^{-1}$ oxygen consumed with ± 5% accuracy). The method is now recognized as the most accurate and practical technique for measuring heat release rates. It was proposed in the 'carbon dioxide generation method' [Tewarson 2002] to measure the heat release rate by including the amount of carbon dioxide production rate. But this method is restricted due to its carbon dependent for the fuels tested.

An exhaust hood with a fan-duct system is constructed to collect the flue gas generated in the burning process. Heat release rate can be calculated by measuring how much oxygen in the incoming gas is consumed. For complete combustion, the equations concerned will be relatively simple. But incomplete combustion is likely in the fire tests. Including the concentrations of other species such as carbon monoxide would give a better estimation of the heat release rate.

Equations for calculating the heat release rate by oxygen consumption method were derived in detail by Parker [1982, 1984] years ago, and then by Janssens [1991, 2000, 2002]. These equations were reviewed, modified and applied under many testing conditions [Lattimer and Beitel 1998; Enright and Fleischmann 1999; Brohez et al. 1999; Brohez et al. 2000; Han and Chow 2004; Brohez 2005]. But those equations

derived with some assumptions are applicable under some conditions. There might be great deviations for using those equations without correction under other conditions. Accurate measurement and better estimation are necessary for hazard assessment. Before analysing errors propagation [e.g. Brohez 2005], equations on heat release rate have to be assessed. Parameters concerned should be reviewed clearly to give better estimation of heat release rate.

Calorimeters with controlled-atmosphere [Babrauskas 1992] are also used to study the fire behaviour of materials. There, intake gas is very different from fresh air in a normal calorimeter. The intake gas may be enriched or depleted in oxygen. Combustions in the fire tests would be incomplete under oxygen-leaned conditions [McCaffrey and Harkleroad 1988; Gottuk and Lattimer 2002; Tewarson 2002]. Combustion products such as carbon monoxide might even mix with the incoming gas in an oxygen consumption calorimeter. This would give higher concentration of carbon monoxide than in fresh air. Therefore, concentrations of the incoming gas should be considered under these conditions.

A general equation including the mole fractions of six components on nitrogen, oxygen, carbon dioxide, carbon monoxide, soot and water vapour will be derived first. Simplified expressions in a closed system and an open system under different measuring conditions are then deduced. These conditions are for measuring oxygen only; and for measuring oxygen, carbon dioxide and carbon monoxide. A system with two linear equations on the mole fractions of nitrogen and oxygen; or four linear equations on the mole fractions of nitrogen, oxygen, carbon dioxide and carbon monoxide will be solved.

4.2 The Oxygen Consumption Method

An exhaust hood with a fan-duct system has to be built in oxygen consumption calorimetry to collect flue gas from a burning object as in Figure 4.1. Intake air of mass flow rate $\dot{m}_a$ (in kgs^{-1}) will be drawn to burn with fuel of mass lost rate $\dot{m}_f$ (in kgs^{-1}). Flue gas with mass flow rate $\dot{m}_e$ (in kgs^{-1}) will be extracted through the hood in the fan-duct system. The heat release rate $\dot{q}$ (in kW) can be estimated from the amount of oxygen consumed.

4.2.1 Complete combustion

For complete combustion, $\dot{q}$ is given in terms of the mass flow rate of oxygen in the incoming air $\dot{m}_{O_2}^o$ (in kgs^{-1}), the mass flow rate of oxygen in the exhaust gas $\dot{m}_{O_2}$ (in kgs^{-1}) and the generic constant E_{O_2} (13.1 $MJkg^{-1}$ oxygen consumed) as follows,

$$\dot{q} = E\left(\dot{m}_{O_2}^o - \dot{m}_{O_2}\right) \tag{4.1}$$

4.2.2 Correction for incomplete combustion

Chemical reactions in a real fire are very complicated. Carbon monoxide and soot might be the final products due to incomplete combustion. Equation of heat release rate on complete combustion given by equation (4.1) must be corrected on the carbon monoxide [Parker 1982, 1984; Beaulieu and Dembsey 2005] and soot [Brohez et al. 2000] production, which depend on the flow rate differences of carbon

monoxide and soot between the exhaust gas and incoming gas, and the oxygen assumed to be used $\Delta\dot{m}_{O_2}$ to oxidize these incomplete combustion products.

Total oxygen consumption rate is $\dot{m}^{o}_{O_2} - \dot{m}_{O_2} + \Delta\dot{m}_{O_2}$. Then the heat release rate should be corrected by subtracting the heat required (such as $E_{CO}\Delta\dot{m}^{CO}_{O_2}$ for carbon monoxide) to change incomplete combustion products to carbon dioxide. According to Hess' law, the heat release rate on correction for incomplete combustion is given by:

$$\dot{q} = E\left(\dot{m}^{o}_{O_2} - \dot{m}_{O_2}\right) - \left(E_{CO} - E\right)\Delta\dot{m}^{CO}_{O_2} - \left(E_S - E\right)\Delta\dot{m}^{S}_{O_2} \qquad (4.2)$$

where E_{CO} (about 17.7 $MJkg^{-1}$ of O_2 consumed) and E_S (about 12.3 $MJkg^{-1}$ of O_2 consumed) are the net heat release per unit mass of O_2 consumed [Babrauskas and Grayson 1992] to oxidize carbon monoxide and soot to CO_2 respectively; $\Delta\dot{m}^{CO}_{O_2}$ and $\Delta\dot{m}^{S}_{O_2}$ are the mass consumed rate of oxygen to oxidize carbon monoxide and soot respectively.

Considering the following chemical reactions:

$$2CO + O_2 \rightarrow 2CO_2$$

$$C + O_2 \rightarrow CO_2$$

For the chemical reaction on complete oxidation of carbon monoxide and soot as above, the rate of change of moles for oxygen is half the rate of change of moles for carbon monoxide, but the same as that for soot:

$$\frac{\Delta \dot{m}_{O_2}^{CO}}{M_{O_2}} = \frac{1}{2}\frac{\Delta \dot{m}_{CO}}{M_{CO}} \tag{4.3}$$

$$\frac{\Delta \dot{m}_{O_2}^{S}}{M_{O_2}} = \frac{\Delta \dot{m}_{S}}{M_{S}} \tag{4.4}$$

where M_{O_2}, M_{CO} and M_S are the molecular weights (in kgkmol^{-1}) of oxygen, carbon monoxide and soot respectively, $\Delta \dot{m}_{CO}$ and $\Delta \dot{m}_S$ are the net production rates (in kgs^{-1}) of carbon monoxide and soot respectively.

Putting in equations (4.3) and (4.4), equation (4.2) changes to:

$$\dot{q} = E\left(\dot{m}_{O_2}^{o} - \dot{m}_{O_2}\right) - \left(E_{CO} - E\right)\frac{\Delta \dot{m}_{CO} M_{O_2}}{2M_{CO}} - \left(E_S - E\right)\frac{\Delta \dot{m}_S M_{O_2}}{M_S} \tag{4.5}$$

Equation (4.1) on complete combustion is the basis of oxygen consumption method to calculate the heat release rate; it can be taken as an ideal state equation. Equation (4.5) is still based on the oxygen consumption method, but it is more accurate due to corrections on carbon monoxide and soot production. As the mass flow rate of oxygen, carbon monoxide and soot in the above equations cannot be measured directly, the above equations will be further derived in the following part.

4.3 Derivation of the General Equation

Both the incoming gas and exhaust gas might have at least oxygen, nitrogen, carbon dioxide, carbon monoxide, soot and water vapour. Other species are of relatively low concentration and so inert gas can be included in the nitrogen component, solid species can be included in soot, and some acid products such as hydrochloric acid (HCl) can be included in the water component. This will give a system of six components. The mole fraction of the ith species X_i (where i = 1, …, 6 for O_2, N_2, CO_2, CO, soot and H_2O) of incoming gas (with superscript o) and exhaust gas are:

$$\begin{cases} X_i^o = \dfrac{\dfrac{\dot{m}_i^o}{M_i}}{\dfrac{\dot{m}_a}{M_a}} \approx \dfrac{\dfrac{\dot{m}_i^o}{M_i}}{\sum_1^6 \dfrac{\dot{m}_i^o}{M_i}} & (4.6a) \\ X_i = \dfrac{\dfrac{\dot{m}_i}{M_i}}{\dfrac{\dot{m}_e}{M_e}} \approx \dfrac{\dfrac{\dot{m}_i}{M_i}}{\sum_1^6 \dfrac{\dot{m}_i}{M_i}} & (4.6b) \end{cases}$$

where $\dot{m}_i^o$ and $\dot{m}_i$ are the mass flow rates (in kgs^{-1}) of the ith species in the incoming and exhaust gas respectively; M_i is the molecular weight of the ith species (in kgkmol^{-1}); subscripts a and e are used for total incoming gas and exhaust gas respectively. X_i^o, $\dot{m}_i^o$ and other symbols with superscript o are used for incoming gas, and corresponding symbols without superscript o are used for exhaust gas.

Concentration of soot and water vapour can be measured directly from the sample and then removed before measuring other gases. Assuming dry oxygen, carbon

dioxide and carbon monoxide are measured in a four species system, their relations for intake and exhaust gases are expressed respectively as:

$$\begin{cases} X_i^{A^o} = \dfrac{\dfrac{\dot{m}_i^o}{M_i}}{\sum_1^4 \dfrac{\dot{m}_i^o}{M_i}} & (4.7a) \\ X_i^{A} = \dfrac{\dfrac{\dot{m}_i}{M_i}}{\sum_1^4 \dfrac{\dot{m}_i}{M_i}} & (4.7b) \end{cases}$$

where $i = 1, \ldots, 4$ are for O_2, N_2, CO_2 and CO. Superscript A indicates the mole fractions of species measured in the gas analyzer with soot and water vapour removed, i.e.

$$\begin{cases} X_{O_2}^{A^o} + X_{N_2}^{A^o} + X_{CO_2}^{A^o} + X_{CO}^{A^o} = 1 & (4.8a) \\ X_{O_2}^{A} + X_{N_2}^{A} + X_{CO_2}^{A} + X_{CO}^{A} = 1 & (4.8b) \end{cases}$$

Note that mole fractions of species measured in the gas analyzer as in equation (4.7) are different from those in the total incoming and exhaust gases as in equation (4.6). The values depend on how many species are considered in the measuring system. But they can be transformed between the different systems.

Nitrogen would not be involved in the chemical reactions under normal fires as the temperatures are not high. Therefore, amount of intake nitrogen is taken to be same as that in the exhaust section:

$$X_{N_2}^{A^o}\frac{\dot{m}_a}{M_a}\left(1-X_{Soot}^{o}-X_{H_2O}^{o}\right)=X_{N_2}^{A}\frac{\dot{m}_e}{M_e}\left(1-X_{Soot}-X_{H_2O}\right) \tag{4.9}$$

Putting in equations (4.8a) and (4.8b) to substitute the mole fraction of nitrogen:

$$\frac{\dot{m}_a}{M_a}=\frac{\dot{m}_e}{M_e}\frac{\left(1-X_{H_2O}-X_{Soot}\right)\left(1-X_{O_2}^{A}-X_{CO_2}^{A}-X_{CO}^{A}\right)}{\left(1-X_{H_2O}^{o}-X_{Soot}^{o}\right)\left(1-X_{O_2}^{A^o}-X_{CO_2}^{A^o}-X_{CO}^{A^o}\right)} \tag{4.10}$$

Based on equations (4.6) and (4.7), the mole flow rates of oxygen in the incoming and exhaust gases can be expressed as:

$$\begin{cases}\dfrac{\dot{m}_{O_2}^{o}}{M_{O_2}}=X_{O_2}^{A^o}\dfrac{\dot{m}_a}{M_a}\left(1-X_{H_2O}^{o}-X_{Soot}^{o}\right) & (4.11a)\\[2ex] \dfrac{\dot{m}_{O_2}}{M_{O_2}}=X_{O_2}^{A}\dfrac{\dot{m}_e}{M_e}\left(1-X_{H_2O}-X_{Soot}\right) & (4.11b)\end{cases}$$

An oxygen depletion factor ϕ was defined by Janssens [1991, 2000, 2002] to relate $\dot{m}_{O_2}^{o}$ with $\dot{m}_{O_2}$:

$$\phi=\left(\dot{m}_{O_2}^{o}-\dot{m}_{O_2}\right)/\dot{m}_{O_2}^{o} \tag{4.12}$$

Inserting equations (4.10) and (4.11), ϕ becomes

$$\phi=\frac{X_{O_2}^{A^o}\left(1-X_{CO_2}^{A}-X_{CO}^{A}\right)-X_{O_2}^{A}\left(1-X_{CO_2}^{A^o}-X_{CO}^{A^o}\right)}{X_{O_2}^{A^o}\left(1-X_{O_2}^{A}-X_{CO_2}^{A}-X_{CO}^{A}\right)} \tag{4.13}$$

If the i[th] species is not measured, X_i in equations (4.8) to (4.13) is zero. For complete combustion with fresh intake gas, $X_{CO}^{A^o} = X_{CO}^{A} = 0$.

Combining equations (4.11) and (4.12), equation (4.10) for relating $\dot{m}_a$ and $\dot{m}_e$ is expressed as:

$$\frac{\dot{m}_a}{M_a} = \frac{X_{O_2}^{A}\left(1 - X_{Soot} - X_{H_2O}\right)}{(1-\phi)\cdot X_{O_2}^{A^o}\left(1 - X_{Soot}^{o} - X_{H_2O}^{o}\right)}\frac{\dot{m}_e}{M_e} \tag{4.14}$$

If some samples cannot be measured, $\dot{m}_a$ can also be approximately related to $\dot{m}_e$ by defining an expansion factor α (note that $\alpha = 1 + X_{O_2}^{o}\left(\beta - 1\right)$ where β is the mole ratio of products generated to oxygen consumed, of value ≤ 2 . Therefore, $1 \leq \alpha \leq 1 + X_{O_2}^{o}$, α is often taken as 1.105 for unknown fuel) [Parker 1982, 1984; Janssens 1991, 2000, 2002] as:

$$\frac{\dot{m}_e}{M_e} = (1-\phi)\frac{\dot{m}_a}{M_a} + \alpha\phi\frac{\dot{m}_a}{M_a} \tag{4.15}$$

Based on equations (4.6) and (4.7) for carbon monoxide and soot, the rate of change of moles for carbon monoxide and soot between the intake gas and exhaust gas respectively are:

$$\begin{cases} \dfrac{\Delta \dot{m}_{CO}}{M_{CO}} = X_{CO}^{A} \dfrac{\dot{m}_e}{M_e}\left(1 - X_{Soot} - X_{H_2O}\right) - X_{CO}^{A^o} \dfrac{\dot{m}_a}{M_a}\left(1 - X_{Soot}^{o} - X_{H_2O}^{o}\right) & (4.16a) \\ \dfrac{\Delta \dot{m}_S}{M_S} = X_{soot} \dfrac{\dot{m}_e}{M_e} - X_{soot}^{o} \dfrac{\dot{m}_a}{M_a} & (4.16b) \end{cases}$$

Putting in equation (4.14) to express $\dot{m}_a$ with $\dot{m}_e$, equation (4.16) becomes:

$$\begin{cases} \dfrac{\Delta \dot{m}_{CO}}{M_{CO}} = \dfrac{\dot{m}_e}{M_e}\left(1 - X_{Soot} - X_{H_2O}\right) \cdot \left(X_{CO}^{A} - \dfrac{1}{1-\phi} \dfrac{X_{O_2}^{A}}{X_{O_2}^{A^o}} X_{CO}^{A^o} \right) & (4.17a) \\ \dfrac{\Delta \dot{m}_S}{M_S} = \dfrac{\dot{m}_e}{M_e} \left[X_{soot} - X_{soot}^{o} \dfrac{X_{O_2}^{A}\left(1 - X_{Soot} - X_{H_2O}\right)}{(1-\phi) \cdot X_{O_2}^{A^o}\left(1 - X_{Soot}^{o} - X_{H_2O}^{o}\right)} \right] & (4.17b) \end{cases}$$

Combining equations (4.5), (4.11), (4.14) and (4.17), the general equation for calculating heat release rate is expressed as:

$$\begin{cases} \dot{q} = \left\{ E\phi - \dfrac{(E_{CO} - E)}{2} \left(\dfrac{X_{CO}^{A}(1-\phi)}{X_{O_2}^{A}} - \dfrac{X_{CO}^{A^o}}{X_{O_2}^{A^o}} \right) - (E_S - E) \left[\dfrac{X_{Soot}(1-\phi)}{X_{O_2}^{A}\left(1 - X_{Soot} - X_{H_2O}\right)} \right. \right. \\ \qquad \left. \left. - \dfrac{X_{Soot}^{o}}{X_{O_2}^{A^o}\left(1 - X_{Soot}^{o} - X_{H_2O}^{o}\right)} \right] \right\} \dfrac{\dot{m}_a M_{O_2} X_{O_2}^{A^o}}{M_e} \left(1 - X_{Soot}^{o} - X_{H_2O}^{o}\right) & (4.18a) \\ \dot{q} = \left\{ \dfrac{E\phi}{1-\phi} - \dfrac{(E_{CO} - E)}{2} \left(\dfrac{X_{CO}^{A}}{X_{O_2}^{A}} - \dfrac{1}{1-\phi} \dfrac{X_{CO}^{A^o}}{X_{O_2}^{A^o}} \right) - \dfrac{(E_S - E)}{1-\phi} \left[\dfrac{X_{Soot}(1-\phi)}{X_{O_2}^{A}\left(1 - X_{Soot} - X_{H_2O}\right)} \right. \right. \\ \qquad \left. \left. - \dfrac{X_{Soot}^{o}}{X_{O_2}^{A^o}\left(1 - X_{Soot}^{o} - X_{H_2O}^{o}\right)} \right] \right\} \dfrac{\dot{m}_e M_{O_2} X_{O_2}^{A}}{M_e} \left(1 - X_{Soot} - X_{H_2O}\right) & (4.18b) \end{cases}$$

where $\dot{m}_a$ is related to $\dot{m}_e$ by equations (4.14) and (4.15). The mole fractions of soot can be calculated by equation (4.6), in which the mass flow rate of soot $\dot{m}_S$ (in kgs^{-1})

in the intake or exhaust gases can be measured by direct sampling or calculated from optical smoke measurement by:

$$\dot{m}_S = C_S \dot{V} = \frac{k_s \dot{V}}{\sigma_S} \tag{4.19}$$

where C_S is the mass concentration of smoke particles (in kgm^{-3}), $\dot{V}$ is the volumetric flow rate (in m^3s^{-1}); σ_S is the specific area per unit mass of soot, often called specific extinction area on soot mass basis (m^2kg^{-1}) and k_s is the extinction coefficient of smoke.

Note that the rate of consuming carbon monoxide by combustion under some conditions might be higher than the production rate (the value of $\Delta\dot{m}_{O_2}^{CO}$ is negative). However, oxygen consumed to oxidize carbon monoxide into carbon dioxide is similar to burning a common fuel (using E = 13.1 $MJkg^{-1}$, not E_{CO} = 17.6 $MJkg^{-1}$). The value of heat release rate is reduced by equation (4.1). Therefore, the heat ($-(E_{CO}-E)\Delta\dot{m}_{O_2}^{CO}$) calculated by burning carbon monoxide should be added by considering the carbon monoxide consumption rate. The above equations are still applicable, though the differences in carbon monoxide and the corresponding oxygen consumed $\Delta\dot{m}_{O_2}^{CO}$ between the intake and exhaust gas are negative. By similar analysis, the above equations are also applicable to both soot production and soot oxidization.

The equation on calculating the heat release rate will be more accurate with more samples measured. The general equation is the most accurate, but it has to be simplified as fewer samples can be measured in real conditions.

4.4 Simplified Equations

The general equation (4.18) can be simplified for deducing forms commonly reported in the literature.

4.4.1 Closed system

The general equation (4.18) is applicable to the controlled environment with a closed system, whether the value of soot is a constant or not. To simplify the general equation, soot can be first neglected by taking X^{o}_{Soot} and X_{Soot} as 0 in the above equations. Next, equations can be further simplified under the conditions whether water and carbon monoxide are measured or not as in the following.

- When only soot is not measured in the six component system

In this case, only soot is neglected by taking X^{o}_{Soot} and X_{Soot} as 0 in the above equations. The general equation (4.18) becomes:

$$\begin{cases} \dot{q} = \left[E\phi - \dfrac{(1-\phi)\cdot(E_{CO}-E)}{2}\left(\dfrac{X_{CO}^{A}}{X_{O_2}^{A}} - \dfrac{1}{1-\phi}\dfrac{X_{CO}^{A^o}}{X_{O_2}^{A^o}} \right) \right] \dfrac{M_{O_2}}{M_a} X_{O_2}^{A^o} \dot{m}_a \left(1 - X_{H_2O}^{o}\right) & (4.20a) \\ \dot{q} = \left[\dfrac{E\phi}{1-\phi} - \dfrac{(E_{CO}-E)}{2}\left(\dfrac{X_{CO}^{A}}{X_{O_2}^{A}} - \dfrac{1}{1-\phi}\dfrac{X_{CO}^{A^o}}{X_{O_2}^{A^o}} \right) \right] \dfrac{M_{O_2}}{M_e} X_{O_2}^{A} \dot{m}_e \left(1 - X_{H_2O}\right) & (4.20b) \end{cases}$$

where ϕ is given by equation (4.13). If $\dot{m}_e$ is measured instead of $\dot{m}_a$, $\dot{m}_a$ in equation (4.20a) will be calculated by equation (4.15).

- When soot and water are not measured in the six component system

If water is not measured, it might be easier to estimate in the incoming gas than in the exhaust gas. The general equation or equation (4.20) is transformed into:

$$\dot{q} = \left[E\phi - \frac{(1-\phi)\cdot(E_{CO}-E)}{2}\left(\frac{X_{CO}^{A}}{X_{O_2}^{A}} - \frac{1}{1-\phi}\frac{X_{CO}^{A^o}}{X_{O_2}^{A^o}} \right) \right] \frac{M_{O_2}}{M_a} X_{O_2}^{A^o} \dot{m}_a \left(1 - X_{H_2O}^{o}\right) \quad (4.21)$$

where ϕ is given by equation (4.13). If $\dot{m}_e$ is measured instead of $\dot{m}_a$, equation (4.15) can be used as:

$$\dot{m}_a = \frac{M_a \cdot \dot{m}_e}{M_e\left[1+(\alpha-1)\phi\right]} \quad (4.22)$$

Or it is simplified by assuming M_e is the same as M_a as:

$$\dot{m}_a = \frac{\dot{m}_e}{1+(\alpha-1)\phi} \quad (4.23)$$

Note that there is no difference in accuracy between measuring only three species (carbon dioxide, carbon monoxide and oxygen) and measuring only two species (carbon monoxide and oxygen). Equation (4.21) is the same for these two conditions, but $X_{CO_2}^{A^o}$ and $X_{CO_2}^{A}$ are zero for measuring only two species in the system. Equation (4.13) for measuring only carbon monoxide and oxygen is given by:

$$\phi = \frac{X_{O_2}^{A^o}\left(1 - X_{CO}^{A}\right) - X_{O_2}^{A}\left(1 - X_{CO}^{A^o}\right)}{X_{O_2}^{A^o}\left(1 - X_{O_2}^{A} - X_{CO}^{A}\right)} \tag{4.24}$$

- When only oxygen is measured

Similar to the above analysis, measuring only oxygen will get the same results as in measuring only 'oxygen and carbon dioxide' in calculating the heat release rate, when the carbon monoxide production rate is negligible for both. Whenever carbon dioxide is not measured, it is removed in the sample gas before measuring the oxygen concentration.

Components of water, soot, carbon monoxide and carbon dioxide are all taken as zero in equations (4.13) and (4.18):

$$\dot{q} = E\phi \frac{M_{O_2}}{M_a} X_{O_2}^{A^o} \dot{m}_a \left(1 - X_{H_2O}^{o}\right) \tag{4.25}$$

where $\dot{m}_a$ can be expressed by equation (4.22) or (4.23) if $\dot{m}_e$ is measured instead of $\dot{m}_a$; the oxygen depletion factor ϕ becomes:

$$\phi = \frac{X_{O_2}^{A^o} - X_{O_2}^{A}}{X_{O_2}^{A^o}\left(1 - X_{O_2}^{A}\right)} \tag{4.26}$$

Note that open system can be taken as a special case of closed system where the parameters in the intake part are constant. The equations commonly used in the literature for open system can be derived by simplifying the above general equation as in the following.

4.4.2 Open system

For convenience, the incoming gas is not measured dynamically in common experiments. An exhaust hood with a fan system is installed to collect the exhaust gas for measurement. A common assumption is to take the incoming gas to be the same as ambient air with constant concentrations of oxygen, nitrogen, carbon dioxide and water vapour. Normally, carbon monoxide in the incoming air is neglected by taking $X_{CO}^{A^o}$ to be 0. Water vapour is measured directly from the sample gas and removed before measuring oxygen, carbon dioxide and carbon monoxide.

- When oxygen, carbon dioxide, carbon monoxide, water vapour and soot are all measured

Only the soot and carbon monoxide in the incoming gas are taken as zero. Equation (4.18) becomes:

$$\dot{q} = \left[\frac{E\phi}{1-\phi} - \frac{(E_{CO} - E)}{2} \frac{X_{CO}^{A}}{X_{O_2}^{A}} - (E_S - E) \frac{X_{Soot}}{X_{O_2}^{A}\left(1 - X_{Soot} - X_{H_2O}\right)} \right] \frac{\dot{m}_e M_{O_2} X_{O_2}^{A}}{M_e} \left(1 - X_{Soot} - X_{H_2O}\right) \quad (4.27)$$

where the oxygen depletion factor ϕ in equation (4.13) becomes:

$$\phi = \frac{X_{O_2}^{A^o}\left(1 - X_{CO_2}^{A} - X_{CO}^{A}\right) - X_{O_2}^{A}\left(1 - X_{CO_2}^{A^o}\right)}{X_{O_2}^{A^o}\left(1 - X_{O_2}^{A} - X_{CO_2}^{A} - X_{CO}^{A}\right)} \quad (4.28)$$

- When only oxygen, carbon dioxide, carbon monoxide and water vapour are measured

In this case, X_{Soot}^{o} and X_{Soot} are taken as 0 due to only soot is not measured in the exhaust part. Equation (4.28) is simplified as:

$$\dot{q} = \left[\frac{E\phi}{1-\phi} - \frac{(E_{CO} - E)}{2} \frac{X_{CO}^{A}}{X_{O_2}^{A}} \right] \frac{\dot{m}_e M_{O_2} X_{O_2}^{A}}{M_e} \left(1 - X_{H_2O}\right) \quad (4.29)$$

where the oxygen depletion factor ϕ is given by equation (4.28).

- When only oxygen, carbon dioxide and carbon monoxide are measured

In this case, water vapour in the exhaust gas is not measured. Putting in equation (4.14), equation (4.29) becomes:

$$\dot{q} = \left[E\phi - \frac{(1-\phi)(E_{CO} - E)}{2} \frac{X_{CO}^{A}}{X_{O_2}^{A}} \right] \frac{\dot{m}_a M_{O_2} X_{O_2}^{A^o}}{M_a} \left(1 - X_{H_2O}^{o}\right) \tag{4.30}$$

where the oxygen depletion factor ϕ is given by equation (4.28) and $\dot{m}_a$ can be related to $\dot{m}_e$ by equation (4.22) or (4.23).

- When only oxygen is measured

In this case, only oxygen is measured in a system of two species (oxygen and nitrogen). When $\dot{m}_a$ is related to $\dot{m}_e$ by equation (4.23), the above equation is further simplified as:

$$\dot{q} = E\phi \frac{\dot{m}_e}{1 + \phi(\alpha - 1)} \frac{M_{O_2}}{M_a} \left(1 - X_{H_2O}^{o}\right) X_{O_2}^{A^o} \tag{4.31}$$

where the oxygen depletion factor ϕ is given by:

$$\phi = \frac{X_{O_2}^{A^o} - X_{O_2}^{A}}{X_{O_2}^{A^o}\left(1 - X_{O_2}^{A}\right)} \tag{4.32}$$

Gas concentrations both in the incoming gas and in the exhaust gas can be measured accurately for carrying out experiments in a closed system. But it might be difficult to dynamically measure all the incoming gas accurately in an open system. Gas concentrations in the exhaust part are easier to measure if all chemical species are collected for an open system, and the intake mass flow rate $\dot{m}_a$ in the equations is

usually estimated by $\dot{m}_e$ measured for exhaust gas. In fact, the equations used in an open system can be taken as a special condition of the closed system by taking samples in the intake gas as a constant or zero.

4.5 Discussion on the Equations Derived

Equations on calculating the heat release rates commonly used in the literature [Parker 1982, 1984; Janssens 1991, 2000, 2002; Lattimer and Beitel 1998; Brohez et al. 2000a, 2000b; Enright and Fleischmann 1999; Han and Chow 2004; Brohez 2005; Babrauskas 1992; McCaffrey and Harkleroad 1988; Beaulieu and Dembsey 2005; Chow 2004] were basically derived for tests in an open system, where a fan-duct system is used to keep enough fresh ambient air entrained. However, fire tests should not be limited to the over-ventilated environment. Under-ventilated environment is always found in the real fire scenarios. Fire tests in more complicated environments such as controlled-atmosphere calorimetry [Gottuk and Lattimer 2002] should be considered. To study certain types of fire, it is necessary to consider fires involving different atmospheres.

Equation (4.18) and its simplified equations (4.20) to (4.25) are applicable no matter the incoming air is taken as fresh air or "contaminated" with some combustion products as in the large-scale fire tests. Equations used in the literature are for keeping the incoming air fresh with correction in carbon monoxide for incomplete combustion included in the exhaust air.

Moreover, after some mathematical manipulation, the simplified forms of equation (4.18) would give equations (4.27) to (4.31). Basically, these simplified equations are similar to equations commonly used in the literature [Janssens 1991, 2002].

For relating $\dot{m}_a$ to $\dot{m}_e$, simplified equation such as equation (4.23) is commonly used in the literature. Differences between M_e and M_a are shown in Appendix A. $\dot{m}_a$ is defined for the total incoming gas, not only for fresh air.

Two special cases on calculating heat release rate using the above equations will be discussed in the following sections. These are on bench-scale tests with a cone calorimeter in a controlled environment and a full-scale burning test on total flooding gas protection system.

4.6 Controlled Environment in a Cone Calorimeter

Equations commonly used in the literature [Parker 1982, 1984; Janssens 1991, 2000, 2002; Lattimer and Beitel 1998; Brohez et al. 2000a, 2000b; Enright and Fleischmann 1999] might not be applicable in calculating the heat release rate for the tests in a controlled environment. An example of using the above general equation or its simplified form is demonstrated. Deviation due to using a constant value of $X_{O_2}^{A^o}$ will be estimated.

For the bench-scale test in a controlled chamber, the fractions of different gas components of input air can be adjusted. $X_{O_2}^{A^o}$ should be taken as a variable as $X_{O_2}^{A}$, though it is always measured before the test and taken as a constant throughout the test. For convenience, assume that there are 80% nitrogen and 20% oxygen in the intake gas. One of the simplified forms of the general equation on $\dot{q}$, i.e. equation (4.25) for controlled environment, can be derived by taking $X_{O_2}^{A^o}$ as 20%:

$$\dot{q} = 0.2E \frac{0.2 - X_{O_2}^{A}}{0.2\left(1 - X_{O_2}^{A}\right)} \frac{M_{O_2}}{M_a} \dot{m}_a \tag{4.33}$$

If $\dot{q}$ (denoted by $\dot{q}_{eq4..31}$) is estimated by equation (4.31) commonly used in oxygen consumption calorimetry under this testing condition, there might be great deviation in taking the incoming oxygen concentration as 20.95% (or the measured value before the test). The percentage deviation of heat release rate PD_q can be estimated by:

$$PD_q = 100\left(\frac{\dot{q}_{eq4.31}}{\dot{q}} - 1\right) \tag{4.34}$$

Values of PD_q are plotted against exhaust oxygen concentration $X_{O_2}^{A}$ for incoming oxygen concentration $X_{O_2}^{A^o}$ varying from 20 % to 22 % in Figure 4.2. It is observed that lower PD_q would be obtained with more oxygen consumed. Greater deviations would be found under over-ventilated conditions; or when the fire was not fully-developed with less oxygen consumed.

4.7 Test in a Full-Scale Burning Facility

Full-scale testing results on evaluating the suppression of total flooding gas protection system with clean agent heptafluoropropane in an office fire [Chow 2006] was taken out as an example to illustrate how the above equations are applied under special conditions. The curves on the mole fractions of clean agent estimated and oxygen measured in the exhaust duct section are shown in Figures 4.3. Heat release rate calculated by the common equation (4.31) is shown in Figure 4.4.

Reduction in the oxygen concentration for suppression by a gas system is due to combustion consumption and dilution by the discharged clean agent. This condition is different from water suppression conditions [Dlugogorski et al. 1994] where water might be removed before measuring other gases. Most of the gases due to discharging clean agent cannot be removed completely by drying agent. The concentrations and the compositions of the gases in the system are different from those defined in equation (4.31). Appropriate corrections on oxygen concentrations measured have to be made in using equation (4.31) to estimate the heat release rate. Dilution effect on $X_{O_2}^{A^o}$ can be included by using equation (4.25) with result shown in Figure 4.4.

It is observed that after discharging the clean agent, up to 10 % deviation of the two heat release rate curves would be resulted. The deviation should depend on the gas concentrations of the clean agent.

4.8 Measuring Heat Release Rate under Water Suppression Conditions

The general equation derived in the above sections can also be applied to the water suppression conditions. However, the following aspects should be watched.

$\dot{m}_a$ and M_a cannot be taken as in fresh air when water is discharged from the suppression system. Mole fraction of water content in the incoming gas (of rate $\dot{m}_a$) $X^o_{H_2O}$ includes moisture of ambient air $X^a_{H_2O}$ ($X^o_{H_2O} = X^a_{H_2O}$ without water suppression) described by humidity and additional water vapour $X^{ws}_{H_2O}$ due to operating the water suppression system. The additional water content $n^{ws}_{H_2O}$ is not the total discharging water, but a part of discharging water entrained into the exhaust duct. The amount of water entrained depends on the ventilation and evaporation due to heat absorbed while suppressing the fire. The physical meaning is not correct without considering $\dot{n}^{ws}_{H_2O}$ in both the incoming gas and exhaust gas in the equation. Therefore, $\dot{n}^{ws}_{H_2O}$ ($\dot{n}^o_{H_2O} = \dot{n}^a_{H_2O} + \dot{n}^{ws}_{H_2O}$) should be considered in a way similar to nitrogen N_2 in mass balancing.

Part of water vapour in the exhaust duct is generated from combustion $\dot{n}^{comb}_{H_2O}$. The total mole flow rate of water vapour in the exhaust gas $\dot{n}^e_{H_2O}$ ($\dot{n}^e_{H_2O} = \dot{n}^o_{H_2O} + \dot{n}^{comb}_{H_2O}$) is then greater than that in the incoming gas $\dot{m}^o_{H_2O}$ (in kg/s).

To relate $\dot{m}_a$ to $\dot{m}_e$, an expansion factor α (≥ 1) commonly used is corrected as α^w used in water suppression with derivation shown in Appendix B:

$$\dot{m}_a = \frac{\dot{m}_e}{1+\phi\left(\alpha - 1 - 0.105 X^o_{H_2O}\right)} \tag{4.35}$$

The expansion factor varied from $\left(\alpha - 0.21 X^o_{H_2O}\right)$ to α in the presence of water $X^o_{H_2O}$. The percentage error on the heat release rate varied from 0 to $\frac{21\phi X^o_{H_2O}}{1+\phi(\alpha-1)}\%$ for all combustibles (or approximated as $10\phi X^o_{H_2O}\%$ for α of 1.105). Therefore, the percentage error might be up to 1% when ϕ about 0.3 and $X^o_{H_2O}$ about 30%.

4.9 Summary

The heat release rate is proposed to be calculated using a general equation on oxygen consumption method given by equation (4.18). This was derived by balancing chemical species both in the incoming gas and in the exhaust gas. Simpler forms under different conditions can then be achieved by neglecting some terms.

Simplified equations on calculating heat release rate are only applicable under some conditions which have to be clarified [Lattimer and Beitel 1998]. Corrections on E, α and molecular weights are necessary when the testing conditions are different from those assumed in the equations. All the parameters should be reviewed carefully before using the relevant equations. Once the equations concerned are clarified, uncertainty analysis [e.g. Enright and Fleischmann 1999; Brohez 2005] can then be applied to give a better estimation of the measured heat release rate.

Equation (4.18) is applicable to almost all fire environments. Accurate results can be obtained if more gas analyzers are available. Corrections on carbon monoxide and soot due to incomplete combustion were considered both in the intake gas and exhaust gas. They are applicable to both increasing and decreasing concentrations of carbon monoxide and soot in the combustion products.

The simplified forms by equations (4.20) to (4.25) are also applicable to both closed and open systems, though the accuracy might be reduced due to fewer samples are measured. Other simplified equations used in the open system are consistent to those equations commonly used in the literature.

CHAPTER 5 IMPORTANCE OF FURNITURE TESTED UNDER FLASHOVER

5.1 Introduction

In response to having so many arson fires in small enclosures such as karaoke boxes [Chow 2002] and train vehicles [SCMP 2003, 2004], it is essential to study the burning behaviour of furniture under well-developed fire after flashover. Assessing furniture under small accidental fires of 100 kW to 300 kW as in the gas ignitor for standard test ISO 9705 [1993] appears to be insufficient.

An accidental fire may start from burning a small object such as a litter bin. The fire is localized with some combustibles ignited. It would take time to have the whole room involved in fire. Once a fire is well-developed after flashover, furniture would be exposed to higher external heat fluxes and then easier to burn. Higher thermal radiation feedback will give a higher pyrolysis rate and faster chemical reactions. The heat release rate will be higher to give a more hazardous environment. It is necessary to understand how furniture are burnt after flashover, not just ignite a small part by a small heat source.

Studies on the fire behaviour of furniture were done years ago [Babrauskas 1982, 1984; Sundstöm 1996]. The heat release rate and other parameters on burning furnitures were measured in furniture or room calorimeters. Furniture fires

developed up to flashover were studied. However, most of the tests started from a smaller ignition source. There were not many studies on burning furniture in a flashover fire. Note that burning furniture might lead to flashover in a small enclosure. Therefore, studies on furniture exposed to a flashover fire should be carried out.

Full-scale burning tests on studying the heat release rates of selected furniture samples under accidental and flashover fires were carried out in a room calorimeter [ISO 9705: 1993]. Furniture samples were tested with a cone calorimeter [ISO5660: 2002] to better understand the results from full-scale burning tests.

5.2. Full-scale Burning Tests

5.2.1. Full-scale testing arrangements

Nine tests were carried out on three sets of four-seater sofas and two wood desks as in Figure 5.1. Sofa samples were comprised of wood frame, foam filling and leather covering. The desk samples were made of oak. The room calorimeter is shown in Figure 5.2 including the locations of thermocouples for measuring the air temperature.

The nine testing arrangements are:

- Burning under an accidental fire with 0.5 litre of gasoline in a 0.2 m diameter pool.

  R5A1: Testing sofa sample SF1

  R5A2: Testing sofa sample SF2 with less amount of foam than SF1

  R5A3: Testing SF1 under a lower exhaust rate by reducing the fan power

  R5A4: Testing SF1 treated with fire retardant

  R5A5: Testing a wood desk

  R5A6: Testing SF1 and a wood desk

- Testing under flashover condition

  R5B1: Testing SF2 by setting up a bigger pool of diameter 1 m with 12 litres gasoline to onset flashover in the room first.

- Measuring the heat release rates of the gasoline pool fires

  R5C1: Testing a 1 m pool fire of 12 litres gasoline to onset flashover.

  R5C2: Testing with a pool fire of 0.5 litre gasoline, used as a small starting fire for tests T1 to T6 to simulate an accidental fire.

In tests R5A1 to R5A6, the furniture was put near to the rear wall. The gasoline pool fire was placed adjacent to the furniture. For test R5B1, a bigger pool of 1 m diameter with 12 litres gasoline was put at the centre of the room to onset flashover first.

The surface of the sofa sample in test R5A4 was protected by a commercial fire retardant coating commonly used in the Far East including China and Hong Kong.

Test R5A3 was conducted at a lower exhaust rate to check whether flue gas can be extracted completely. The exhaust fan-duct system as shown in Figure 5.3 should be set at sufficient fan power to avoid leakage of flue gases.

A thermal radiative heat flux meter was placed at the floor level as shown in Figure 5.2. Thermocouples were put in positions labeled in Figure 5.2 as:

C : Corner of the wall near the room opening

M : Centre of the room

T : Near the ceiling

Rc (R1 to R6) : Near the rear wall corner

Rm (R7 to R12): Near the middle of the rear wall

D1 to D4 : Room opening

D5 : A point at the top of exhaust hood near the duct

5.2.2. Full-scale testing results

Results on heat release rate curves and heat fluxes at floor level position are shown in Figures 5.4 and 5.5 respectively.

A summary of the key information such as mass of samples m, burning time t_B, peak heat release rate (pkHRR) $\dot{q}_{\max}$, time to first peak heat release rate t_{fp} and peak heat flux $q''_{\max}$ is shown in Table 5.1. The typical temperature profiles of Tests R5A1, R5A5, R5A6 and R5A7 are shown in Figures 5.6 to 5.9. The vertical temperature profiles and average room air temperatures in those tests were measured and shown in Figures 5.10 and 5.11 respectively. The average room temperature is calculated by the temperatures measured from different thermocouple positions in the center, corner and opening side of the room with several heights. The measured average room air temperatures are compared with the standard temperature/time curve of BS476 [1972] as shown in Figure 5.11 to assess the potential hazard of burning furniture in an enclosure.

Dark smoke was generated and spreading out of the room. It was difficult to judge flashover using the criterion of flame coming out from the opening. Therefore, gas temperature measured near to the ceiling was used as the criterion for determining flashover. The value was taken to be 600 °C in this study.

The following key points were observed:

- Room air temperature rise caused by the furniture fire was high for quite a long time under flashover. Even without flashover, the maximum temperature might reach a dangerous level and affect the building structures.

- Treating sofa materials with this selected commercial sample of fire retardants would only delay the ignition time t_{ig} by several minutes under an accidental small fire source. Once ignited, the materials burnt as unprotected sofa in test R5A1. This point is verified by the bench-scale cone tests in the following section.

- Under flashover condition in test R5B1, SF2 was ignited quickly with most of the combustibles burnt up. Note that the amount of gasoline used was only to onset flashover as shown in the results for test R5C1.

5.2.3. Analysis on heat release rate and total heat released

The following points are observed on the heat release rate of burning furniture:

- Burning the sofa foam SF1 without the treatment of fire retardants in test R5A1 would give a $\dot{q}_{\max}$ over 1 MW as shown in Figure 5.4. Burning it with fire retardant applied on the surface in test R5A4 did not reduce the $\dot{q}_{\max}$. However, the time to peak heat release rate t_{fp} was delayed by over 2 min. This will allow

a longer time for evacuation, which is very useful in dealing with crowd movement and control.

- Burning the sofa with a lower exhaust rate will give a longer burning duration due to inadequate ventilation, but roughly the same value of $\dot{q}_{\max}$. The time to peak heat release rate t_{fp} can be extended to 1.5 min.

- Burning the sofa SF2 under a flashover fire (i.e. test R5B1) is very different from burning it in an accident as in test R5A2. The peak heat release rate is up to 3 MW in Test R5B1. The effect will be illustrated by the net heat release rate in the following.

The net heat release rate $\dot{q}_{net}$ of burning the combustibles can be computed from the total heat release rate $\dot{q}$ and the heat release rate of the fire source only $\dot{q}_{source}$:

$$\dot{q}_{net} = \dot{q} - \dot{q}_{source} \qquad (5.1)$$

The results on the net heat release rate of burning furniture are plotted in Figure 5.12. It is observed that most single items of furniture gave a net heat release rate higher than 1 MW with burning duration several minutes in an accidental fire. The net peak heat release rate for sofa SF2 in test R5B1 represented by curve G is 0.568 MW higher than that in test R5A2 as represented by curve B. If there are more adjacent combustibles, such flaming fires would ignite them to give a much higher heat release rate. The net peak heat release rate curve F in Figure 9 is 2.02 MW instead of

1.02 MW, due to igniting an adjacent wood desk by the burning sofa. Note that the net peak heat release rate was only 0.61 MW for burning only one wood desk.

The net total heat released THR_{net} (in MJ) can be obtained by integrating the net heat release rate curve $\dot{q}_{net}$ (in kW) from ignition time t_{ig} to the last time t_{stop} :

$$THR_{net} = 10^{-3} \int_{t_{ig}}^{t_{stop}} \dot{q}_{net} dt \tag{5.2}$$

The results of the net total heat release rate THR_{net} for the seven tests are shown in Figure 5.13.

It is observed that there are great differences between burning one sofa alone and burning the sofa together with other combustibles, especially under a post-flashover fire. The value of THR_{net} in burning SF1 and a wood desk in test R5A6 was 868 MJ. The value is higher than 728 MJ by adding up the value of THR_{net} of 353 MJ for SF1 in test R5A1 and 375 MJ for wood desk in test R5A5. The value of THR_{net} for SF2 was 451 MJ in test R5B1, but only 402 MJ in test R5A2. Complete combustion under higher temperature would give higher heat release rate.

The effective heat of combustion $\Delta h_{c,eff}$ can be calculated by the net total heat released THR_{net} and the mass consumed Δm :

$$\Delta h_{c,eff} = \frac{THR_{net}}{\Delta m} \tag{5.3}$$

The computed values of $\Delta h_{c,eff}$ in the full-scale burning tests are shown in Table 5.1. The values of $\Delta h_{c,eff}$ were measured to be 17 $MJkg^{-1}$ to 21 $MJkg^{-1}$ for most samples, except being 12 $MJkg^{-1}$ for desk.

Burning the sofa SF2 under a flashover fire (i.e. test R5B1) is very different from burning it in an accident as in test R5A2. This is clearly illustrated by the net peak heat release rates of 1.2 MW in test R5B1 and 0.7 MW in test R5A2 as shown in Figures 5.12 and 5.13, though the net total heat released did not increase so much. Therefore, testing furniture under a flashover fire will give a better assessment on fire safety.

5.3. Bench-scale Burning Tests

5.3.1 Testing arrangements of furniture foam and wood

Typical furniture wood and foams with and without fire retardants for constructing local furniture were selected for safety evaluation by a cone calorimeter. The samples were cut into squares of surface area 10 cm by 10 cm and labeled as:

C5A1: Foam without fire retardant tested under 70 kWm^{-2};

C5A2: Foam without fire retardant tested under 50 kWm^{-2};

C5A3: Foam without fire retardant tested under 35 kWm^{-2};

C5A4: Foam without fire retardant tested under 20 kWm^{-2};

C5B1: Foam with fire retardant tested under 70 kWm^{-2};

C5B2: Foam with fire retardant tested under 50 kWm^{-2};

C5B3: Foam with fire retardant tested under 35 kWm^{-2};

C5B4: Foam with fire retardant tested under 20 kWm^{-2}.

C5C1: Wood tested under 70 kWm^{-2};

C5C2: Wood tested under 50 kWm^{-2};

C5C3: Wood tested under 35 kWm^{-2};

C5C4: Wood tested under 20 kWm^{-2}.

5.3.2 Analysis on burning foam and wood

The results on the key parameters such as ignition time t_{ig}, peak heat release rate per unit area $\dot{q}_{A,\max}$, time to first peak of heat release rate curve t_{fp}, total heat released per unit area, effective heat of combustion $\Delta h_{c,eff}$, burning time t_B and average heat release rate per unit area over the burning time $\dot{q}_{A,avg}$ are shown in Table 5.2. Results on heat release rate per unit area are shown in Figure 5.14.

From the cone calorimeter tests, burning the furniture wood under heat fluxes higher than 35 kWm^{-2} and all the furniture foam would give almost complete combustion. No obvious improvement was observed for the foam treated with fire retardant under a flashover fire, except delaying the ignition time.

The values of $\Delta h_{c,eff}$ were 21 $MJkg^{-1}$ to 25 $MJkg^{-1}$ for furniture foam; and 13 $MJkg^{-1}$ to 16 $MJkg^{-1}$ for furniture wood. It appears that the values of $\Delta h_{c,eff}$ for furniture in

tests R5A1 to R5A6 are lower than those samples tested by a cone calorimeter due to the items were exposed to lower radiative heat fluxes.

5.4. Summary

Full-scale burning tests on different furniture arrangements were carried out. Wood and foam materials used in the furniture were tested with a cone calorimeter under radiative heat fluxes up to 70 kWm^{-2}. The burning behaviours of furniture under a well-developed fire were studied.

The values of effective heat of combustion of the same materials measured in full-scale and in bench-scale tests are similar under similar heat fluxes. Samples burnt more completely with higher heat release rate and total heat released under higher external heat fluxes. From both the full-scale and bench-scale tests, burning up all furniture under a flashover fire will give a much higher net heat release rate and total heat released, in comparing with burning only part of the combustibles in an accidental fire before flashover. The fire hazard would be much higher when a piece of furniture not yet ignited was involved in a flashover fire due to burning other combustibles. This point should be considered carefully in designing fire safe furniture for scenarios with possibility to have well-developed fires.

As fire retardants are only required to be tested by ignitability tests [FSD 2000] with a small flame at the moment , response to higher temperature fire scenarios such as a

fully developed fire is unknown. Furniture samples treated with fire retardant should be tested under a flashover fire, not only testing its ignitability.

CHAPTER 6 RADIATION AND FLASHOVER

6.1 Importance of Radiation

Convection is important at the preflashover stage of a building fire. Thermal radiation would be more significant when the fire develops with a hotter smoke layer. It was identified to be the key mode of heat transfer in developed room fires [Tien et al. 2002; de Ris 1979]. Thermal radiation in terms of electromagnetic wave would be emitted from objects at non-zero temperature [e.g. Hottel and Sarofim 1967; Edwards 1985; Modest 1993; Mbiock and Weber 2000] as summarized in Appendix C. The radiation flux radiated from an object is proportional to the fourth power of its temperature. Ignition of combustibles, flame spread, heat release rate and time to flashover all depend on that [Yuen et al. 2003; Yuen and Chow 2004; Li and Chow 2004]. Radiation will affect the fire temperature and pose direct threat to humans. Fire temperatures measured by burning different furniture as in Chapter 5 can be taken as a reference to study the heat transfer.

As the radiation flux radiated from an object is proportional to the fourth power of its temperature, radiation increases more rapidly with temperature than convection. The fraction of heat transfer from thermal radiation will increase with temperature rising. Radiation will dominate when a fire develops to a certain stage at higher temperature. For example, the radiative heat transfer from the flames to the fuel surfaces was found to exceed convective heat transfer when the characteristic fuel length is greater than 0.2 m by de Ris [1979]. Blocking of radiation heat by an agent such as

water mist is an important fire suppression mechanism [e.g. Ravigururajan and Beltran 1989]. However, in many fire studies, the modeling of radiative heat transfer is often treated in a simple way or even ignored. Significant errors in the predictions at the post-flashover stage might be resulted.

Combustion products in a fire depend on the fuel, ventilation and environment. Smoke is considered as a mixture of entrained air, unburnt fuel such as soot and combustion products such as carbon monoxide (CO), carbon dioxide (CO_2), water vapour (H_2O) and others. The absorptivity and emissivity of smoke are very important in predicting thermal radiation in a fire.

The Krichhoff's Law can be applied to study the emissivity ε_T and absorptivity α_T of a real object in the fire. Under steady temperature, the monochromatic emissivity from a certain direction is equal to the absorption from the same direction. When the incident radiation is independent of the incident angle (diffuse reflect) and has the same spectral proportions as a blackbody radiator (gray body), the Krichhoff's law can be revised as:

$$\varepsilon_T = \alpha_T \tag{6.1}$$

6.2 Radiation Properties of Gases and Soot

At the early stage of a room fire, there are two layers of hot smoke and cold air. The smoke layer is composed of soot, CO, CO_2, H_2O, and entrained air. Diatomic gas

molecules with symmetric structure (such as oxygen O_2 and nitrogen N_2) would have very little absorption and emission, considered as transparent. But gas molecules with diasymmetric structure such as CO_2 and H_2O have higher absorption and emission. In a smoke layer, CO_2, H_2O and soot would yield over 95% of radiant absorption and emission [Novozhilov 2001].

For a monochromatic beam of radiation with an initial intensity $I_{\lambda 0}$ passing through a smoke layer of thickness L_s and extinction coefficient k_s, the intensity of the radiation $I_{\lambda L_s}$ is [Tien et al. 2002; Hottel and Sarofim 1967; Edwards 1985; Modest 1993; Mbiock and Weber 2000]:

$$I_{\lambda L_s} = I_{\lambda 0} e^{(-k_s L_s)} \tag{6.2}$$

The absorptivity of the smoke layer to the monochromatic beam α_λ is:

$$\alpha_\lambda = \frac{I_{\lambda 0} - I_{\lambda L_s}}{I_{\lambda 0}} = 1 - e^{(-k_s L_s)} \tag{6.3}$$

For an arbitrary shaped smoke with volume V and area of the boundary surface A, the mean thickness of smoke layer L_s can be estimated by:

$$L_s = 3.6\frac{V}{A} \tag{6.4}$$

An emissivity chart for CO_2 and H_2O based on experimental data was formulated by Hottel and Sarofim [1967]. The total emissivity charts were summarized by Edwards [1985] for water vapour and carbon dioxide. The emissivity depends on the pressure, temperature and the mean beam length. These charts are only suitable for use at a standard atmospheric pressure, and have to be corrected at different pressures. For the mixtures of these two gases, an additional band overlap correction factor is needed. The equivalent gray gas emissivity ε_g for a mixture of CO_2 and H_2O is [Tien et al. 2002]:

$$\varepsilon_g = C_{CO_2}\varepsilon_{CO_2} + C_w\varepsilon_w - \Delta\varepsilon \tag{6.5}$$

In the above equation, C_{CO_2} and C_w are the pressure correction factors of carbon dioxide and water, respectively; ε_{CO_2} and ε_w are the emissivities of CO_2 and H_2O at 1 atm respectively; and $\Delta\varepsilon$ is the band overlap correction factor for the mixture. In most fire engineering applications, the pressure correction factor is taken as 1, and the band overlap correction is about half of the emissivity of CO_2. The total emissivity for a mixture of CO_2 and H_2O is:

$$\varepsilon_g = 0.5\varepsilon_{CO_2} + \varepsilon_w \tag{6.6}$$

Soot particles are produced from incomplete combustion. The soot particles inside the smoke and flame are at higher temperature, their radiation spectra are continuous, and depend on their temperature, size and shape. The emissivity equation for soot is similar to the absorption of monochromatic beam as follows:

$$\varepsilon_s = 1 - e^{(-\kappa L_s)} \tag{6.7}$$

Note that κ is the equivalent absorption coefficient for soot, which is proportional to the temperature T and fraction f_v of soot in the smoke, and can be expressed as:

$$\kappa = 3.72 \frac{C_0}{C_2} f_v T \tag{6.8}$$

C_0 is a constant ranging from 2 to 6 and might depend on the soot refraction index [Snegirev 2004]. C_2 is the Planck's second constant, taking a value of 1.44×10^{-2} mK. The total emissivity of a gas-soot mixture can be approximated by using the empirical correlation:

$$\varepsilon_T = 1 - e^{(-\kappa L_s)} + \varepsilon_g e^{(-\kappa L_s)} \tag{6.9}$$

In calculating the total emissivity, the emissivities of CO_2 and H_2O are obtained through charts. This is not convenient and so for many engineering applications, simplified methods [Fletcher et al. 1994] are used.

$$\alpha_T = \alpha_g + \alpha_s \tag{6.10}$$

The absorption coefficients for gas phase α_g may be approximated by the following correlation [Novozhilov 2001; Fletcher et al. 1994]

$$\alpha_g = 0.28e^{(-\frac{T}{1135})} \tag{6.11}$$

The soot absorption and emission is proportional to the soot volume fraction, f_v. If the scattering of radiation by soot particles is negligible, the absorption coefficient for soot may be obtained from the Planck mean absorption coefficient data [Tien et al. 2002; Fletcher et al. 1994]

$$\alpha_s = 1264 f_v T \tag{6.12}$$

Another expression for the absorption coefficient of soot produced by ethylene diffusion flame was proposed by Kent and Honnery [1990] as follows:

$$\alpha_s = 1862 f_v T \tag{6.13}$$

Putting in the Smith's model [Adiga et al. 1990], the overall absorption coefficient for the soot and gas mixture is:

$$\alpha_T = \alpha_g + \alpha_s - \alpha_s \alpha_g \tag{6.14}$$

6.3 Flashover

The importance of the phenomenon of flashover in a compartment fire is well known for many years [Drysdale 1999]. Physically, flashover is a term used to characterize

the rapid transition of a relatively small local fire to a large fire in which the whole compartment is involved. When flashover occurs, the fire "jumps" from the growth stage to the development stage, and would lead to great damages to the building structure and properties. Flashover has been consistently observed in disastrous fires [Rasbash 1991] leading to severe losses of human lives and properties.

Experimentally, studies on flashover were reported both in actual fires and in full-scale burning tests. There are now quantitative criteria consistently observed as conditions for the onset of flashover as:

- Upper gas layer temperature exceeds 600 ^{o}C;
- Heat flux at the floor exceeds 20 kWm^{-2};
- Flame coming out of openings.

A summary of the conditions for the onset of flashover reported by different studies is shown in Table 6.1 [Peacock et al. 1999; Hagglund et al. 1974; Parker and Lee 1974; Fang 1975; Lee and Breese 1978; Babrauskas 1979; Budnick and Klein 1979; Fang and Breese 1980; Thomas et al. 1980; McCaffrey and Quintiere 1981].

Numerical and theoretical studies of flashover have focused primarily on predicting the behaviour of the gas layer temperature in a compartment fire using various forms of the zone model [Emmons 1978; Quintiere 1989; Chow 1998,1999,2001]. The concept of thermal instability in a compartment fire was initiated by Thomas et al. [1980]. This concept led to further works [Bishop et al. 1993; Graham et al. 1995] in which the onset of flashover was "predicted" by computational techniques of

nonlinear dynamics [Thompson and Steward 1986; Liang et al. 2002]. In all of the existing numerical and theoretical studies, the gas layer temperature is the primary dependent variable and the gas temperature criterion (> 600 °C) is used as the quantitative criterion for flashover.

As shown in Table 5.1, both the gas temperature and heat flux criteria for the onset of flashover are recorded. Physically, the heat flux criterion is expected to be more critical since the secondary ignition of the combustibles in a compartment is a major factor leading to flashover. The heat flux to the floor (and more specifically, radiant heat flux) is the main source of energy leading to the secondary ignition. However, gas layer temperature exceeding 600 °C without a radiation source (such as the wall or soot particulates which can serve as a radiating medium) is insufficient to generate the necessary heat flux at floor required for flashover.

6.4 Thermal Radiation and Flashover

To generate a floor heat flux of 20 kWm^{-2} for a temperature difference of 600 °C based only on convection, for example, would require a heat transfer coefficient of about 33 $Wm^{-2}K^{-1}$ if the whole compartment is assumed to be one zone at the same temperature. In general, the lower gas layer is expected to be at a temperature lower than 600 °C. The actual heat transfer coefficient required for flashover is thus higher than 33 $Wm^{-2}K^{-1}$. This value exceeds the range of heat transfer coefficient generally expected in a compartment fire environment (natural convection and low speed force convection). Therefore, thermal radiation is the dominant mode of heat transfer

causing flashover.

The importance of the radiant feedback mechanism in the onset of flashover is recognized by almost every theoretical study of flashover [Emmons 1978; Quintiere 1989; Chow 1999; Bishop et al. 1993; Graham et al. 1995]. But due to the complexity of radiation and the uncertainty of the radiation model used in the analysis, all of the existing studies do not use the heat flux criterion as a factor in determining the condition of flashover. Over the past ten years, significant advances have achieved both in the understanding of the radiative properties of the various combustion species in a fire and the mathematical modeling of three-dimensional radiative transport in a participating medium [Siegel and Howell 2002]. These advances can be readily implemented in a zonal model to give an improved assessment of the onset of flashover.

Since smoke particulates are expected to be a major component contributing to the radiative emission and absorption of the hot gas/particulates layer in the room during a compartment fire. The relationship between the smoke particulates volume fraction, gas layer temperature with the radiative emission and absorption of the hot layer should be studied. Various parameters both from the perspective of the hot gas/particulates layer temperature and the radiant heat flux to the floor are important to the onset of flashover.

6.5 Summary

Convection is important at the early stage of a building fire. However, thermal radiation would be more significant when the fire develops to give a hotter smoke layer. It plays a very important role in real room fires by contributing significantly to flashover, igniting other combustibles and flame spread. Fire temperatures deduced from burning different furniture as in above can be taken as a reference to study the radiative heat transfer.

In this chapter, the thermal radiation properties of smoke were reviewed. The relations between thermal radiation and flashover were discussed. Modelling thermal radiation is important in simulating room fires to give more accurate results.

CHAPTER 7 A ZONE FIRE MODEL FOR FLASHOVER

7.1 Introduction

Once flashover occurs, the magnitude of threat of a fire to life and property increases significantly. The ability to predict flashover has attracted great attention in the fire research community. A fire model is a very useful tool in simulating the fire. Based on some existing theories, a zone model with radiation effect was developed to study flashover [Yuen et al. 2003].

A simplified two-layer zone fire model [Bishop et al. 1993] was used as the basis of the present study. While this model can give only an overall picture with no fine details, it contains all the relevant physics and is sufficient for the present purpose, which is to illustrate the importance of using an accurate radiation model in assessing flashover.

A simple compartment with length L_R, width W_R and height H_R is considered as shown in Figure 7.1. The height of the vent H_V is taken as the same as the height of the room H_R. In addition, the fire base is assumed to be a rectangle with width W_f and length L_f situated at the floor of the room. The thermal balance equations are used in studying flashover in room fires [Bishop et al. 1993].

7.2 Key Equations

Following the previous mathematical development [Bishop et al. 1993], the temperature T of the hot gas/particulates layer with thermal capacity c_p and mass flow rate $\dot{m}$ is governed by

$$\frac{dT}{dt} = \frac{\dot{G} - \dot{L} - \dot{H}}{c_p \dot{m}} \tag{7.1}$$

where $\dot{G}$ is the energy gain rate of the hot layer and $\dot{L}$ is the rate of energy loss from the hot layer; $\dot{H}$ is the enthalpy increase of the hot layer. $\dot{G}$ depends on whether the ratio of the mass air flow rate to the fuel volatilization rate is greater than (fuel controlled fire) or less than (ventilation controlled fire) the stoichiometric ratio. Assuming that all energy of combustion goes into the hot layer, $\dot{G}$ is given by

$$\dot{G} = \begin{cases} \chi \dot{m}_f \Delta h_c & \left(\frac{\dot{m}_a}{\dot{m}_f} \geq r \right) \\ \frac{\chi \dot{m}_a \Delta h_c}{r} & \left(\frac{\dot{m}_a}{\dot{m}_f} < r \right) \end{cases} \tag{7.2}$$

where χ is the combustion efficiency, $\dot{m}_a$ is the mass flow rate of air into the compartment, $\dot{m}_f$ is the rate of volitalisation, Δh_c is the net heat of combustion and r is the stoichiometric ratio.

The volitalisation rate $\dot{m}_f$ of fuel depends on the heat transfer from the fire and the compartment surrounding the fire base. It is given by

$$\dot{m}_f = \frac{\left(\dot{q}''_{ff} + \dot{q}''_{f,surr}\right)}{\Delta h_g} \tag{7.3}$$

where $\dot{q}''_{ff}$ is the heat flux from the fire to the fire base, $\dot{q}''_{f,surr}$ is the heat flux from the surrounding (hot layer and walls) to the fire base, Δh_g is the heat of gasification and A_f is the area of the fuel surface given by

$$A_f = \pi R^2 \tag{7.4}$$

The heat loss from the fuel surface (due to convection and radiation) is assumed to be negligible compared to the large incoming heat flux from the flame and the surrounding hot layer.

Following Emmons [Emmons 1978], the fire is assumed to have the form of a cone and the heat flux from the flame to the base is given by

$$\dot{q}''_{ff} = \dot{q}''\left(1 - e^{-bR}\right) \tag{7.5}$$

where $\dot{q}''$ is the total potential heat flux generated by the free burning fire and b is an exponential coefficient. The formulation of $\dot{q}''_{f,surr}$ depends on the radiation model, it will be discussed in the next section.

The mass flow rate of air into the compartment is assumed to be driven by buoyancy flow [Rockett 1976] and is given by

$$\dot{m}_a = \frac{2}{3} C_D \rho_0 W_v H_v^{1.5} \sqrt{2g\left(1-\frac{T_a}{T}\right)(N-D)}\left(N+\frac{D}{2}\right) \tag{7.6}$$

with D being the fractional height of the discontinuity plane given by

$$D = \frac{Z_d}{H_v} \tag{7.7}$$

where Z_d is the discontinuity height. N is the fractional height of the neutral plane, it is taken empirically to be

$$N = D + 0.5(1-D)^2 \tag{7.8}$$

The rate of energy loss from the hot layer is given by

$$\dot{L} = \dot{H}_o + \dot{q}_w \tag{7.9}$$

where $\dot{H}_o$ is the enthalpy flow rate out of the vent given by

$$\dot{H}_o = \dot{m}_e c_p (T - T_a) \tag{7.10}$$

with $\dot{m}_e$ being the mass flow rate out of the vent. Assuming that there is no accumulation of mass in the compartment, $\dot{m}_e$ is related to $\dot{m}_a$ and $\dot{m}_f$ by

$$\dot{m}_e = \dot{m}_a + \dot{m}_f \tag{7.11}$$

$\dot{q}_w$ is the heat loss rate from the hot smoke layer to the wall. Its expression depends on the convective heat loss $\dot{q}_{w,c}$ and radiation heat loss $\dot{q}_{w,r}$ as expressed as:

$$\dot{q}_w = \dot{q}_{w,c} + \dot{q}_{w,r} \tag{7.12}$$

where convective heat loss is given by:

$$\dot{q}_{w,c} = A_w h_c \left(T - T_w\right) \tag{7.13}$$

where h_c is a convective heat transfer coefficient; T_w and A_w are temperature and surface area respectively of the surrounding wall.

The relevant radiation models will be discussed in the next section. A consequence of equation (7.11) is that there is no net enthalpy increase ($\dot{H} = 0$) within the compartment. The mass of the hot gas/particulates layer is given by

$$m_s = \rho_a L_R W_R \left(H_R - Z_d\right) \tag{7.14}$$

In equation (7.14), the density of the hot gas/particulates layer is assumed to be constant at ρ_a. While this assumption is in general not accurate as the gas layer temperature rises and the soot concentration increases, it is retained in the present work so that the current result can be compared with previous works [Emmons 1978; Quintiere 1989; Chow 1999; Bishop et al. 1993; Graham et al. 1995] which used this assumption. From the perspective of illustrating the effect of radiation on flashover, this assumption is not expected to have a significant quantitative impact.

Finally, the differential equation for the rate of change of the fire radius is given by

$$\frac{dR}{dt} = V_f \left[1 - e^{\left(\frac{R - R_{\max}}{R_{edge}} \right)} \right] \tag{7.15}$$

where R_{edge} is the distance over which the effect of the edge of the fuel is felt and R_{max} is the maximum radius, representing the size of the fuel sample. V_f is the flame spread rate which can be taken as [Takeda 1987]

$$V_f = \frac{K_f \dot{m}_a}{\rho_0 W_v N H_v} \tag{7.16}$$

with K_f being a flame spread constant.

Note that Z_d is taken as a constant. Previous experience on zone modeling simulation indicated that the smoke layer interface height depends only on the opening height

for a steady burning fire. The objective of this study is to illustrate the importance of thermal radiation and so such a simplified approach was used.

7.3 Radiation Model

For those flashover works reported in the literature [Emmons 1978; Quintiere 1989; Chow 1999; Bishop et al. 1993; Graham et al. 1995], $\dot{q}''_{f,surr}$ and $\dot{q}_w$ are derived by assuming emissivity ε for the gas or particulates layer is constant. For example, the following expressions were used in the model by Bishop et al. [1993]:

$$\dot{q}''_{f,surr} = \sigma\left[\varepsilon T^4 + (1-\varepsilon)\, T_w^4 - T_a^4\right] \tag{7.17}$$

$$\dot{q}_{w,r} = A_w \varepsilon\sigma\left(T^4 - T_w^4\right) \tag{7.18}$$

To complete the mathematical description of the model, the wall temperature is assumed to be between the layer temperature T and the ambient temperature T_a given by

$$T_w = U_c\left(T - T_a\right) + T_a \tag{7.19}$$

with U_c being an adjustable parameter between 0 and 1.

A fundamental difficulty of this radiation model is that it provides no physical correlation between the layer emissivity ε and measurable parameters such as particulates volume fraction and temperature of the hot layer which are known to have an effect on hot layer emissivity. The model also does not account for the effect of the compartment geometry (dimensions, size of vent and radius of fire base) on the radiation transport.

In the current new model, particulates in the hot layer are assumed to be the primary species for radiative emission and absorption. While the gaseous species (e.g. CO_2 and H_2O) are known to contribute to the flame radiative emission, their contribution is generally small. For example, a standard furnace 4m high and 2m in diameter consisting of a stoichiometric mixture of CO_2 and H_2O (generated from the combustion of methane) at one atmosphere only has an emittance of 0.11 [Siegel and Howell 2002]. Indeed, the presence of soot particulates and luminous radiation from the hot layer are known to be important factors in the occurrence of flashover. The effect of gaseous radiation on flashover is thus secondary compared to that of radiation from the soot particulates.

Assuming that the size of the particulates is small so that the Rayleigh's limit of particle absorption is valid, the absorption coefficient of the hot gas/particulates layer can be written as [Siegel and Howell 2002]

$$a_\lambda = \frac{36\pi f_v}{\lambda} \frac{n\kappa}{\left(n^2-\kappa^2+2\right)^2+4n^2\kappa^2} \tag{7.20}$$

where n and κ are optical constants for soot which are known functions of λ. The emittance of a soot cloud of thickness L_S is

$$\varepsilon(T, L_s) = \frac{1}{\sigma T^4} \int_0^\infty I_{\lambda b}(T) \left(1 - e^{-aL_s}\right) d\lambda \tag{7.21}$$

Equations (7.21) and (7.20) have been evaluated for soot generated by some common fuel (acetylene and propane) and numerically, it was shown [Yuen and Tien 1976] that the emittance can be approximated by an equivalent gray model as

$$\varepsilon(T, L_s) = 1 - e^{(-\kappa L_s)} \tag{7.22}$$

with κ being an equivalent absorption coefficient which is determined to be

$$\kappa = \frac{3.6 C_0 f_v T}{C_2} \tag{7.23}$$

where f_v is the particulates volume fraction, C_0 is a constant depending on the fuel and C_2 is the second radiation constant.

In the present work, a gray soot model with an absorption coefficient given by equation (7.23) will be utilized. The radiative emission from the gaseous combustion products will be ignored. Analysis with a more detailed non-gray soot model and the inclusion of radiation from gaseous species will be considered in future works.

Since the size of the fire grows with a growth rate given by equation (7.14), the volume fraction of the hot gas/particulates layer is assumed to be proportional to the fire radius R. Specifically, the current model assumes

$$f_v = \frac{R}{R_{\max}} f_{v,0} \tag{7.24}$$

with $f_{v,0}$ being a characteristic volume fraction which is a function of the fuel.

Assuming that the fuel surface can be treated as a square of length L_f given by

$$L_f = \sqrt{\pi} R \tag{7.25}$$

Exact expressions for the exchange factor between the fire base, the hot gas/particulates layer and the surrounding wall can be readily obtained using the tabulated data and superposition procedure as outlined in Yuen and Takara [Yuen and Takara 1997]. The definition of exchange factor and its mathematical properties are described in ref. [Yuen and Tien 1976]. For a cubic enclosure with $W_R = L_R = H_R = 40$ cm, $Z_d = 0$ (i.e. the hot layer fills the whole compartment) and a fire base with $L_f = 30$ cm, for example, the exchange factor between the fire base and the hot layer ($s_f g$), the exchange factor between the fire base and the top wall ($s_f s_t$) and the exchange factor between the hot layer and the top wall ($g s_t$) are shown in Figure 7.2. It is important to note that these factors depend strongly on the absorption coefficient. The radiation transport thus depends strongly on the hot layer temperature and the particulates volume fraction.

Based on the concept of exchange factor, the expression for $\dot{q}''_{f,surr}$ can be written as

$$A_f \dot{q}''_{f,surr} = \sigma T^4 \cdot gs_f(\kappa) + \sigma T_a^4 \cdot s_v s_f(\kappa_a) + \sigma T_w^4 \left[s_t s_f(\kappa_w) + s_l s_f(\kappa_w) + s_r s_f(\kappa_w) + s_i s_f(\kappa_w) + s_{o-v} s_f(\kappa_w) \right] \tag{7.26}$$

$gs_f(\kappa)$ is the exchange factor between the hot layer and the fire base. $s_x s_f(x = t,l,r,i,o-v,v)$ stands for the exchange factor between the top wall (t), left wall (l), right wall (r), inner wall (i), outer wall (o), the vent opening (v) and the fire base respectively. The subscript o-v stands for the outer wall section minus the vent opening. The subscript in the absorption coefficient κ indicates the temperature (wall, vent or hot layer temperature) at which it is evaluated. In a similar manner, the expression for radiation heat loss rate $\dot{q}_{w,r}$ is given by

$$\dot{q}_{w,r} = \sigma T^4 \left[gs_t(\kappa) + gs_b(\kappa) + gs_l(\kappa) + gs_r(\kappa) + gs_i(\kappa) + gs_o(\kappa) \right] - \sigma T_a^4 \cdot gs_v(\kappa_a) - \sigma T_w^4 \left[gs_t(\kappa_w) + gs_{b-f}(\kappa_w) + gs_l(\kappa_w) + gs_r(\kappa_w) + gs_i(\kappa_w) + gs_{o-v}(\kappa_w) \right] \tag{7.27}$$

where the subscript b stands for the bottom floor. Equations (7.1) to (7.15), together with equations (7.20) to (7.27) constitute a complete mathematical description of the present transient compartment fire model. In addition to predicting the transient behaviour of the hot layer temperature, the radiative heat flux to the compartment floor can be readily evaluated by

$$(L_R W_R) \cdot \dot{q}''_b = \sigma T^4 \cdot gs_b(\kappa) + \sigma T_a^4 \cdot s_v s_b(\kappa_a) + \sigma T_w^4 \left[s_t s_b(\kappa_w) + s_l s_b(\kappa_w) + s_r s_b(\kappa_w) + s_i s_b(\kappa_w) + s_{o-v} s_b(\kappa_w) \right] \tag{7.28}$$

Equation (7.28) can be used as a basis of evaluation for the heat flux criterion of flashover.

The radiation exchange factors can be computed based on the methods by Yuen and Takara [Yuen and Takara 1997]. Equations (7.1) to (7.18), together with the evaluation of the radiation exchange factors, represent a complete mathematical representation of the model.

In summary, a set of governing equations, together with the necessary numerical value for the radiative exchange factor [Yuen and Takara 1997], are now developed for the analysis of flashover in an enclosure. The effect and importance of the radiation effect can be illustrated clearly with comparison between this model and those presented in literature [Bishop et al. 1993].

Once a model has been developed, it must be rigorously tested to assure the model yields acceptable results. The model had been compiled in FORTRAN and many numerical calculations were successfully made.

7.4 Results and Discussion

Numerical data are generated to examine the effect of vent opening W_v, particulates volume fraction $f_{v,0}$ and the wall temperature parameter U_c on the transient temperature rise of the hot gas/particulates layer and the radiative heat flux to the compartment floor. These parameters are selected because they are expected

physically to be important parameters affecting the occurrence of flashover. The effect of other parameters will be investigated in future works. For the value of other parameters, the present work follows the approach of Bishop et al. [1993]. They are chosen to describe a typical fire burning on a circular PMMA slab developed on a scaled (i.e. 40 cm inside cube) compartment. For a direct comparison, numerical data are also generated with the Radiation Approach by Bishop et al. with a layer emissivity of $\varepsilon = 0.41$ (value used in reference [Bishop et. al 1993]).

For the case with $U_c = 0$ ($T_w = T_a$, the "cold wall" case), the layer temperature for different vent openings are shown in Figure 7.3. The corresponding heat flux to the compartment floor are shown in Figure 7.4. The layer temperature illustrates an interesting relation between radiation and vent openings. When the vent opening is small (for example, $W_v = 5$ cm) and the fire is ventilation controlled, the primary effect of radiation appears to be the heat loss to the surrounding wall. The case with the smaller particulates volume fraction (hence less radiation heat loss) has the higher layer temperature. An increase in the particulates volume fraction increases the radiative heat loss (to the surrounding) and thus lowers the layer temperature. When the vent opening is large ($W_v > 10$ cm) and the fire is fuel controlled, the effect of radiative feedback to the fuel surface appears to be more important. The layer temperature increases with increasing particulates volume fraction. The increased radiative feedback to the fuel surface increases the burning rate and therefore the layer temperature.

Note that results of the Radiation Approach by Bishop et al. (which does not depend on particulates volume fraction) agrees with the optically thick (high particulates

volume fraction) case for the ventilation controlled fire (W_v = 5 cm) and it agrees with the optically thin (low particulates volume fraction) case for the fuel controlled fire. This result demonstrates the physical difficulty of the Radiation Approach by Bishop et al.. By assuming a constant emissivity for the hot gas layer and the wall in an ad-hoc fashion, the model cannot yield a consistent interpretation of the physics, even in a limiting sense.

From the flashover perspective, results in Figure 7.3 and the temperature criterion would suggest that flashover occurs in the ventilation controlled case with low particulates volume fraction ($f_{v,0} \leq 10^{-6}$ for W_v = 5 cm, $f_{v,0} \leq 10^{-5}$ for W_v = 10 cm). The temperature criterion is also satisfied for the high volume fraction case ($f_{v,0} \geq 10^{-5}$) with W_v = 20 cm. The temperature criterion is never satisfied for all particulates volume fraction for the fuel controlled fire (W_v = 30 cm). The conclusion about flashover, however, is quite different if the heat flux criterion and results in Figure 7.4 are utilized. Specifically, heat flux criterion is not satisfied for all particulates volume fraction for the fully ventilation controlled fire (W_v = 5 cm) and the fully fuel controlled fire (W_v = 30 cm). For the W_v = 5 cm case, the high layer temperature is attained when the particulates volume fraction is small. There is insufficient emission and therefore the radiative heat flux to the compartment floor remains low. For the W_v = 30 cm case, the temperature of the hot layer might be not high enough to generate the necessary radiative heat flux. Results in (b) to (d) of Figure 7.4 suggest that flashover occurs in cases with high particulates volume fraction ($f_{v,0}$ = 10^{-3}, 10^{-4}, 10^{-5}) for fires which are neither totally ventilation controlled nor totally fuel controlled (W_v = 10, 20, 30 cm). Note that in the W_v = 30 cm case, the heat flux criterion is satisfied even though the hot layer temperature is

only about 500 °C. It is important to note that the association of flashover with high particulates volume fraction is consistent with the observation that the presence of smoke and luminous flame is a necessary condition for flashover. Results in Figures 7.4 and 7.5 demonstrate readily that the temperature criterion alone might not be an adequate condition for the identification of flashover. An accurate model for thermal radiation heat transfer and a correct assessment of the radiative heat flux to the compartment floor are necessary for an effective assessment of flashover.

Temperature results with $U_c = 1$ ($T_w = T$, the "hot wall" case), are shown in Figure 7.5 and the corresponding heat flux to the compartment floor are shown in Figure 7.6. The slight oscillation in the numerical result is due to the explicit numerical scheme used in the present calculation. It has no negative impact on the accuracy of the result.

The transient temperature behaviour for different W_v are quite similar. Since there is no heat loss from the hot layer to the wall, the primary heat loss from the hot layer is that from the mass flow out of the vent. For ventilation controlled fire ($W_v = 5$ cm), the radiative feedback to the fuel surface is not a controlling factor on the combustion rate, the steady state temperature is independent of the radiative properties of the layer and is thus insensitive to the particulates volume fraction. For fuel controlled fires ($W_v = 20, 40$ cm), the radiative feedback effect has a more important effect on combustion and the particulates volume fraction has a stronger effect on the layer temperature. The radiative heat flux to the compartment floor also shows similar behaviour for different vent opening and particulates volume fraction. In general, the radiation of the wall dominates the heat transfer and has a major

effect on the final steady state hot layer temperature and heat flux to the compartment floor. Because of the large radiative heat flux from the wall, the two flashover criteria are readily satisfied in all cases. It is observed that all the predicted flashovers are quite "catastrophic" as there is a nearly vertical jump both in the temperature and in the radiative flux to the compartment floor. Physically, this suggests that a fire in a highly insulated compartment will likely lead to a flashover. This is consistent with physical expectation.

7.5 Summary

Radiative heat transfer is demonstrated to be a dominant factor in onsetting flashover. A zone model without accurate model of radiation would not give good results.

Using a non-gray particulate radiation model and the zonal method, a zone model is developed to determine the conditions leading to flashover. Soot produced in fire should be considered to improve the radiation heat transfer model. Numerical studies on the effect of vent opening, particulate volume fraction and the external heat transfer coefficient on the transient temperature rise and flashover were carried out. Both the external heat transfer coefficient and the particulate volume fraction are shown to be parameters which can lead to thermal instability and, subsequently onsetting flashover. The size of the vent opening also has a significant effect on the hot layer temperature and wall temperature during a fire. An accurate radiation model is important to the accurate assessment of these effects. The present model

can be used as a basis for a more detailed non-linear analysis to identify the different types of instabilities and their relation to the transition to flashover.

CHAPTER 8 SUPERPOSITION ON THE HEAT RELEASE RATES

8.1 Introduction

The heat release rate generated by burning combustibles in a room fire has to be understood in hazard assessment. Different combustibles, including both movable and fixed fuel load [Chow and Cheung 1996], are stored in buildings. The rate of heat release in burning these materials together should be estimated. In most projects, only the heat release rates of individual materials or single items are available. How the curves can be combined to estimate the resultant heat release rate curve [Babrauskas and Grayson 1992; Göransson 1993] should be understood.

The principle of superposition [Mowrer and Williamson 1990; Chow and Au Yeung 2003; Chow 2002] was proposed to add up the heat release rate curves of every combustible item to give the total heat release rate of the arrangement. This concept will be explored in this chapter. How the resultant heat release rate of two different polymeric materials can be combined was studied firstly. Polymethylmethacrylate (PMMA), unplasticized polyvinyl chloride (PVC), polycarbonate (PC) and oak wood widely used in the market as consumer products and construction materials are taken as examples. The samples were exposed to the same conditions in a cone calorimeter for measuring the heat release rates under heat fluxes of 50 kWm^{-2} and 70 kWm^{-2}. The samples were tested individually by themselves first, then burnt with another

sample together for comparing with the calculated heat release rate using equation (8.1). Full-scale burning tests on foam cushions with fabric covering were also explored. Many cushions with the same size were tested with different arrangements.

8.2 Testing Arrangements

8.2.1 Examples from bench-scale burning tests

Experimental measurements on one or two sample cubes of PMMA, PVC, PC and wood were conducted in a cone calorimeter. Samples were cut into small cubes of size 20 mm. The samples were placed at the side of the cone tray as shown in Figure 8.1. The radiative heat flux of the cone was set at 70 kWm^{-2} or 50 kWm^{-2}. In following the procedures in the standard tests [ASTM E 1354 – 04a], samples were placed at 25 mm below the cone. In this study, some samples were also tested by moving down to 50 mm below the cone [Vanspeybroeck et al. 1993]. This will give different ventilation conditions as in real fire scenarios. Different heat release rate curves can then be achieved.

The testing arrangements as shown in Table 8.1 are summarized in the following:

Test C8A: Two sample cubes at two sides of the tray with arrangements:

- C8A1: PMMA and PC at 70 kWm^{-2}, 25 mm under the cone
- C8A2: PMMA and PVC at 70 kWm^{-2}, 25 mm under the cone
- C8A3: PMMA and PVC at 70 kWm^{-2}, 50 mm under the cone

- C8A4: PMMA and PVC at 50 kWm^{-2}, 50 mm under the cone
- C8A5: PMMA and wood at 50 kWm^{-2}, 50 mm under the cone

Test C8B: PMMA cube only at one side of the tray with arrangements:

- C8B1: PMMA at 70 kWm^{-2}, 25 mm under the cone
- C8B2: PMMA at 70 kWm^{-2}, 50 mm under the cone
- C8B3: PMMA at 50 kWm^{-2}, 50 mm under the cone

Test C8C : PC cube only at one side of the tray with only one test:

- C8C1: PC at 70 kWm^{-2}, 25 mm under the cone

Test C8D : PVC cube only at one side of the tray with arrangements:

- C8D1: PVC at 70 kWm^{-2}, 25 mm under the cone
- C8D2: PVC at 70 kWm^{-2}, 50 mm under the cone
- C8D3: PVC at 50 kWm^{-2}, 50 mm under the cone

Test C8E : Wood cube only at one side of the tray with only one test:

- C8E1: Wood at 50 kWm^{-2}, 50 mm under the cone

Each testing arrangement was tested several times to check the repeatability [ISO3534 1993]. Only one typical set of results was used to study the superposition. Results on the heat release rate per unit area $\dot{q}_A$ measured in the cone and the total heat released per unit area Q_A for each test are shown in Figures 8.2 to 8.6.

In a real fire, combustibles placed together are exposed to different radiative heat fluxes. Therefore, different external radiative heat fluxes and separation distances among them should be assessed. For the two samples tested in this study, there was a constant heat flux emitted from the cone $\dot{q}''_{fC}$, a heat flux from the adjacent burning sample $\dot{q}''_{fa}$ and a heat flux fedback from the flames $\dot{q}''_{ff}$ acting on the burning surface of the sample as shown in Figure 8.1c. The distances between the two samples might become shorter than 6 cm (even 2 cm for PVC) due to melting and swelling upon burning. There might be stronger interaction between the two combustibles due to the shorter distance. Although $\dot{q}''_{fa}$ might be higher than $\dot{q}''_{fC}$, both heat fluxes are likely to be less than $\dot{q}''_{ff}$. Unless at very high values, external heat fluxes such as $\dot{q}''_{fC}$ would only be important in ignition. Effects of these couplings should be further studied quantitatively but not included in this study.

PVC samples were difficult to ignite under lower heat fluxes. Therefore, higher heat fluxes of 50 kWm^{-2} and 70 kWm^{-2} were used. As observed in the tests, PVC sample melted quickly and gasified into fuel vapour. Large quantity of smoke with irritating smell was liberated upon exposure to the heat fluxes. Among the four samples tested, PVC was the most difficult to burn with the longest ignition time. Further, PVC cubes did not burn steadily with charring. Taking test C8A4 as an example, the heat release rate oscillated with several peaks.

There was smouldering at first in burning the wood samples. Char was formed later at the burning stage. PMMA was ignited easily and burnt completely with a steady rate. PC sample was also difficult to burn. However, once ignited, it burnt vigorously

with smoke liberated. Except PMMA, some residues were left in burning other samples.

Rate of heat transfer inside the sample from the external heat flux depends on the effective exposure area and the distance away from the conical heater. The heat flux might be reduced by 5 to 15 kWm^{-2} when the distance of sample from the heater was moved from 25 mm to 50 mm when set at 50 and 70 kWm^{-2}. There were differences in the exposure areas for the different samples upon burning. The melted PVC is an obvious example. Results of heat release rate per unit area deduced from the cone would be affected. The exposing areas for all sample cubes were taken to be the same upper surface area of 4 cm^2. The accuracy of the heat release rate would be affected by the above factors. However, those effects should be the same to all samples, giving very little deviations in judging the superposition principle.

8.2.2 Examples from full-scale burning tests

All the specimens of foam cushion with fabric covering were made into the same size of 60 cm × 60 cm × 5 cm. One or several cushions combined were tested with different arrangements as shown in Figure 3.4. All these tests were ignited with 0.5 litre of gasoline in a round pan beside the samples. Net heat release rate and net total heat released were used in comparing the superposition results by subtracting the heat release rate and total heat released from the ignition source. The ignition times were adjusted slightly to give an obvious comparison on peak heat release rates.

The details of the different arrangements are summarized in the following:

- C^1, C^2, C^3, C^4, C^5, C^5 and C^6 are used to label the net heat release rates and net total heat released by burning 1,2...6 cushions respectively. C^{1h} and C^{1v} are the net heat release rates of one cushion tested with horizontal position and vertical position respectively.

- $C^4 + C^2$, $C^3 + C^2 + C^{1h}$, $2\ C^3$, $2(C^2 + C^{1h})$, and $2(C^{1v} + 2C^{1h})$ are the superposition results with burning 6 cushions under different testing arrangements. These results will be used to compare with C^6.

- $C^2 + C^{1h}$ and $C^{1v} + 2\ C^{1h}$ are superposition results with burning 3 cushions under different testing arrangements. These results can be used to compare with C^3. Two times of their values are same to those for $2(C^2 + C^{1h})$, $2(C^{1v} + 2C^{1h})$ and $2\ C^3$ respectively.

8.3 Superposition of Heat Release Rate Curves

Whether the individual heat release rate curves of two different materials can be added together (i.e. superposition) to give the resultant heat release rate while burning both of them will be assessed by the measured results [e.g. Peacock et al. 1994; Mowrer and Williamson 1990; Chow and Au Yeung 2003; Chow 2002; ISO 9705: 1993; Smith and Shaw 1999].

The combined heat release rate $\dot{q}$ (in kW) [Chow and Au Yeung 2003; Chow 2002] for burning two samples A and B with heat release rates $\dot{q}_a$ (in kW) and $\dot{q}_b$ (in kW) is suggested to be [e.g. Mowrer and Williamson 1990]:

$$\dot{q} = \dot{q}_a + \dot{q}_b \tag{8.1}$$

Equation (8.1) can be used for full-scale testing results. For the bench-scale testing results of the heat release rate per unit area curves $\dot{q}_{A,a}$ (in kWm^{-2}) and $\dot{q}_{A,b}$ (in kWm^{-2}) of two samples A and B, the transient heat release rate per unit area estimated $\dot{q}_A$ (in kWm^{-2}) is:

$$\dot{q}_A = \frac{1}{2}\left(\dot{q}_{A,a} + \dot{q}_{A,b}\right) \tag{8.2}$$

Experimental results of $\dot{q}_{A,a}$ and $\dot{q}_{A,b}$ for burning two different samples A and B respectively and the combined results of $\dot{q}_A$ from equation (8.2) are compared in Figures 8.2 to 8.6.

Full-scale testing results on burning 6 cushions together C^6 and the superposition results with 6 cushions combined $C^4 + C^2$, $C^3 + C^2 + C^{1h}$, $2\ C^3$, $2(C^2 + C^{1h})$, and $2(C^{1v} + 2C^{1h})$ are shown in Figure 8.7.

Adding the heat release rate curves of two combustibles by superposition is useful in predicting real fire scenarios when the combustibles are not placed too close to each other. The results can at least be taken as a minimum estimation.

There might be some other effects which are more obvious for bigger fires. A correction factor might be required in using superposition. Assuming these effects can be neglected under a specified standard external heat flux higher than normal heat fluxes, the net heat release rate for one sample by burning it only will be the same as that burning together with other combustible under the same conditions. Therefore, the upper limits of predicted results can be determined by applying the results tested under the same standard external heat fluxes. Testing result of each sample exposed to the same conditions can be added, though more tests should be carried out to confirm this.

Another method is to calculate the increase in heat flux by the adjacent burning item. The geometries of the two combustibles and the relevant flames, the variable heat flux and other potential factors should be considered. These aspects will be further reported separately later.

8.4 Functional Analysis

Instead of comparing the estimated results from superposition with the experiments in qualitative terms such as 'good', 'satisfactory' or 'bad', functional analysis proposed for evaluating fire models by Peacock et al. [1999] is used. Fire model predictions had been compared with test data by Friday and Mowrer [2001] with such approach.

As both experimental and predicted data can be described by transient curves, functional analysis would quantify the difference between two curves in terms of magnitude and shape. The data points within each curve are described by vectors, summing them up would give a resultant single vector for each curve. The distance between the resultant vectors for the predicted and measured curves is an error. This error can be normalized to provide a relative difference, or norm, between the curves. The following parameters will be calculated:

- The parameter *norm* is a measure of the relative difference in magnitude of the two curves.
- The parameter *inner product or cosine* describes the angular difference between the resultant vectors to provide a quantitative measure on the similarity of the curve shape.

For better agreement between the experimental and predicted curves, the value of norm is expected to be closer to zero, and the value of cosine is expected to be closer to one.

Following the recommendation by Peacock et al. [1999], the Euclidean norm with n data is calculated by the i^{th} experimental data e_i $(i = 1, \cdots, n)$ and prediction value of the model p_i at the i^{th} time increment t_i with s data points to be considered at each increment inside as:

$$\frac{|e-p|}{|e|} = \frac{\sqrt{\sum_{i=1}^{n}(e_i - p_i)^2}}{\sqrt{\sum_{i=1}^{n}(e_i)^2}} \tag{8.3}$$

The secant inner product cosine is:

$$\frac{\langle e,p\rangle}{|e|\cdot|p|}=\frac{\sum_{i=s+1}^{n}\left[\frac{(e_i-e_{i-s})\cdot(p_i-p_{i-s})}{s^2(t_i-t_{i-1})}\right]}{\sqrt{\sum_{i=s+1}^{n}\left[\frac{(e_i-e_{i-s})^2}{s^2(t_i-t_{i-1})}\right]\cdot\sum_{i=s+1}^{n}\left[\frac{(p_i-p_{i-s})^2}{s^2(t_i-t_{i-1})}\right]}} \tag{8.4}$$

The parameter s (≥ 1) would smoothen the results to give better estimates of large-scale differences. Higher values of s might not overcome the effects of small-scale noise between dense data, depending on the shapes of the curves. Values of s will be varied as 1, 2, 3, 4 and 5 in this study to investigate its effect on the secant inner product cosine.

8.5 Functional Analysis on the Superposition Results

8.5.1 Superposition of curves under the same heat fluxes in bench-scale tests

Norms and inner product cosines were calculated for the curves of $\dot{q}_A$ and THR for each case under the same radiative heat fluxes. The values were computed over the burning duration period of 400 s and 600 s for radiative heat fluxes of 70 kWm^{-2} and 50 kWm^{-2} respectively.

Functional analysis results of the point-to-point comparison are presented in Table 8.1. It is observed that the values of norm are lower than 0.23, indicating very good

predictions on curve magnitude. The shapes of the curves are in fact very close as shown in the figures.

For s equal to 1, the computed values of cosine at higher heat fluxes are higher than 0.72. However, the values of cosine for $\dot{q}_A$ are 0.16 for test C8A4 and 0.60 (with wood at 50 kWm^{-2}) for test C8A5. A possible reason might be that wood and PVC samples were not burnt steadily under the lower heat flux of 50 kWm^{-2}.

Values of cosine would be higher for higher values of s. For example, the values of cosine for tests C8A4 and C8A5 would be changed to 0.25 and 0.80 respectively by taking s as 5.

Results on comparing the curves with functional analysis suggested that superposition is better for tests under higher heat fluxes.

8.5.2 Superposition of curves under different heat fluxes in bench-scale tests

For real fire scenarios, the heat release rate of burning a combustible will be affected by the total heat feedback, and the total external heat fluxes which might be varied with the distance and exposure area. Result of one sample tested in other conditions can be taken as a reference curve which might be varied under the same initial conditions. Deviation of the calculated results by superposition can be estimated by functional analysis.

If the curves under different heat fluxes are added together, say C8B3 (under 50 kWm^{-2}) with C8C1 (under 70 kWm^{-2}) instead of C8B1 with C8C1, both the norm and cosine compared with test C8A1 deviated from the matching value of 0 and 1.0. The values of norm and cosine are 0.46 and 0.56 respectively for C8B3 with C8C1 when s is 1. The value of cosine only increased to 0.66 when s is 5.

For curves under the same heat but at different distances below the cone, say combining C8B2 of 70 kWm^{-2} for 50 mm and C8C1 for 25 mm, the values of norm and cosine are 0.21 and 0.83 respectively. The value of cosine increased up to 0.93 when s is 5. Therefore, combining the curves measured under the same heat but at different distances below the cone would not give results deviated so much from the experiment.

8.5.3 Superposition of curves from full-scale burning tests

Norms and inner product cosines were calculated for the curves of heat release rate and total heat released for different arrangements. The values were computed over the burning duration period of 600 s.

Functional analysis results of the point-to-point comparison are shown in Table 8.2. It is observed that the values of norm are lower than 0.33 for the results of $C^4 + C^2$, $C^3 + C^2 + C^{1h}$, $2\ C^3$, indicating good predictions on curve magnitude. While $2(C^{1v} + 2C^{1h})$ got a worst value of 0.57. Except $2(C^{1v} + 2C^{1h})$ and $C^{1v} + 2C^{1h}$ have cosine values of 0.53 and 0.61 respectively, most superposition results got higher values of cosine. The shapes of the curves are very close as shown in Figure 8.7.

The above analyses for the bench-scale burning tests were further demonstrated by the full-scale testing results. Burning conditions have important influence on the superposition results.

8.6 Summary

From the above study, the heat release rate of burning two material samples together can be estimated by superposition principle. The ignition time, burning time and peak heat release rate are key points to be considered for superposition.

Functional analysis suggested that the predicted curves agreed better with the measured curves for the tests under higher heat fluxes or other similar burning conditions. Results of superposition would be better when different combustibles are exposed to higher external heat fluxes such as a flashover fire with relatively less interaction, or when they are placed not so closely together with relatively independent burning.

The heat release rate deduced from a simple superposition might be underestimated for real fires when the combustibles are placed close to each other, and with lower external heat fluxes from the ceiling, walls and smoke layer. But those results can be taken as an estimation on the minimum values. For better estimations of the combined heat release rate, coupling effects between the combustibles, external heat and ambient conditions should be considered.

CHAPTER 9 SMOKE AND TOXICITY

9.1 Introduction

Thermal properties and smoke toxicity upon burning combustibles are two key aspects to be considered in fire hazard assessment. Smoke is confirmed to be the major threat in accidental fires, especially in places with high combustible contents. Smoke inhalation accounted for up to 75% of all fire deaths, which might be due to the toxicants liberated. Many test methods have been developed to determine the toxic potency of smoke [ISO9122-4 1993; ISO13344: 1996; NFPA269 2000; ASTM1678 2002] released from different materials during combustion. However, different fire scenarios were used in developing the test methods in different laboratories, the calculation methods are different and even different gas species are analyzed.

Eight different bench-scale test methods were introduced in ISO9122-4. However, none can be used easily and only three of them are available in Japan. There were criticisms on the design principles of the University of Pittsburgh test method. The NBS Cup Furnace method was superseded by the NIST/SwRI radiant furnace test which is considered to be the optimum test method for animal-based testing, but the test is not readily available. No special advantages for gas-analysis based testing were offered. Other methods [Babrauskas 1996, 1997, 2000] are DIN 53436 tube furnace, US radiant furnace (modified) and ISO 5660 cone calorimeter [ISO5660 2002] tests. These three methods can be used to assess the smoke toxicity. It is well-

known that bench-scale tests with a cone calorimeter have many functions, the apparatus is relatively simple and hence easy to operate.

The cone calorimeter is demonstrated to be a useful bench-scale apparatus to evaluate the thermal properties. Even some key parameters on smoke, such as the smoke extinction area, the carbon dioxide and carbon monoxide concentrations can be measured. As most cone tests are conducted under well-ventilated conditions, there are arguments on whether the cone calorimeter is suitable for assessing the smoke toxicity. There might be misinterpretation in using the gas concentration measured in the duct of the cone calorimeter.

In this thesis, the calculation procedure for the 'lethal concentration of the fire effluent emitted to produce death in 50 % of test animals for a specified exposure time' LC_{50} and the fractional effective dose FED based on the cone data will be clarified. The objective is to inspect how the concentrations of toxic gases from burning combustibles can be derived from such bench-scale tests.

A general summary of the calculation method for determining the 'lethal concentration of the fire effluent emitted to produce death in 50 % of test animals for a specified exposure time' (LC_{50}) was outlined in ISO 13344. There appears to be some problems in using the gas concentration measured in the exhaust duct of the cone calorimeter in following ISO 13344. The calculation procedure for LC_{50} and fractional effective dose (FED) based on the testing results of the cone calorimeter should be clarified. The key point lies in how the concentrations of toxic gases are derived. An appropriate control volume with all toxic products collected should be

taken. Clarifying this point will allow using the cone calorimeter to assess the smoke toxicity.

Polycarbonate (PC) sheets tested with a cone calorimeter are taken as an example to illustrate the calculation procedure. The values of LC_{50} deduced by measuring only the carbon monoxide will be discussed.

9.2 Equations Commonly Used on FED and LC_{50}

Fractional effective dose (FED) is defined [ISO13344 1996] as:

The ratio of the concentration and time product for a gaseous toxicant produced in a given test to that product of the toxicant that has been statistically determined from independent experimental data to produce lethality in 50% of test animals within a specified exposure and post-exposure time.

Since the exposure time in this expression is cancelled over the numerator and denominator, FED becomes simply a ratio of the average concentration C_i (in ppmv or gm^{-3}) of the i^{th} toxic gas to its LC_{50} value LC_i (in ppmv or gm^{-3}) for the same exposure time:

$$FED_i = \frac{C_i}{LC_i} \tag{9.1}$$

A toxic potency parameter commonly used for assessing smoke of a material or fire effluent is the lethal concentration LC_{50} (in ppmv or gm^{-3}) that causes death in 50 % of the animals for a specified exposure time. The value of LC_{50} is related to all the toxic gases liberated. The value of LC_{50} for the i^{th} toxicant LC_i is statistically determined from independent experimental data to produce lethality in 50 % of test animals within a 30-min exposure plus 14 days post-exposure [ISO13344 1996].

With reference to more than a single toxicant, the term FED represents the summation of FED_i for individual toxicants in the combusting atmosphere as [ISO 13344 1996]:

$$FED = \sum_i FED_i \tag{9.2}$$

The predicted LC_{50} (in ppmv or gm^{-3}) for a testing sample is calculated from the specimen mass loss Δm, FED and the total air volume V (in m^3):

$$LC_{50} = \frac{\Delta m}{FED \cdot V} \tag{9.3}$$

The FED concept came from the "N-Gas Model" [ISO13344 1996] based on the hypothesis that a small number (N) of gases in the smoke account for a large percentage of the observed toxic potency. Based on the experiments, the results of the mixed gas tests were reduced to an algebraic equation which was empirically determined for the exposure of test animals to mixtures of gases such as carbon

monoxide CO, carbon dioxide CO_2, hydrogen cyanide HCN, hydrogen chloride HCl and reduced oxygen O_2:

$$FED = \frac{m[CO]}{[CO_2]-b} + \frac{21-[O_2]}{21-LC_{50,O_2}} + \frac{[HCN]}{LC_{50,HCN}} + \frac{[HCl]}{LC_{50,HCl}} + \frac{[HBr]}{LC_{50,HBr}} \qquad (9.4)$$

The parameters m and b in the above equation are the slope and intercept respectively of the fitted curve describing the combined effects of CO and CO_2. The toxic effect from absorbing CO increases with the increase in CO_2 concentration.

A linear expression simplified for FED (in ppmv) is given as [ISO13344 1996; NFPA269 2000; ASTM 1678 2002]:

$$FED = \frac{[CO]}{5000} + \frac{[HCN]}{150} + \frac{[HCl]}{3800} + \frac{[HBr]}{3000} + \frac{[NO]}{1000} + \frac{[NO_2]}{200} \qquad (9.5)$$

The values of all gas concentrations are the average values obtained by integrating their corresponding concentration-time curves on C_i over the testing period t_B divided by t_B. Usually, t_B is taken as 30 mins [ISO13344: 1996].

9.3 Correction Factor for Measuring Carbon Monoxide Only

Among all the toxic gases liberated from test samples containing carbon, CO is the dominant one in most fires. Most likely, only the carbon monoxide concentration [CO] (which in fact is a time-averaged value) is measured. The FED obtained is then

only an estimation of the minimum consequence as the effects of other gases are not included. Taking the peak value of [CO] (denoted by pk[CO]) and putting it into equation (9.5):

$$FED = \frac{pk[CO]}{5000} \tag{9.6}$$

The effects of other species are proposed to be described by a factor k_{co} ($k_{co} \geq 0$) of [CO], and rewriting equation (9.6) as:

$$FED = \frac{(1+k_{co})\cdot[CO]}{5000} \tag{9.7}$$

In view of equation (9.5):

$$FED = \frac{[CO]}{5000}\left(1+\frac{100}{3}\cdot\frac{[HCN]}{[CO]}+\frac{25}{19}\cdot\frac{[HCl]}{[CO]}+\frac{5}{3}\cdot\frac{[HBr]}{[CO]}+5\cdot\frac{[NO]}{[CO]}+25\cdot\frac{[NO_2]}{[CO]}\right) \tag{9.8}$$

k_{co} is given by:

$$k_{co} = 33.3\cdot\frac{[HCN]}{[CO]}+1.3\cdot\frac{[HCl]}{[CO]}+1.7\cdot\frac{[HBr]}{[CO]}+5\cdot\frac{[NO]}{[CO]}+25\cdot\frac{[NO_2]}{[CO]} \tag{9.9}$$

The range of k_{co} ($k_{co} \geq 0$) can be estimated by applying the testing results reported by Babrauskas:

- Full-scale burning tests

Three tests reported in the literature [Babrauskas 1996, 1997, 2000] on steel faced sandwich panels with three different insulation materials polyurethane foam, rock wool and polystyrene foam (EPS) respectively were considered. The plastic facing film was used on the steel face in the three full-scale tests. These tests are labeled as R9A1, R9A2 and R9A3 in this study.

The values of k_{co} are 1.7, 0.26 and 2.6 for tests R9A1, R9A2 and R9A3 respectively when the mole fraction of each gas in the total gases produced is applied.

- Cone calorimeter tests

The three sandwich samples used in the full-scale burning tests [Babrauskas 1996, 1997, 2000] were also tested by a cone calorimeter under two different heat fluxes of 35 kWm^{-2} (labeled as C9A1, C9A2 and C9A3) and 50 kWm^{-2} (labeled as C9B1, C9B2 and C9B3). Each material was tested twice with and without the plastic protection film covering the steel surface.

Under 35 kWm^{-2}, the values of k_{co} are 3.4 and 3.4 for tests C9A1 with and without the plastic protection film; 3.2 and 1.9 for tests C9A2; 0.05 and 0.46 for tests C9A3. Under 50 kWm^{-2}, the values of k_{co} are 3.2 and 2.3 for tests C9B1 with and without the plastic protection film; 1.5 and 1.7 for tests C9B2; 0.03 and 1.7 for tests C9B3.

The values of k_{co} ($k_{co} \geq 0$) lie between 0 to 3.4 as shown in Figure 9.1. Higher values are given for those with higher concentrations of HCN and HCl.

In calculating k_{co} by equation (9.9), the units of the concentrations of gases should match with those in the FED equation. As there were no transient data reported in the literature [Babrauskas 1996, 1997, 2000], the mean concentrations of gases were calculated in terms of the total mole numbers of each gas concerned.

As the combustion products are generated in a transient manner, real-time measurements are necessary. The values measured can be applied directly in the above equations for burning fuel with or without adequate ventilation. Gas concentration would increase with more fuel consumed. A peak value can be resulted at the time when the fuel is burnt out.

The ventilation conditions in the tests including ISO 13344 [1996] and ISO 9122-4 [1993] are not specified in detail at present. Any one of the above equations can be used to compare the hazard of different samples in different testing facilities. For well-ventilated burning condition such as in a cone calorimeter, the measured pk[CO] can be put into equation (9.6) to calculate FED. The average values of [CO] as described in the following should be used to calculate LC_{50} together with FED.

9.4 Equations Used in the Literature

LC_{50} can be calculated from FED measured in a burning facility with a chamber volume specified as V_c and mass lost of sample Δm as:

$$LC_{50} = \frac{\Delta m}{FED \cdot V_c} \tag{9.10}$$

There are three key papers on assessing the smoke toxicity with bench-scale tests reported in the literature [Babrauskas 1996, 1997, 2000]. The results in those three papers are consistent for 'higher values' of FED with V_c of 0.01 m^3. However, the calculated values in those tables deviate from the gas concentrations listed in their experiments. It appears that those reported results might not be calculated by the equations using the transient concentrations measured in a cone calorimeter or full-scale burning tests. The method used to calculate FED and LC_{50} might be as follows.

The measured [CO] with and without adequate ventilation would be very different, giving different FED and LC_{50}. Therefore, the results under different conditions of the measurement should be checked. Note that reproducibility [ISO3534-1 1993] is the precision under conditions where the test results are obtained with the same method on identical test items in different laboratories with different operators using different equipments. As there is no standard method to follow, it might be difficult [ISO9122-4 1993] to use the cone calorimeter for assessing the smoke toxicity due to over-ventilated fires.

In calculating the effects of exposing animals to all toxic gases, and calculating the FED for use later to determine LC_{50} by equation (9.10), the results of gas concentrations such as [CO] extracted from the burning facility with over-ventilated conditions ('cone data' or other well-ventilated full-scale tests) have to be adjusted.

Gases are assumed to be accumulated in an enclosure (similar to setting V_c to be 10 m^3 for full-scale tests and 0.01 m^3 for cone calorimeter). This will not only be used for calculating LC_{50} by equation (9.10), but also for calculating the FED first.

9.5 Calculation Procedure for Cone Calorimeter

Six sets of tests on PC glazing sheets with (labelled as C9C1 to C9C6) and without (labelled as C9D1 to C9D6) a protective coating film were conducted in a cone calorimeter [Han and Chow 2005]. Heat fluxes of 30 kWm^{-2} to 70 kWm^{-2} were used. A summary of the testing conditions is shown in Table 9.1. The PC sheets were cut into 10 cm by 10 cm with a thickness of 4 mm and a mass of about 50 g.

The volume V_c is set to be 0.01 m^3, and it is assumed that all the toxic gases can be collected in this volume. The gas concentrations are calculated over time. The new transient concentration of CO, $[CO]_t$, is given by the integrated volume V_{CO}^{0-t} in terms of mass m_{CO}^{0-t} and density of CO ρ_{CO}^{0-t}:

$$[CO]_t = \frac{V_{CO}^{0\to t}}{V_c} = \frac{m_{CO}^{0\to t}}{0.01\rho_{CO}} \tag{9.11}$$

At any time t_i, the transient volume of CO $V_{CO}^{0\to t_i}$ is calculated by the volumetric flow rate of exhaust gas in the cone calorimeter $\dot{V}_{Cone}$:

$$V_{CO}^{0\to t_i} = \int_0^{t_i} [CO]_{Cone} \dot{V}_{Cone} dt \qquad (9.12)$$

The mean value of CO concentration over the total measuring time at intervals n of 1 minute, $[CO]_{avg}$, is calculated by:

$$[CO]_{avg} = \frac{1}{n}\sum_1^n [CO]_t^i = \frac{1}{n}\frac{\sum_1^n V_{CO}^{0\to t_i}}{V_c} \qquad (9.13)$$

As the testing time t_B is usually taken as 30 mins, n is equal to 30. Note that the concentration in the above equation is expressed as a volume ratio. It might be necessary to change it to other units for later calculations.

The results of FED and LC_{50} calculated by equation (9.10) are shown in Table 9.1.

In comparing with those values measured from a chamber without adequate air supply to give an under-ventilated fire [ISO 13344: 1996(E); NFPA 269 2000; ASTM E 1678-02], the values of FED and LC_{50} deduced in this study are higher. The values of FED deduced here lie between 32 to 64, which are much higher than the reported range of results from 0.5 to 1.5 [e.g. ISO 13344: 1996(E)] measured by similar equipments. However, the measured results in this study are consistent with

those reported in literature [Babrauskas 1996, 1997, 2000]. Calculating FED is taken as an 'intermediate' step to deduce LC_{50}.

The values of LC_{50} calculated in this study lie between 73 to 142, which are much higher than those from 4.3 to 50 reported in the literature [Babrauskas 1996, 1997, 2000]. The selected sample of PC might have a lower toxicity than other materials tested in the literature [Babrauskas 1996, 1997, 2000]. Besides the materials themselves, there are other uncertainties. Measuring only [CO] in this test is a main reason. Another possibility might be due to the relatively lower [CO] in over-ventilated fires.

Note that for PC, there is a CHO aromatic structure. PC without additive would not liberate HCN and HCl gases. Therefore, taking k_{co} to be 0 by measuring [CO] only is satisfactory.

9.6 Summary

The calculation procedure for estimating the lethal toxic potency LC_{50} and FED in burning polymer with a cone calorimeter was clarified in this study. The toxic gases yields other than their concentrations measured in a cone calorimeter should be considered. Toxic gases are supposed to mix uniformly into a specific total air volume. If there is no detailed information on the actual total air volume, an arbitrary value of 0.01 m^3 was proposed for the bench-scale cone calorimeter tests.

The values of LC_{50} for polycarbonate deduced by measuring only the carbon monoxide were discussed. Carbon monoxide must be measured to assess the toxicity of combustion products for most of the materials.

The cone calorimeter is a good bench-scale facility to assess the smoke toxicity provided that a correct calculation method and testing conditions are used. The results should be correlated with full-scale testing results for better assessment.

CHAPTER 10 FIRE SAFE FUNITURE AND FIRE SAFETY RANKING SYSTEM

10.1 Introduction

Both the thermal effect and smoke aspect including smoke obscurity and smoke toxicity should be considered in designing fire safe furniture. Many factors might affect the fire behaviour of burning furniture. One important external factor to be considered is ignition source such as burning under a flashover fire. The possibility to onset flashover and furniture fire behaviour under flashover should be analyzed.

Experimental testing results are necessary to study the fire behaviour of common furniture and their material constituents. Full-scale burning tests on typical sofa and tables, and bench-scale results on furniture materials including wood, foam, cloth and plastic samples commonly used were carried out under different fire conditions.

Fire safety ranking system is useful to assess the fire safety level of furniture. An equivalency system using numerical values followed by an appropriate criterion was always used in the fire safety ranking system [Chow and Lui 2001].

10.2 Fire Safety Ranking System

10.2.1 Fire safety ranking of furniture materials

Furniture materials such as wood, plywood, foam, fabric, plastics materials including PVC, PMMA, PC should be assessed.

Some parameters on burning some furniture materials are shown in Tables 10.1 to 10.2.

10.2.2 Fire safety ranking of furniture

The following two aspects should be considered:

- Different furnitures are assessed to compare their fire behaviours under same burning conditions.

- Same furnitures are assessed to compare their fire behaviours under different burning conditions.

10.2.3 Criteria for attributes

There are several ways to work out the attributes in a ranking system.

- Based on fire codes: A safety ranking system can be worked out by following the local fire codes, say, giving full marks for those satisfying the new codes.

- Based on fire science and engineering: A safety ranking system can be set up by referring to hazard assessment on different furniture. Safety criteria can be worked out with reference to
  - Critical times for furniture fire, such as time to ignition, time to peak heat release rate, and time to flashover
  - Fire retardant treatment or not
  - Heat release rate and total heat released
  - Smoke release rate or total smoke released
  - Toxicity such as by the value of LC_{50}

But it is difficult to establish take appropriate criteria to assess the attribute of the above aspects. Therefore, it is not the right time to put in primitive data in deciding the attributes. More experiments should be carried out to set up a database for the fire safety ranking system.

A fire risk diagram combining key parameters can be taken as a good substitute for fire safety ranking system. The fire properties commonly measured are the basis for the fire safety ranking system and fire risk diagram.

10.3 Properties Parameters

Both full-scale and bench-scale experiments are important for fire hazard assessment. Results from bench-scale tests are used as an example to illustrate the properties parameters

10.3.1 Thermal parameters

- Ignition temperature (in ^{o}C)

- Time to ignition (TTI), t_{ig} (in s)

- Peak heat release rate (pkHRR), $\dot{q}_{A,\max}$ (in kWm^{-2})

- Time to first $\dot{q}_{A,\max}$ after ignition, t_{fp} (in s)

- Average heat release rate in time t s (such as 60s, 180s or burning duration t_B) after ignition, $\dot{q}_{A,avg}$ (in kWm^{-2}), given by:

$$\dot{q}_{A,avg} = \frac{1}{t}\int_{t_{ig}}^{t_{ig}+t} \dot{q}_A dt \qquad (10.1)$$

- Total heat released (THR) Q_A (in MJm^{-2}), calculated from:

$$Q_A = \int_0^{\infty} \dot{q}_A dt \qquad (10.2)$$

- Mass loss rate $\dot{m}$ (in gs^{-1}) or mass loss percentage of sample m_L (in %)

- Effective heat of combustion (EHC) $\Delta h_{c,eff}$ (in MJkg^{-1})

10.3.2 Smoke and toxicity parameters

10.3.2.1 Smoke parameter only

Smoke parameter include extinction coefficient, smoke release rate and total smoke released during some time, and smoke extinction area.

Total smoke released at the end of the test, *TSR* (a non-dimensional quantity), is calculated by integrating the curve of the smoke release rate S_R (in s^{-1}) over the burning time t_B:

$$\mathrm{TSR} = \int_0^{t_B} \mathrm{S_R}\,\mathrm{dt} \tag{10.3}$$

10.3.2.2 Toxicity parameter

Toxicity of combustion products is always assessed through smoke contents. Concerning smoke toxicity, measuring only carbon monoxide CO would give the peak Fractional Effective Dose (FED). This can be deduced from the peak concentration of CO, pk[CO] in ppm (in this way, FED is also expressed in ppm and correction is necessary for assessing the smoke toxicity). The toxic potency LC_{50} for CO denoted by LC_{CO} is taken to be 5000 ppm:

$$FED = \sum_i C_i / LC_i \tag{10.4}$$

where C_i (in ppmv or gm^{-3}) is the average concentration of the i^{th} toxic gas and LC_i (in ppmv or gm^{-3}) is LC_{50} value for the same gas.

In addition, smoke toxicity can be assessed by calculating the lethal concentration LC_{50} of the fire effluent emitted to produce death in 50 % of test animals for a specified exposure time. LC_{50} can be estimated by the specimen mass loss Δm, bench-scale volume in a cone calorimeter V_c (0.01 m^3), and the fractional effective dose (FED) as:

$$LC_{50} = \frac{\Delta m}{\text{FED} \cdot V_c} \tag{10.5}$$

The calculation procedure of equation (10.5) follows the method described in Chapter 9.

10.4 Fire Risk Diagram

As discussed by Petrella [Petrella 1994] and expanded later by Chow [Han and Chow 2005], two parameters x and y can be computed to establish the thermal contribution of materials. The first parameter is the flashover propensity x (in $kJm^{-2}s^{-2}$) given by:

$$x = \frac{\dot{q}_{A,\max}}{t_{fp}} \tag{10.6}$$

Based on the experimental results, materials can be rated in an arbitrary scale of x as:

Low risk to flashover	LRF	: 0.1 to 1.0
Intermediate risk to flashover	IRF	: 1.0 to 10
High risk to flashover	HRF	: 10 to 100

The second parameter is y on the THR (in MJm^{-2}), i.e.

$$y = Q_A \tag{10.7}$$

Similarly, materials are rated as:

Very low risk of heat generation	VLRH	: 0.1 to 1.0
Low risk of heat generation	LRH	: 1.0 to 10
Intermediate risk of heat generation	IRH	: 10 to 100
High risk of heat generation	HRH	: 100 to 1000

The third parameter is z (in m^3kg^{-1}), taken as reciprocal of LC_{50} to quantify the smoke hazard as:

$$z = \frac{1000}{LC_{50}} \tag{10.8}$$

Similarly, materials are rated as:

Low risk of toxic hazard	LRTH	: 0 to 1.0
Intermediate risk of toxic hazard	IRTH	: 1.0 to 10

High risk of toxic hazard	HRTH	: 10 to 100
Very high risk of toxic hazard	VHRTH	: > 100

There are three parameters x, y, z to quantify fire risks. Values of x, y and z calculated from the testing results should be shown in table, and plotted in figure as a 'risk diagram' with ranges of LRF, IRF, HRF, VLRH, LRH, IRH, HRH, LRTH, IRTH, HRTH and VHRTH also shown in the figure. A risk diagram can be used to link the three parameters x, y, z in a three dimensional figure. The results on burning furniture foams were taken as an example with results shown in Table 10.3 and Figure 10.1.

10.5 Summary

Many relevant factors should be considered together in designing fire safe furniture and fire safety assessment of furniture. One aspect is for special purpose or requirement such as the furniture would not ignite below threshold conditions such as a specified temperature or heat flux; the other aspect is to assess the overall risk. To better control the fire risk and to reduce the hazard of furniture fire, a set of criteria should be set to give specific requirements in selecting materials and manufacturing products.

Fire safety ranking system with a risk diagram is proposed to assess furnitures. It is important to set up a database on the local furniture materials by carrying out the

above tests. Results from bench-scale tests and full-scale tests should be better correlated.

CHAPTER 11 CONCLUSIONS

As furniture plays a prominent role in fatal fire scenarios, a detailed investigation of the probable hazards due to furniture fires is necessary. An in-depth study on local furniture was carried out in this project.

It is very important to study the fire behaviours of common furniture and their constituent materials using the experimental facilities. Experimental studies on local furniture with a cone calorimeter and room calorimeter were investigated. Full-scale burning tests on typical furniture under different arrangements were carried out in the full-scale burning facility in northern China. In addition, more results were measured from bench-type experiments with a cone calorimeter. Typical furniture materials including wood, foam, cloth and plastic materials commonly used were tested under different fire conditions. Key parameters such as the heat release rate, smoke release rate, concentrations of carbon monoxide and carbon dioxide generated by burning constituent materials were measured. The possibility of causing flashover in a room and smoke toxicity were analyzed.

Test results illustrated that thermal properties of materials, fire retardant, total combustible mass, smoke production and toxic potency, geometry and configuration are all important aspects that need to be considered for assessing the fire safety of furniture. Ignitability might be the primary consideration of fire safety in many regulations. However, furniture not easy to ignite might not have a lower fire risk. They can be more hazardous in real fires. Materials that passed the bench-scale tests

such as the cigarette ignition test might be ignited easily in a post-flashover fire. This suggests that materials tested under high radiative heat fluxes would give more realistic results. Burning conditions such as the heat release rate of the furniture assembly in a flashover fire and under a small fire should be considered. Toxicity effect is another concern in developing fire safe furniture.

Burning furniture in a room might cause flashover. As observed from full-scale and bench-scale tests in this study, burning furnitures not yet ignited under a flashover fire would give a much higher heat release rate, in comparing with burning only part of the combustibles in an accidental fire without flashover. Therefore, furniture not yet ignited is suggested to be tested in a well-developed fire. As fire retardants are only required to be tested by ignitability tests with a small flame [FSD code 2000], their response to higher temperature fire scenarios such as a fully developed fire is unknown. Furniture samples treated with fire retardant should be tested under a flashover fire, not only testing its ignitability. These points should be considered carefully in designing fire safe furniture under developed fires.

Heat release rate was identified as the most important parameter. A general equation on calculating heat release rate by the oxygen consumption method was further derived. Correction for incomplete combustion, and the equations used in different environments such as fire suppression conditions were discussed. Most simplified equations on calculating heat release rate are only applicable under some specific conditions. They are applicable to other conditions provided that appropriate corrections have been made. The equations must match with the testing conditions including connections of the sample analyzers. Corrections on parameters used in the

equations such as effective heat of combustion and molecular weights are necessary when the testing conditions are different from those assumed in the equations. All the parameters should be reviewed carefully before using the relevant equations.

The principle of superposition, i.e. adding up the heat release rate curve of each combustible item to give the total heat release rate of the arrangement, might be applicable under similar burning conditions such as smaller fires. That was demonstrated by the bench-scale burning tests and full-scale burning tests. The ignition time, burning time and peak heat release rate are key points to be considered for superposition. Functional analysis suggested that the predicted curves agreed better with the measured curves for the tests under higher heat fluxes or other similar burning conditions. Results of superposition might agree better with experiments when different combustibles are exposed to higher external heat fluxes such as a flashover fire with relatively less interaction, or when they are placed not so closely together with relatively independent burning. However, the results of superposition might underestimate real fires when the combustibles are placed close to each other, and with lower external heat fluxes from the ceiling, walls and smoke layer. High external thermal radiation might give more complete combustion. The results can be taken as a minimum estimation. The coupling effects between the combustibles, external heat and ambient conditions should be considered.

Thermal radiation is the key mode of heat transfer in room fires at higher temperatures. It plays a very important role in real room fires by contributing significantly to ignition, flame spread and flashover. Therefore, good modeling of thermal radiation in simulating room fires would give more accurate results in

providing safety. Radiative heat transfer is clearly a dominant factor in the determination of flashover. A theoretical model with an inaccurate model of radiation can generate misleading conclusion about the effect of various design parameters on flashover.

Using a non-gray particulate radiation model and the zonal method, a zone model was developed to determine the conditions leading to flashover. Results from the model illustrated the effect of vent opening, particulate volume fraction and the external heat transfer coefficient on the transient temperature rise and flashover. Both the external heat transfer coefficient and the particulate volume fraction are shown to be parameters which can lead to thermal instability and, subsequently, flashover. The size of the vent opening also has a significant effect on the hot layer temperature and wall temperature during a fire. An accurate radiation model is important for accurate assessment of these effects. The present model can be used as a basis for a more detailed non-linear analysis to identify the different types of instabilities and their relation to flashover.

Smoke toxicity of burning furniture is another important aspect to be considered in fire safety assessment. The calculation procedure for estimating the lethal toxic potency LC_{50} and FED on burning combustibles with a cone calorimeter was clarified. The toxic gases yields other than their concentrations measured in a cone calorimeter should be considered to avoid confusion. Toxic gases are supposed to be dispersed into a specific total air volume. If there is no design information on the building volume, an arbitrary value of 0.01 m^3 was proposed for bench-scale tests. The testing method and calculation procedure might be simplified for some materials.

The cone calorimeter is a good bench-scale facility to assess the smoke toxicity provided that a correct calculation method and testing conditions are used. The results should be related with full-scale testing results for better assessment.

Many relevant factors should be considered together for better evaluating the fire safety of furniture. A fire safety ranking system is proposed for studying the fire safety level of furniture. More experiments should be carried out to investigate the fire behaviours. Results are useful in setting up regulations.

TABLES

Table 3.1: Cone calorimeter results for fabric materials

Parameters		C3A1	C3A2	C3A3	C3A4	C3A5	C3B1	C3B2	C3B3	C3B4	C3B5
Thermal data	m / g	1.220	1.223	1.224	1.226	1.227	1.523	1.527	1.528	1.528	1.529
	t_{ig} / s	2	7	26	66	-	2	3	7	-	-
	$\dot{q}_{A,\max}$ / kWm^{-2}	117	90	78	55	-	116	83	29	11	-
	t_{fp} / s	4	8	7	7	-	1	1	5	-	-
	Q_A / MJm^{-2}	1.6	1.4	1.4	1.0	0	2.5	2.7	1.5	0.6	0
	m_L / %	100	100	100	99	14	100	94	86	71	40
	$\Delta h_{c,eff}$ / MJkg^{-1}	13.1	11.5	11.5	8.2	-	16.4	17.7	11.4	5.5	-
Thermal risk parameters	x / kWm^{-2}s^{-1}	59	13	3	1	0	58	28	4	0	0
	Classification	H	H	I	L	L	H	H	I	L	L
	y / MJm^{-2}	1.6	1.4	1.4	1.0	0	2.5	2.7	1.5	0.6	0
	Classification	L	L	L	L	VL	L	L	L	VL	VL
Smoke parameters	*TSR* / -	15	11	9	15	7	-	8	14	18	11
	pk[CO] / ppm	27	38	28	22	0	117	84	30	12	0
	FED	0.0054	0.0076	0.0056	0.0044	0	0.0234	0.0168	0.006	0.0024	0

Table 3.2: Cone calorimeter results for plywood materials

Parameters	Three-layer thin sandwich plywood				Six-layer plywood				Three-layer thick plywood		
	C3C1	C3C2	C3C3	C3C4	C3D1	C3D2	C3D3	C3D4	C3E1	C3E2	C3E3
m / g	19.39	20.74	33.83	27.47	44.03	45.95	52.21	42.43	100.74	97.73	95.23
t_{ig} / s	113	90	150	130	15	5	14	24	183	32	6
$\dot{q}_{A,\max}$ / kWm^{-2}	408	278	256	253	217	234	213	225	220	223	239
t_{fp} / s	17	12	78	74	183	229	199	201	1032	79	66
m_L / %	99	90	85	97	97	98	93	93	99	99	99
Q_A / MJm^{-2}	25.3	22.6	29.5	27.8	58.1	51.8	56.6	51.1	145.2	142.5	146.2
$\Delta h_{c,eff}$ / $MJkg^{-1}$	13.2	12.1	10.1	10.4	13.6	11.5	11.7	12.9	14.6	14.7	15.5
TSR / -	85	197	198	146	109	336	258	133	552	266	332
pk[CO] / ppm	146	269	231	204	103	309	124	125	338	129	157

Table 3.3: Summary of full-scale burning tests on table and cushions

Test / Parameter	R3A1	R3A2	R3A3	R3A4	R3A5	R3A6	R3A7	R3A8	R3B1	R3B2	R3B3	R3B4	R3B5
m / kg	1	1	1	2	3	6	24	25	4	4	4	4	4
$\dot{q}_{max}$ / kW	142	82	67	232	474	1017	302	899	547	521	329	444	356
Q / MJ	20	20	20	33	47	72	197	435	57	58	45	60	40

Table 5.1: Summary of full-scale burning tests on desk and sofa

Test / Parameter	Small ignition source						Large ignition source (flashover)		
	R5A1	R5A2	R5A3	R5A4	R5A5	R5A6	R5B1	R5C1	R5C2
m / kg	22	20	22	23	31	53	20	9.5	0.4
t_B / s (min)	1664 (28)	2000 (33)	2330 (39)	1643 (27)	2033 (34)	1576 (26)	1715 (29)	317 (5)	718 (12)
$\dot{q}_{max}$ / MW	1.05	0.63	1.12	1.05	0.64	2.06	3.01	2.45	0.04
t_{fp} / s	405	465	496	541	360	365	290	270	475
THR_{net} / MJ	353	402	483	411	375	868	451	418	18
$\Delta h_{c,eff}$ / MJkg^{-1}	17	19	21	20	12	17	22	44	44
q''_{max} / kWm^{-2}	2.93	0.67	1.71	2.92	1.07	9.52	12.72	18.6	-

Table 5.2: Summary of cone calorimeter results on furniture foam and wood

Group / Parameter	Furniture foam								Furniture wood			
	No fire retardant				With fire retardant							
Tests labeled	C5A1	C5A2	C5A3	C5A4	C5B1	C5B2	C5B3	C5B4	C5C1	C5C2	C5C3	C5C4
$\dot{q}''_{fC}$ / kWm^{-2}	70	50	35	20	70	50	35	20	70	50	35	20
m / g	10	10	10	9.6	10	10	10	11	79	80	78	76
t_{ig} / s	1	2	3	4	4	4	10	15	10	24	73	614
$\dot{q}_{A,\max}$ / kWm^{-2}	574	500	430	362	821	758	560	367	256	199	167	232
t_{fp} / s	356	55	57	71	26	35	29	60	14	23	21	174
Q_A / MJm^{-2}	22	24	24	24	24	24	23	23	110	121	124	94
$\Delta h_{c,eff}$ / MJkg^{-1}	21	23	24	25	23	23	22	21	14	15	16	13
t_B / s	111	114	130	135	108	111	130	140	1200	1400	1600	1900
$\dot{q}_{A,avg}$ / kWm^{-2}	203	214	196	178	219	214	192	179	91	93	91	83

Table 6.1: Observations of the flashover criteria

References	Temperature near the ceiling (^{o}C)	Heat flux at floor (kWm^{-2})
Hagglund (1974)	600	-
Parker and Lee (1974)	-	20
Fang (1975)	450-650	17-33
Lee and Breese (1978)	650	17-30
Babrauskas (1979)	600	20
Budnick and Klein (1979)	673-771	15
	634-734	-
Fang and Breese (1980)	706±92	20
Thomas (1980)	520	22
McCaffrey, Quintiere (1981)	600	17.7-25

Table 8.1: Functional analysis on the superposition results for bench-scale burning tests

Curves tested	Parameters	C8A1: PMMA+PC			C8A2: PMMA+PVC			C8A3: PMMA+PVC			C8A4: PMMA+PVC			C8A5: PMMA+Wood		
		Same heat flux	Under different heat fluxes		**Same heat flux**	Under different heat fluxes		Different heat flux	**Same heat flux**	Different heat flux	Under different heat fluxes		**Same heat flux**	Under different heat fluxes		**Same heat flux**
		B1+C1	*B2+C1*	*B3+C1*	**B1+D1**	*B2+D1*	*B3+D1*	*B1+D2*	**B2+D2**	*B3+D2*	*B1+D3*	*B2+D3*	**B3+D3**	*B1+E1*	*B2+E1*	**B3+E1**
$\dot{q}_A$	Norm	0.13	*0.21*	*0.46*	0.17	*0.31*	*0.55*	*0.19*	0.23	*0.51*	*0.70*	*0.5*	0.22	*0.82*	*0.52*	0.15
	Cosine(s=1)	0.86	*0.83*	*0.56*	0.83	*0.53*	*0.16*	*0.44*	0.72	*0.14*	*-0.07*	*-0.02*	0.16	*0.11*	*0.16*	0.60
	Cosine(s=2)	0.90	*0.88*	*0.61*	0.89	*0.59*	*0.18*	*0.49*	0.78	*0.16*	*-0.07*	*-0.01*	0.18	*0.12*	*0.19*	0.65
	Cosine(s=3)	0.91	*0.91*	*0.63*	0.91	*0.62*	*0.20*	*0.54*	0.80	*0.17*	*-0.07*	*-0.01*	0.20	*0.12*	*0.21*	0.70
	Cosine(s=4)	0.92	*0.93*	*0.65*	0.93	*0.65*	*0.21*	*0.59*	0.82	*0.19*	*-0.07*	*0.01*	0.22	*0.13*	*0.23*	0.75
	Cosine(s=5)	0.93	*0.93*	*0.66*	0.94	*0.68*	*0.23*	*0.63*	0.83	*0.20*	*-0.06*	*0.02*	0.25	*0.15*	*0.25*	0.80
Q_A	Norm	0.08	*0.16*	*0.30*	0.16	*0.25*	*0.39*	*0.06*	0.14	*0.31*	*0.05*	*0.51*	0.04	*0.61*	*0.41*	0.11
	Cosine(s=1)	0.99	*0.99*	*0.90*	0.99	*0.97*	*0.84*	*0.98*	0.97	*0.86*	*0.06*	*0.07*	0.97	*0.77*	*0.89*	0.99

Table 8.2: Functional analysis on the superposition results for full-scale burning tests

Curves tested	Parameters	C_6					C_3	
		$C_4 + C_2$	$C_3 + C_2 + C_{1a}$	$2C_3$	$2(C_2 + C_{1a})$	$2(C_{1b} + 2C_{1a})$	$C_2 + C_{1a}$	$C_{1b} + 2C_{1a}$
$\dot{q}$	Norm	0.28	0.33	0.19	0.51	0.57	0.38	0.43
	Cosine(s=1)	0.87	0.95	0.97	0.80	0.53	0.85	0.61
Q	Norm	0.18	0.25	0.21	0.29	0.35	0.14	0.24
	Cosine(s=1)	0.99	0.98	0.98	0.98	0.98	0.99	0.99

Table 9.1: Cone calorimeter results for polycarbonate samples

Heat flux / Test / Properties	30 kWm^{-2}		35 kWm^{-2}		40 kWm^{-2}		50 kWm^{-2}		60 kWm^{-2}		70 kWm^{-2}	
	C9C1	C9D1	C9C2	C9D2	C9C3	C9D3	C9C4	C9D4	C9C5	C9D5	C9C6	C9D6
CO yield / $kgkg^{-1}$	0.1	0.1	0.1	0.1	0.1	0.06	0.07	0.08	0.06	0.05	0.05	0.05
CO_2 yield / $kgkg^{-1}$	1.7	1.7	1.7	1.9	1.8	1.5	1.8	1.9	1.8	1.8	1.8	1.8
pk[CO] / ppm	360	327	363	236	391	323	465	446	475	395	515	501
FED / -	49	40	47	54	64	35	50	50	46	36	40	32
LC_{50} / gm^{-3}	92	115	96	85	73	130	88	90	100	127	112	142

Table 10.1: Comparison of cone calorimeter results

Parameters		$\dot{q}''_{fC}$ / kWm^{-2}	t_{ig} / s	$\dot{q}_{A,\max}$ /kWm^{-2}	t_{fp} / s	Q_A /MJm^{-2}	m / g
Poly-carbonate	Without film	20	-	-	-	-	114
		50	68	447	44	240	113
		70	35	420	64	239	115
	With film	20	-	5	-	0.1	115
		50	34	557	47	235	115
		70	11	456	37	256	115
Three combined tests	PMMA	20	113	622	208	150	69.8
	Wood	20	108	231	20	74	54.4
	PVC	50	26	135	186	110	139
Cloth	Without Fire retardant	10	-	-	-	0	1.24
		20	47	79	10	1.4	1.24
		30	13	104	10	1.7	1.23
		50	3	117	8	1.8	1.23
		70	1	134	4	1.8	1.23
	With Fire retardant	10	-	-	-	0	1.52
		20	-	11	-	0.5	1.52
		30	5	39	6	1.4	1.51
		50	2	76	4	2.2	1.51
		70	1	98	3	2.4	1.51
Foam	Without Fire retardant	10	30	271	93	24	10.6
		20	4	362	75	23.8	10.6
		50	2	500	57	24.2	10.7
		70	1	574	36	22	10.6

Foam	With Fire retardant		10	-	0	-	0	11.2
			20	15	367	75	22.6	11.2
			50	4	758	39	23.8	11.2
			70	4	821	30	23.7	11.2
Polywood	Thickness: 5 cm	Log	20	113	408	17	25.3	19.4
		+ oil		90	278	12	22.6	20.7
		+Fr1		150	256	78	29.5	33.8
		+Fr2		130	253	74	27.8	27.5
	Thickness: 8 cm	Log	50	15	217	183	58.1	44.0
		+ oil		5	234	229	51.8	46.0
		+ Fr1		14	213	199	56.6	52.2
		+ Fr2		24	225	201	51.1	42.4
	Thickness: 18 cm	Original wood	20	183	220	1032	145.2	100.7
			50	32	223	79	142.5	97.7
			70	6	239	66	146.2	95.2

Table 10.2: Ignition temperature for typical furniture materials

Number	Materials	Ignition temperature / °C	
		Pilot ignition	Auto ignition
1	cotton	230 - 270	250 - 300
2	nylon	390 - 480	420 - 500
3	fiberboard	300 - 350	300 - 500
4	wood	200- 500	250 - 600
5	PU foam	300 - 370	370 - 450
6	FR-PUfoam	320 - 460	350 - 500
7	PVC	240 - 400	280 - 460
8	PMMA	260 - 360	300 - 500
9	PC	440 - 530	500 - 600

Table 10.3: Results of thermal and smoke risk parameters for foam

Parameters		Tests							
		C5A1	C5A2	C5A3	C5A4	C5B1	C5B2	C5B3	C5B4
Thermal risk parameters	x / $kJm^{-2}s^{-2}$	9	91	250	574	0	25	190	205
	Classification	IRF	HRF	HRF	HRF	LRF	HRF	HRF	HRF
	y / MJm^{-2}	24.0	23.8	24.2	22.0	0	22.6	23.8	23.7
	Classification	IRH	IRH	IRH	IRH	VLRH	IRH	IRH	IRH
Smoke risk parameter	z / m^3kg^{-1}	0.7	1.1	1.4	1.6	0	5.4	9.5	11
	Classification	LRTH	IRTH	IRTH	IRTH	LRTH	IRTH	IRTH	HRTH

FIGURES

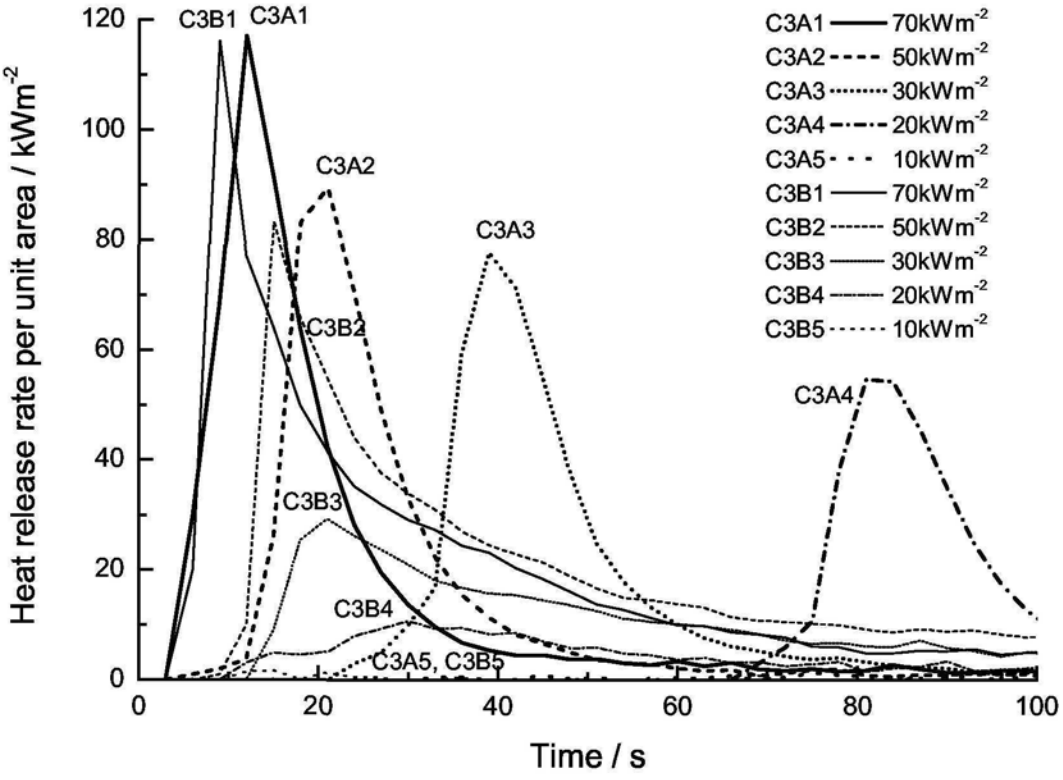

Figure 3.1: Heat release rates per unit area for fabric

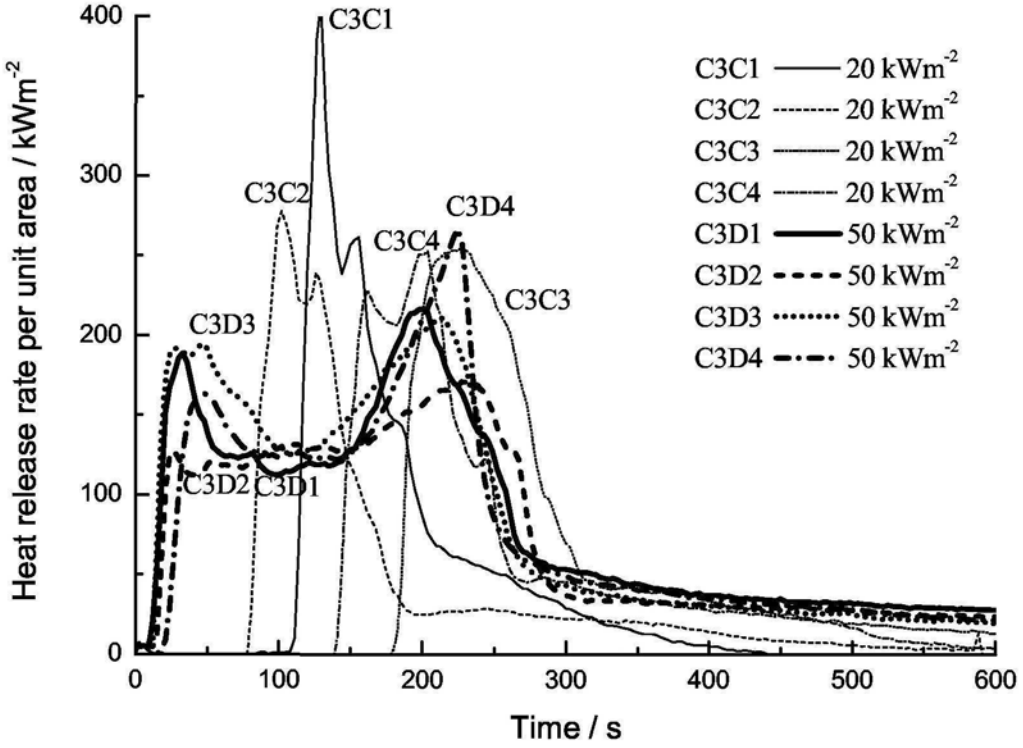

(a) Plywood A and B

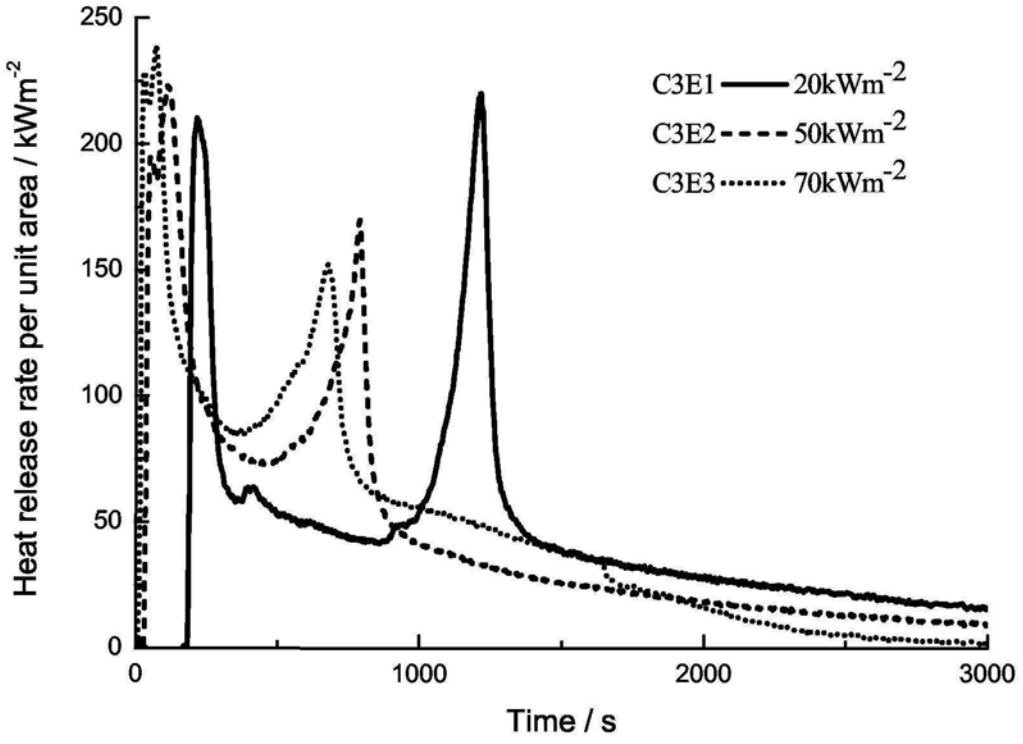

(b) Plywood C

Figure 3.2: Heat release rates per unit area for plywood

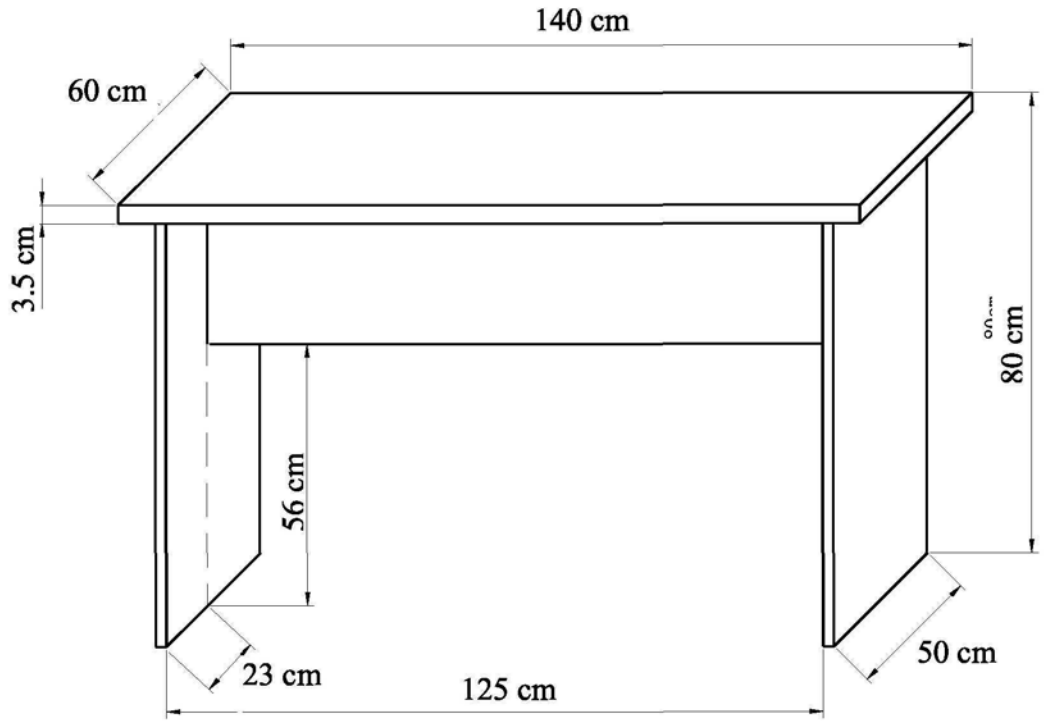

Figure 3.3: Table dimensions

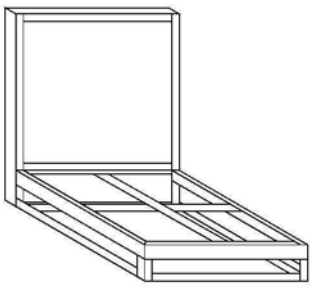

(a) Steel frame

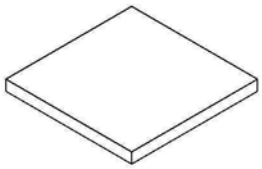

(b) One horizontal cushion

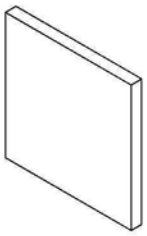

(c) One vertical cushion

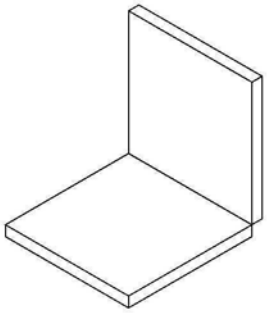

(d) Two cushions

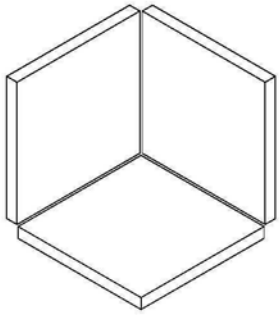

(e) Three cushions

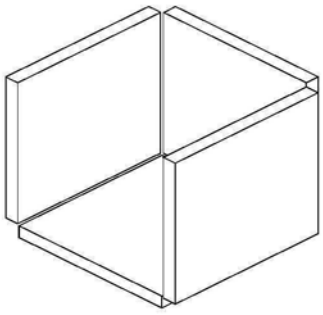

(f) Four cushions

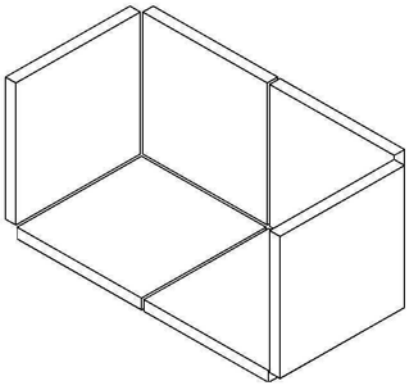

(g) Six cushions

Figure 3.4: Testing arrangements of cushions

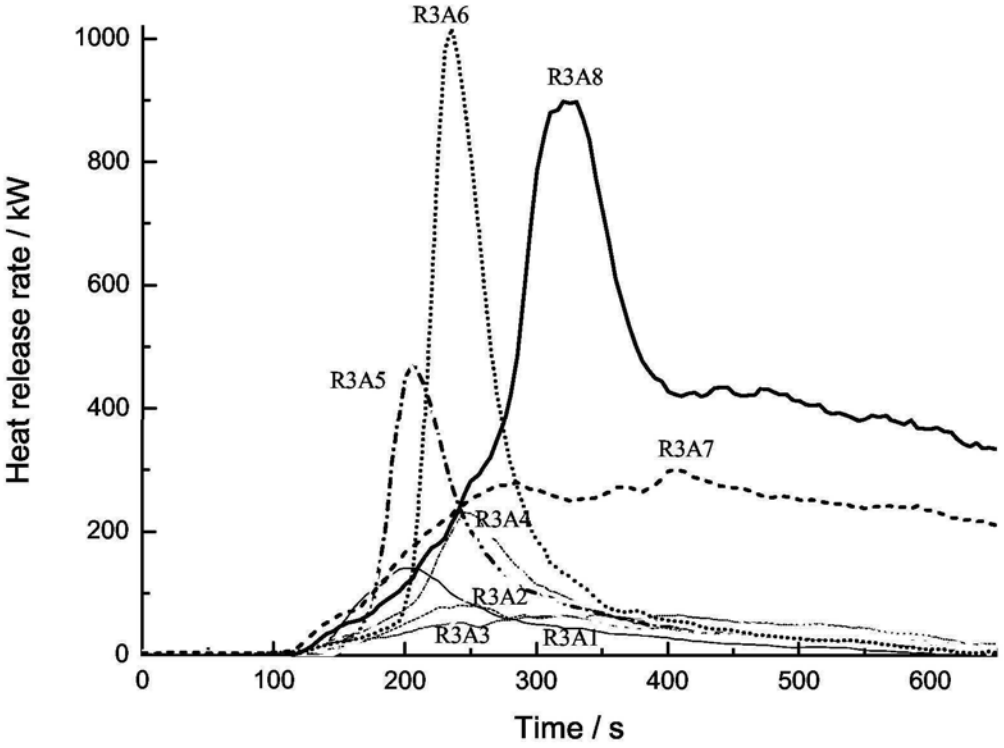

(a) Tests R3A1 to R3A8 on table and cushions

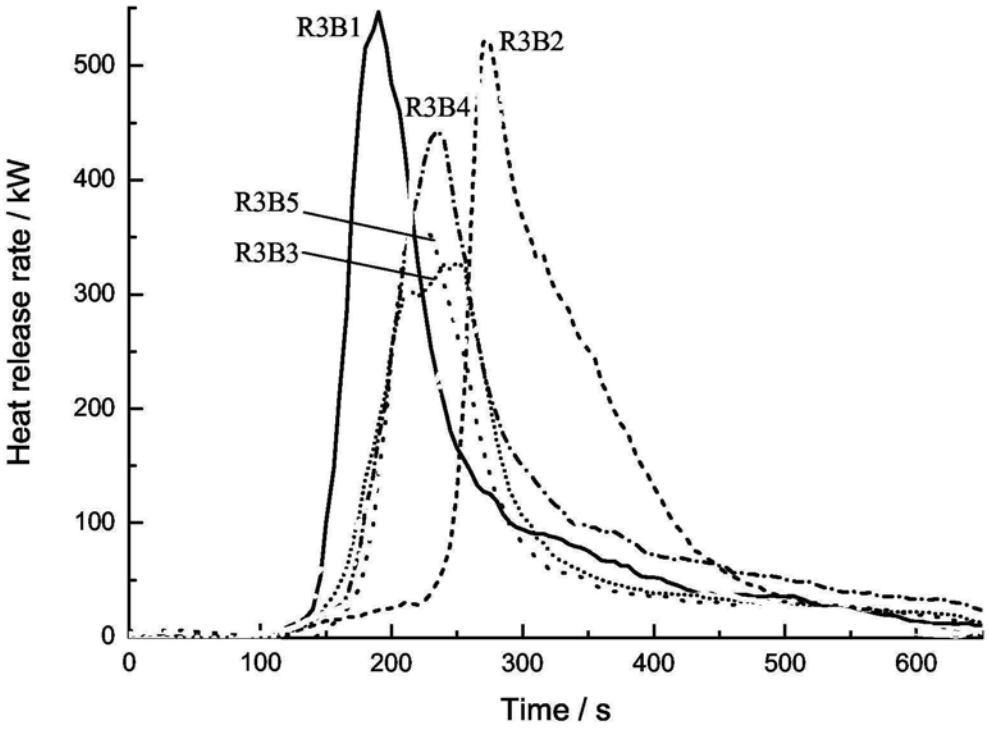

(b) Tests R3B1 to R3B5 on four cushions with different arrangements

Figure 3.5: Heat release rates for table and cushions

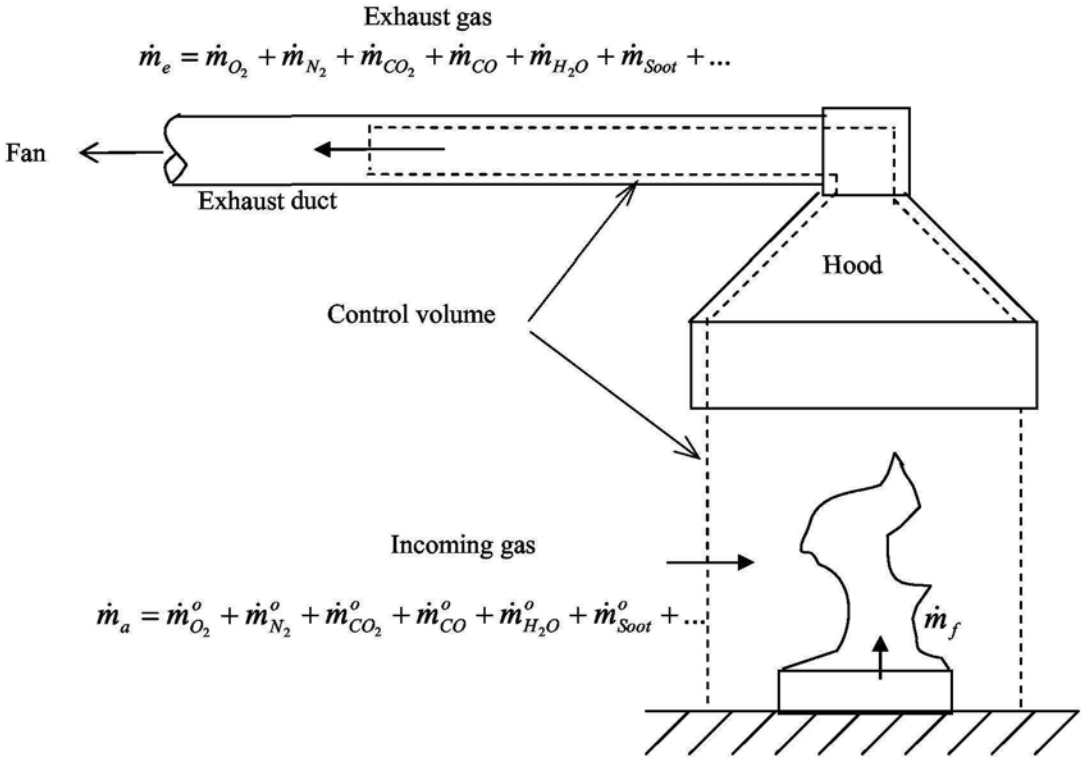

Figure 4.1: Schematic view of oxygen consumption calorimetry

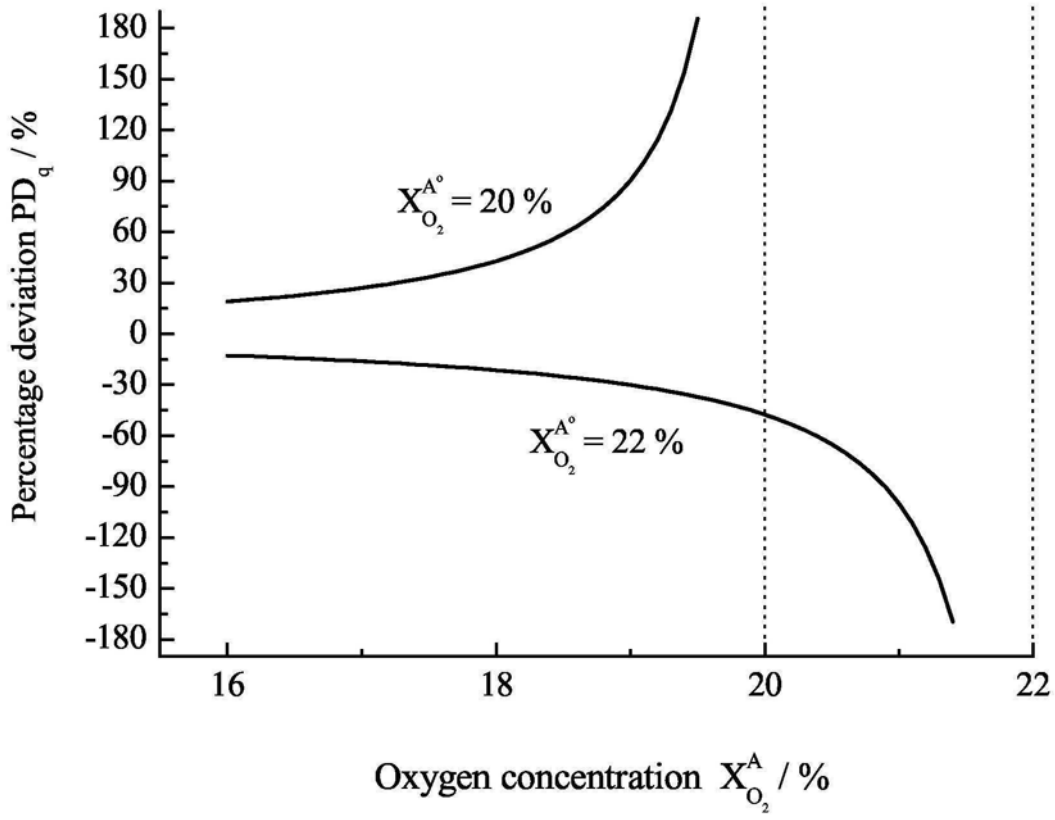

Figure 4.2: Deviation of heat release rates

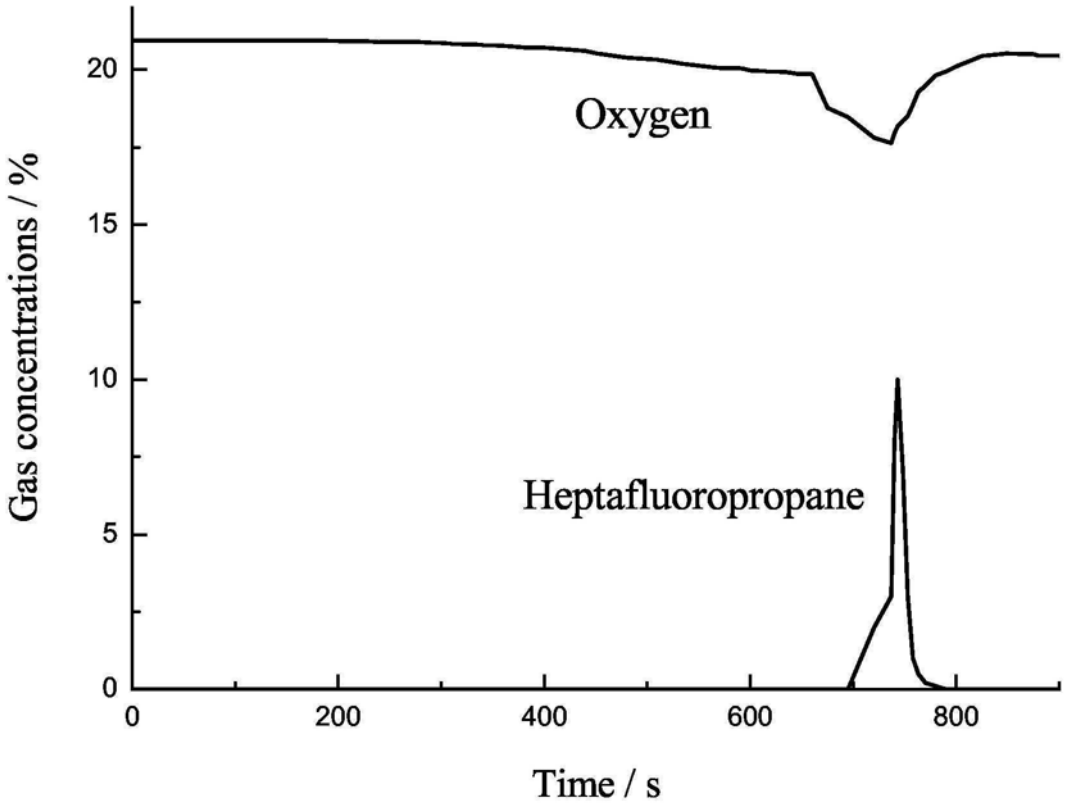

Figure 4.3: Gas concentrations for discharging clean agent

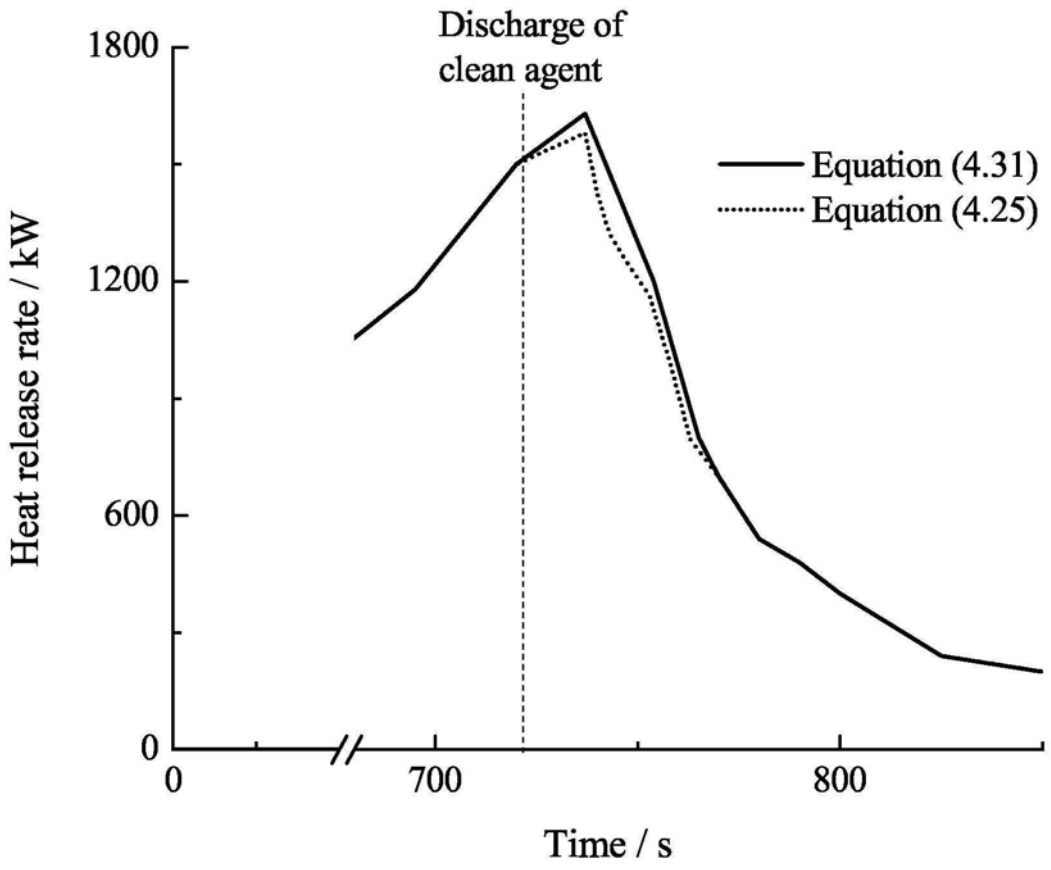

Figure 4.4: Heat release rates for discharging clean agent

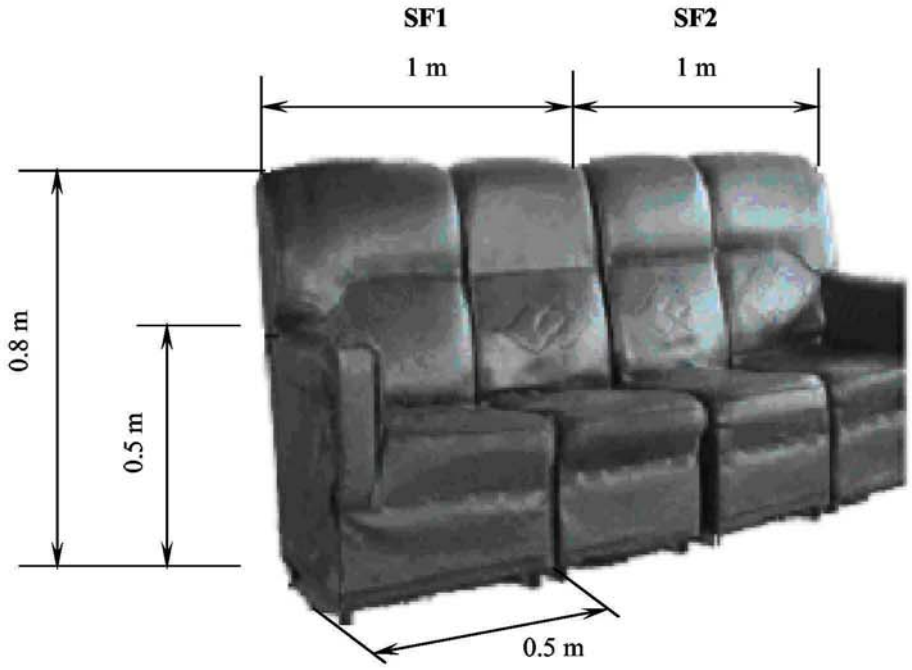

(a) Sofa

(b) Desk

Figure 5.1: Samples of sofa and desk

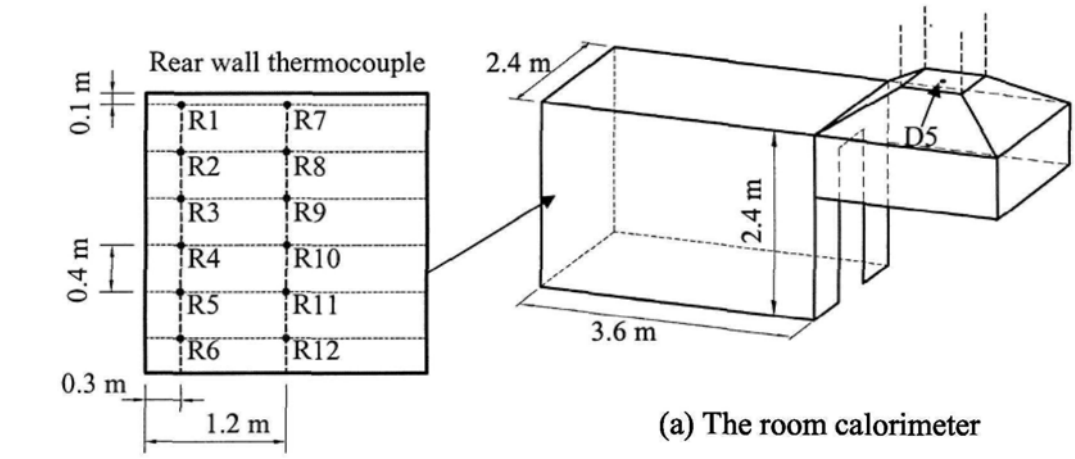

(a) The room calorimeter

(b) Thermocouple at wall

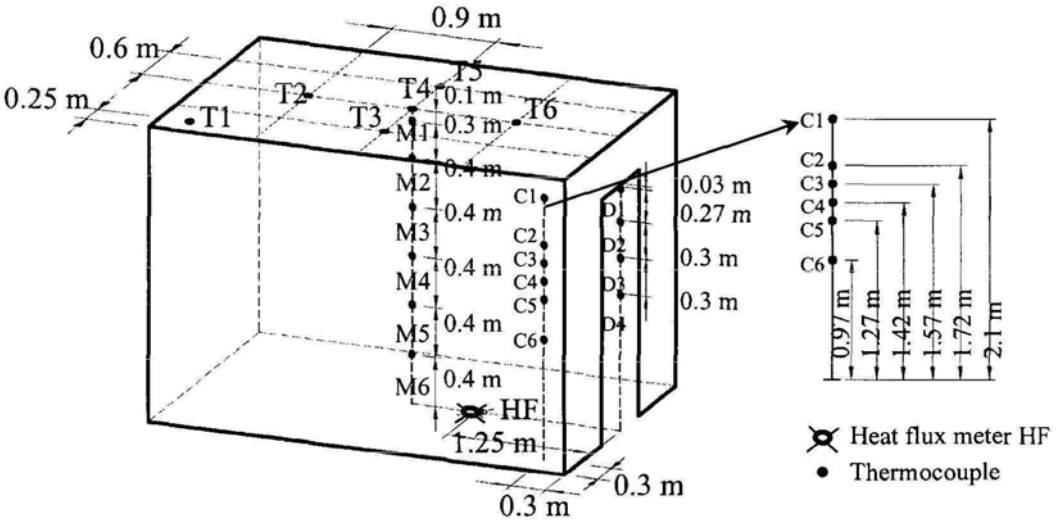

(c) Temperature measuring points

Figure 5.2: The room calorimeter

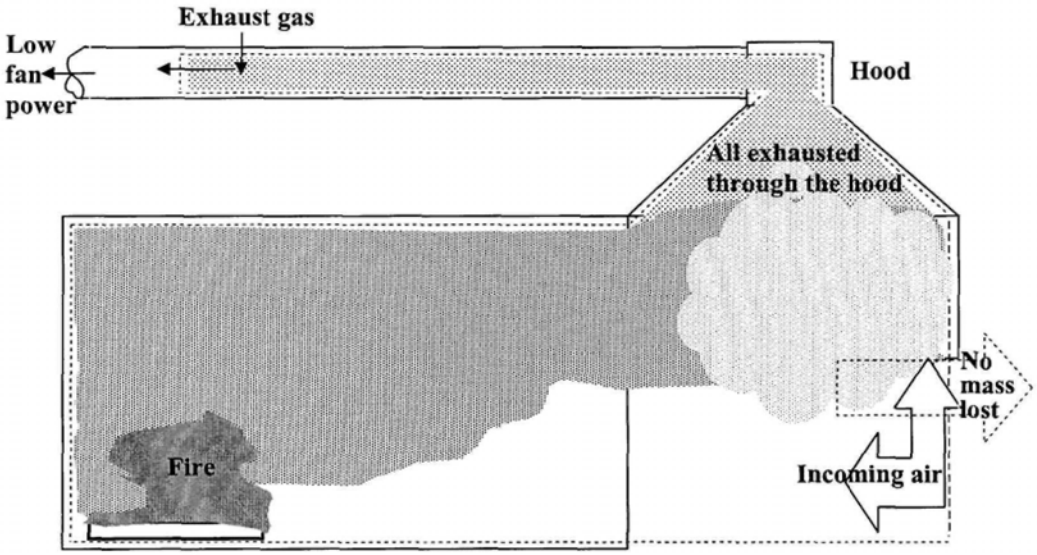

Figure 5.3: Schematic view of test with lower exhaust rate

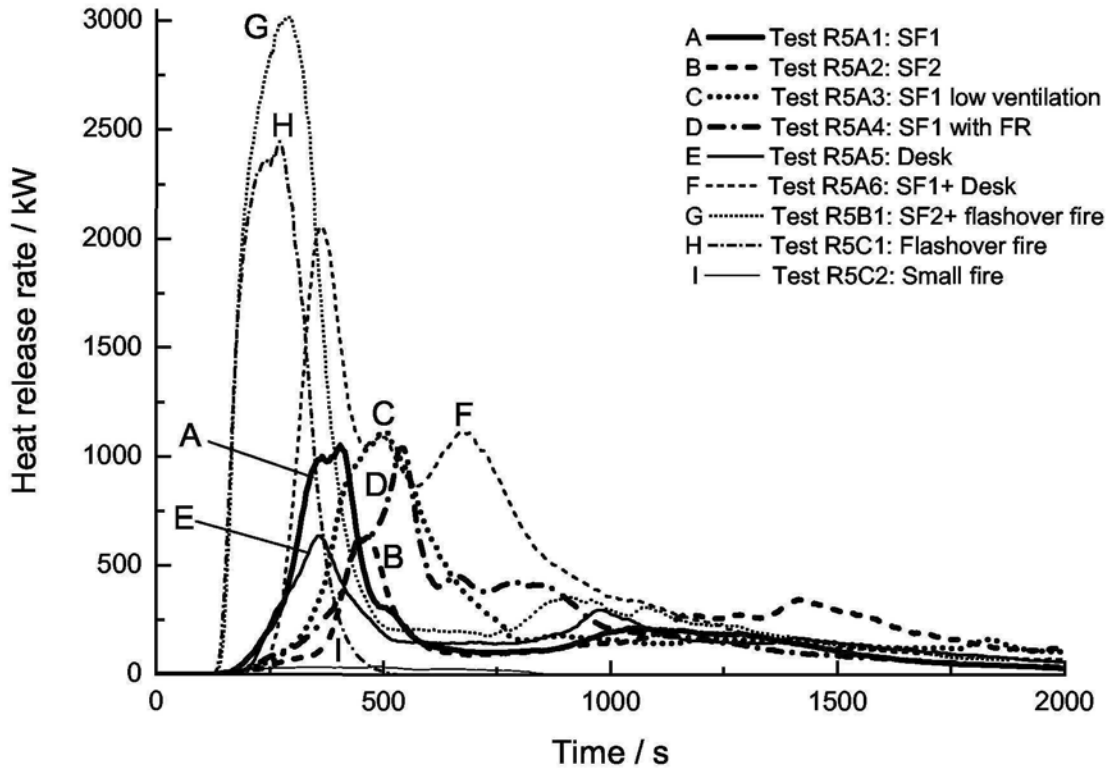

Figure 5.4: Heat release rates of furniture fires

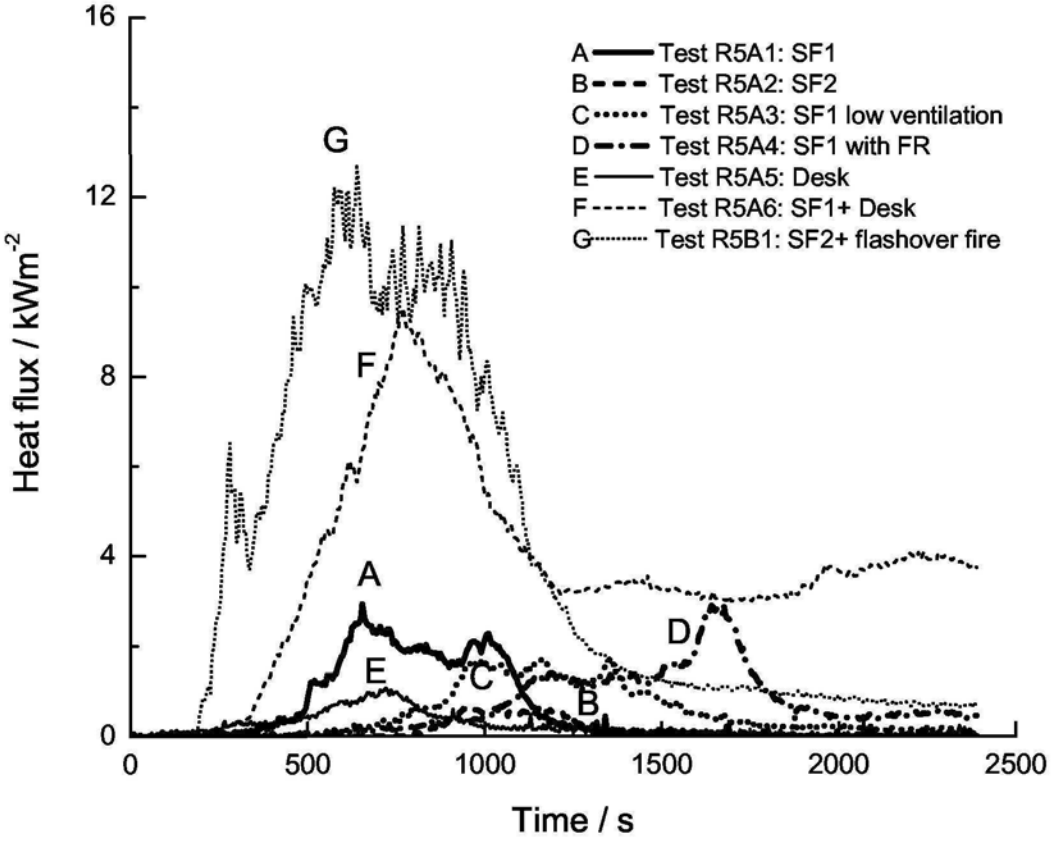

Figure 5.5: Heat fluxes of furniture fires

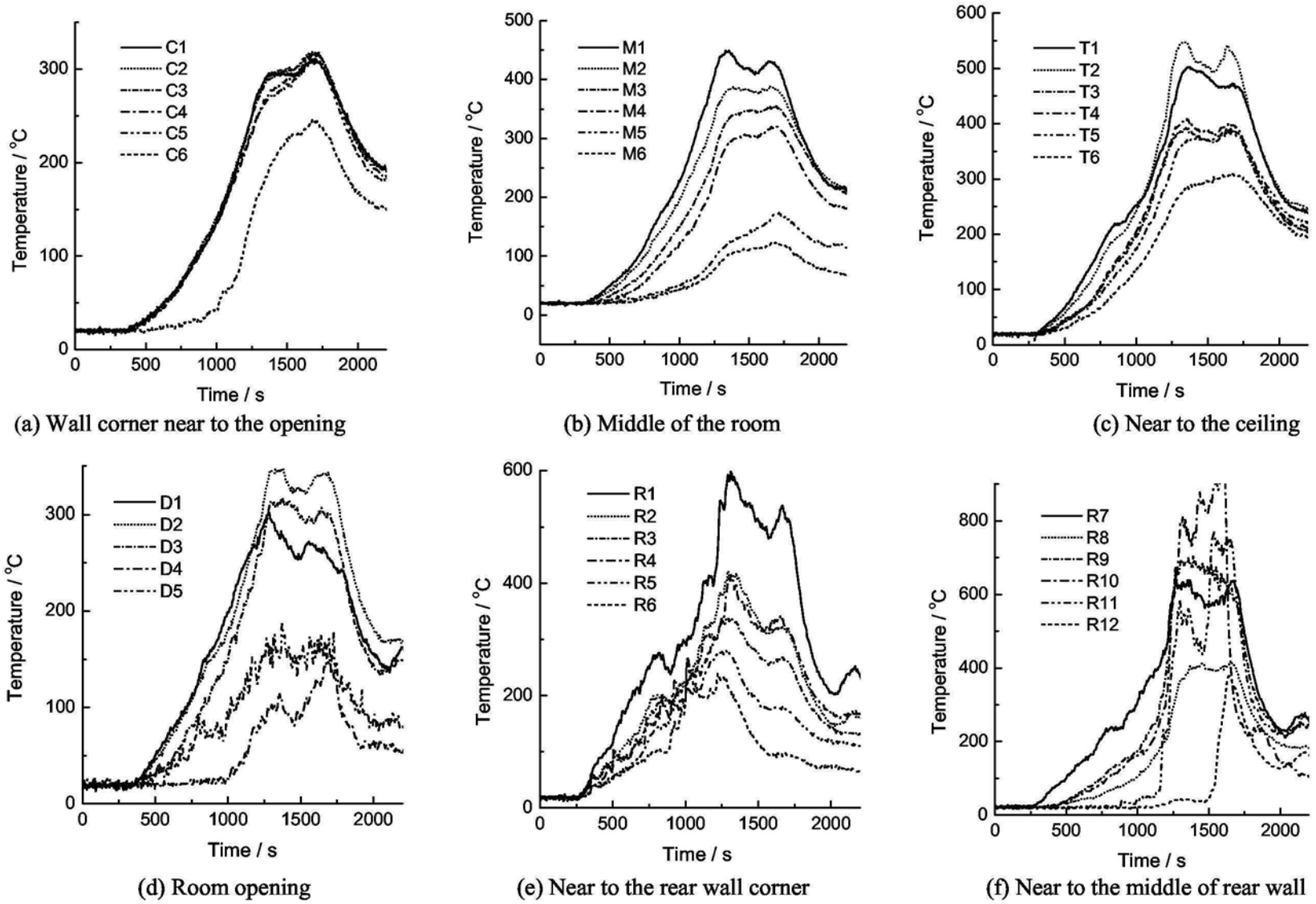

Figure 5.6: Air temperatures for burning a sofa

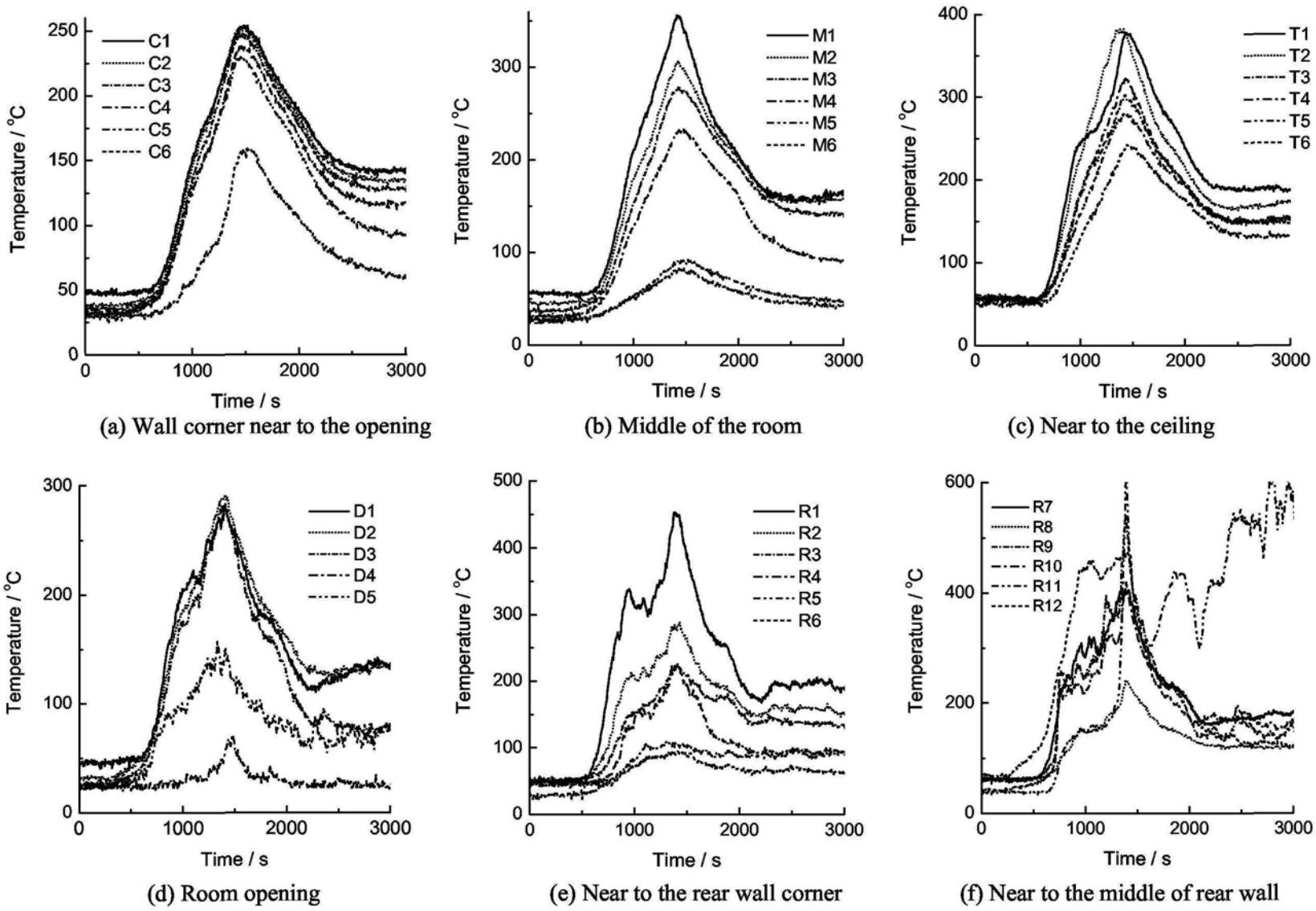

(a) Wall corner near to the opening

(b) Middle of the room

(c) Near to the ceiling

(d) Room opening

(e) Near to the rear wall corner

(f) Near to the middle of rear wall

Figure 5.7: Air temperatures for burning a desk

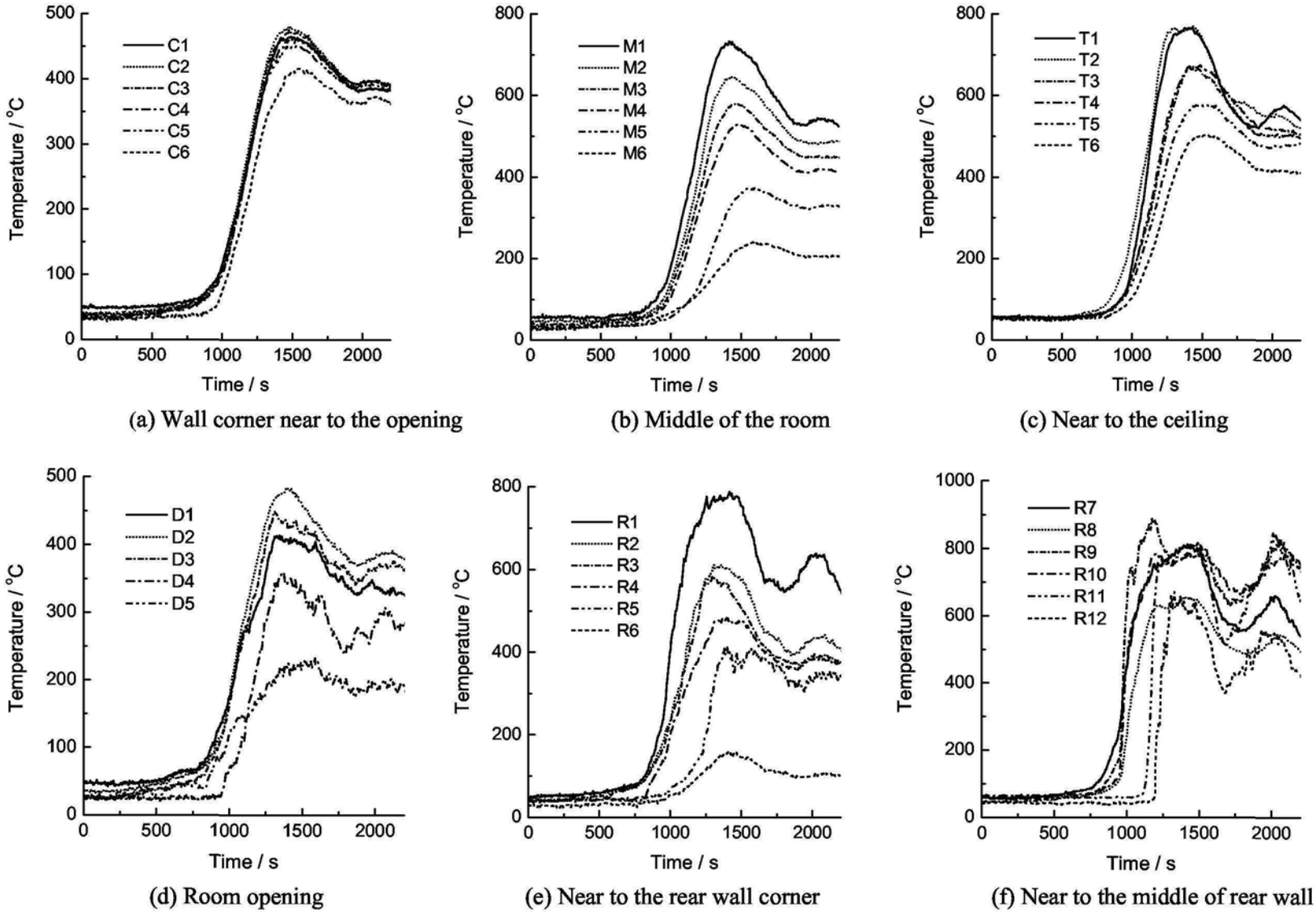

(a) Wall corner near to the opening

(b) Middle of the room

(c) Near to the ceiling

(d) Room opening

(e) Near to the rear wall corner

(f) Near to the middle of rear wall

Figure 5.8: Air temperatures for burning a sofa with a desk

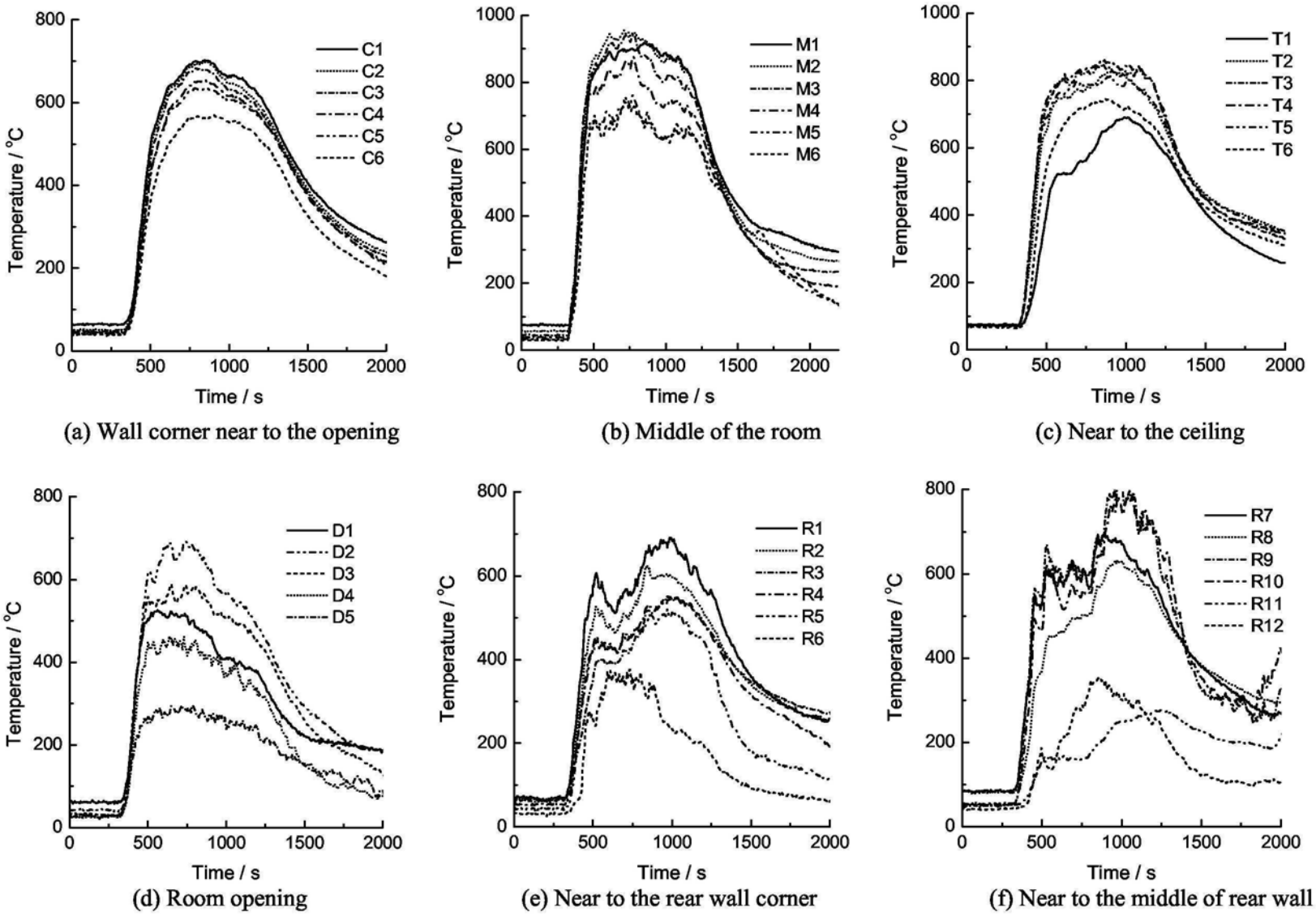

(a) Wall corner near to the opening (b) Middle of the room (c) Near to the ceiling

(d) Room opening (e) Near to the rear wall corner (f) Near to the middle of rear wall

Figure 5.9: Air temperatures for burning a sofa under flashover

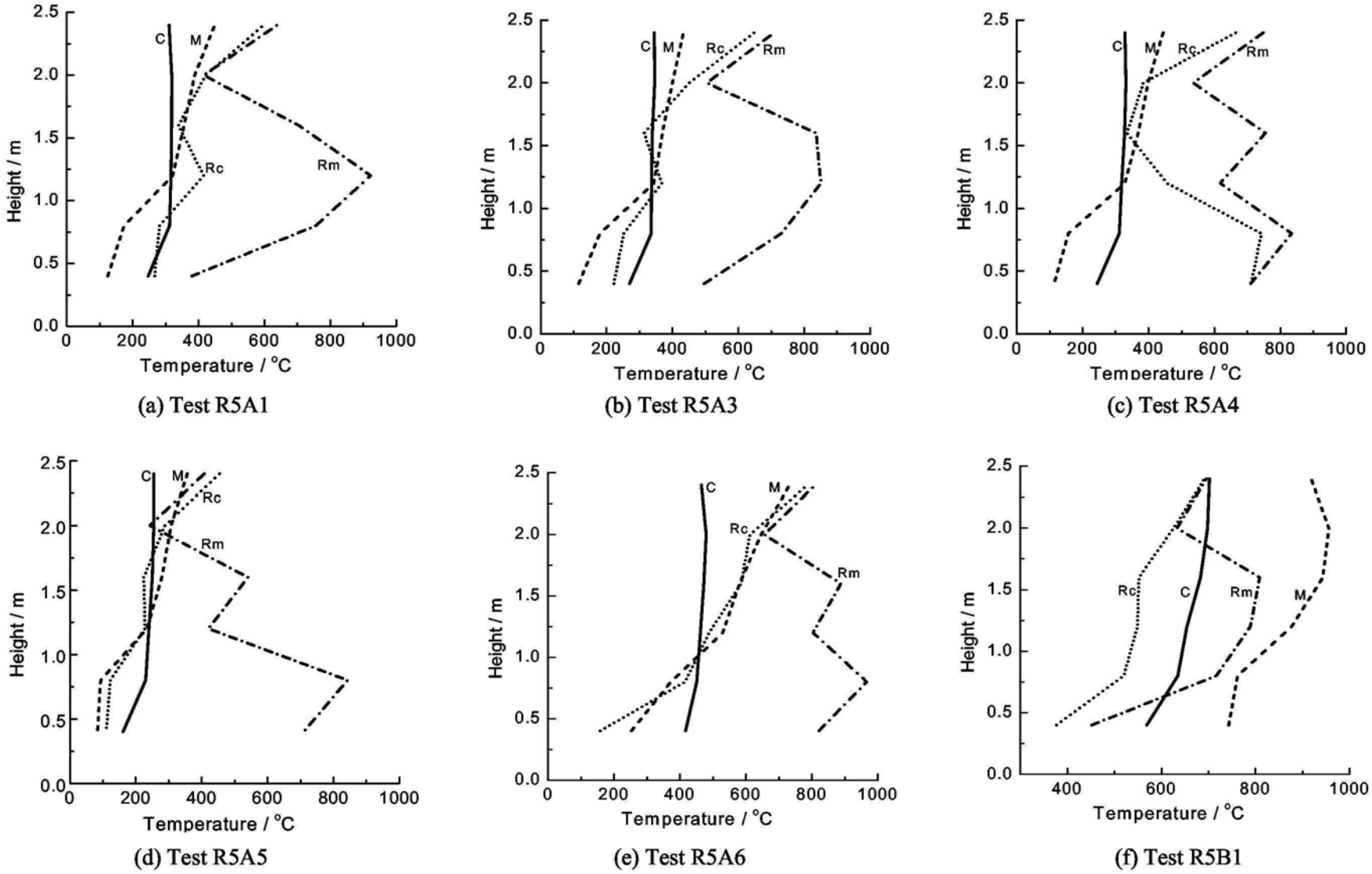

Figure 5.10: Vertical temperature profiles of furniture fires

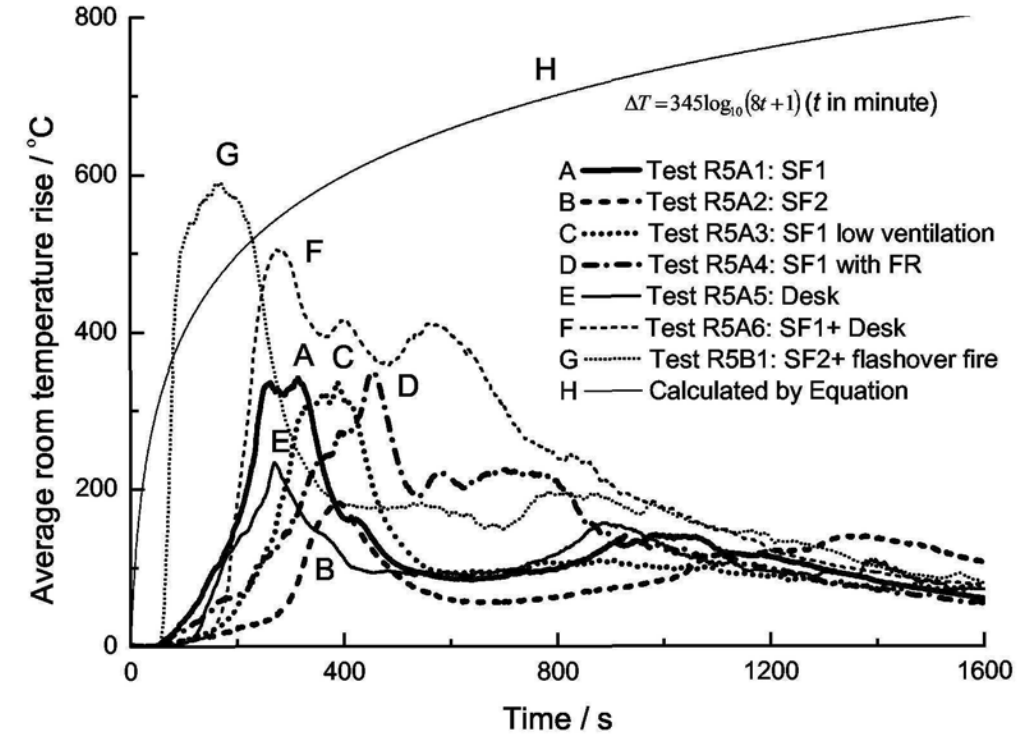

(a): Average temperature rise

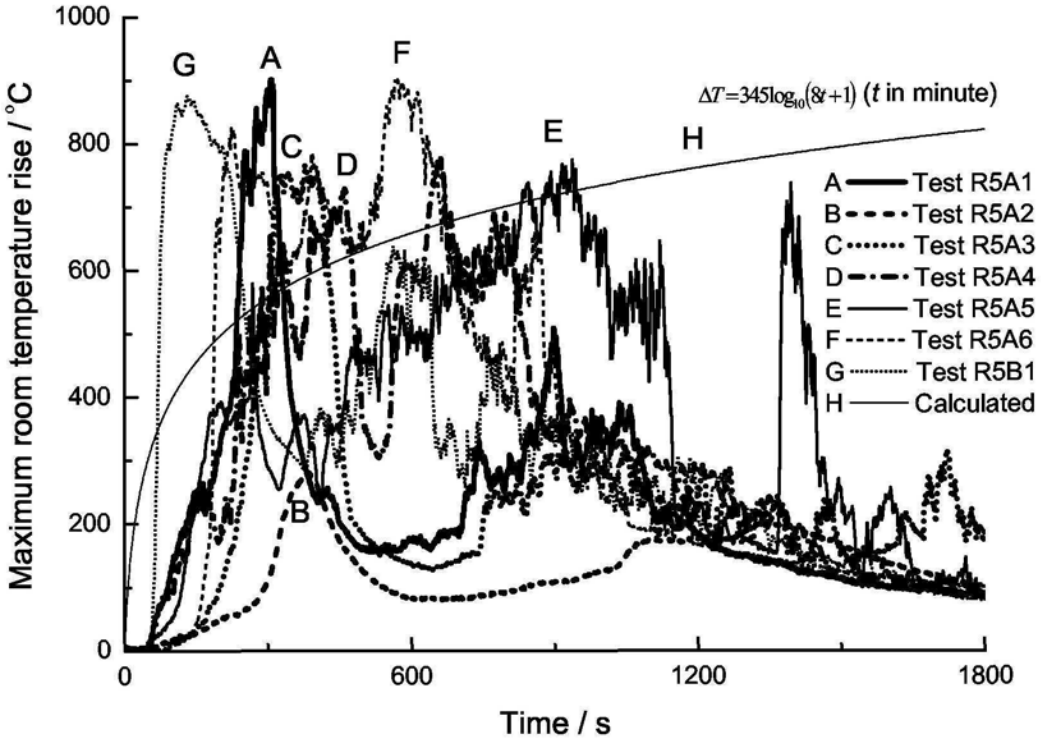

(b): Maximum temperature rise

Figure 5.11: Temperature rise of room air under furniture fires

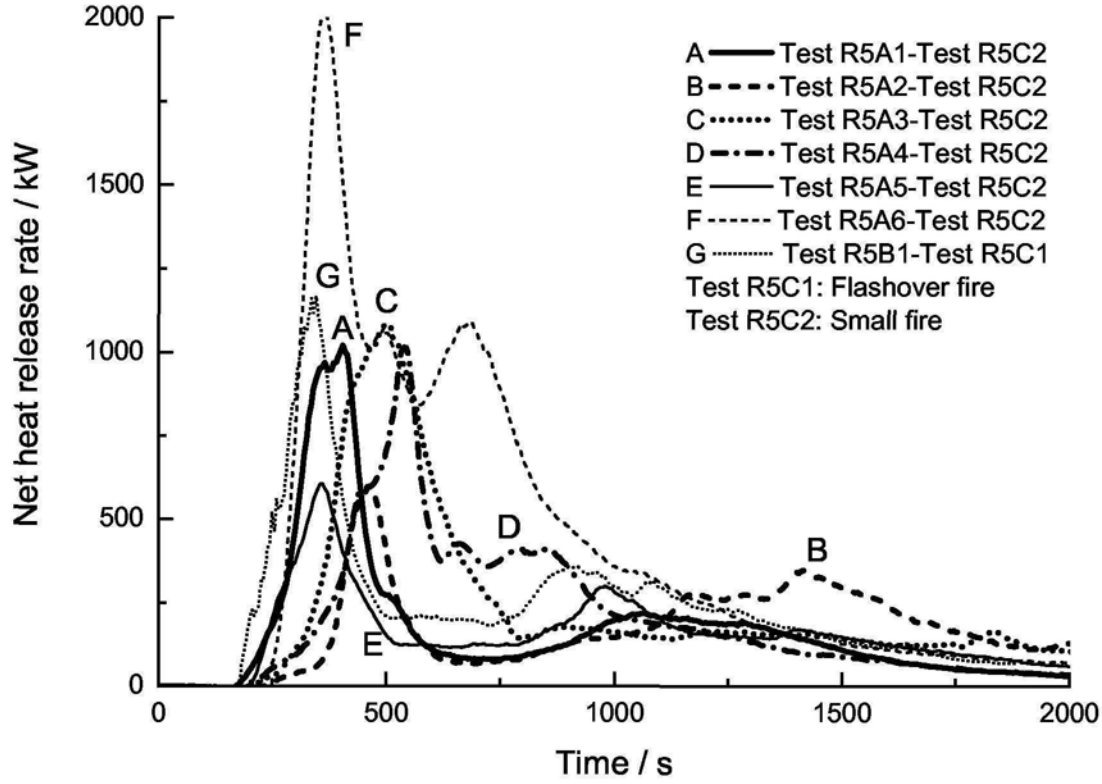

Figure 5.12: Net heat release rate of furniture fires

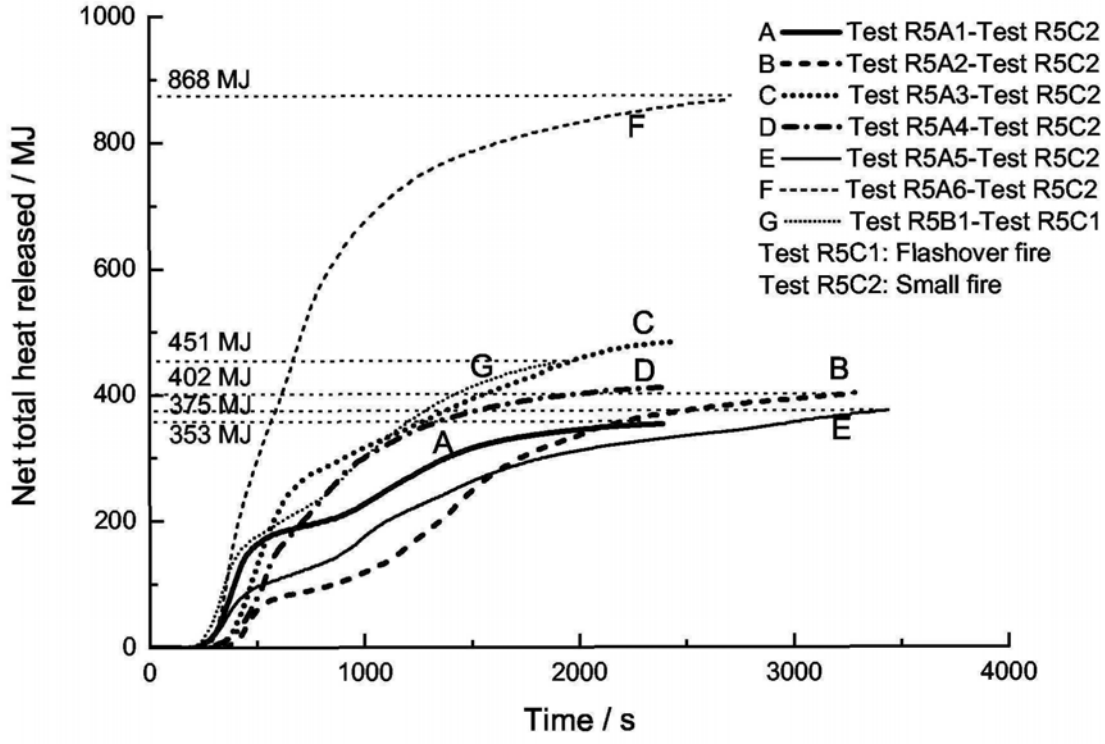

Figure 5.13: Net total heat released of furniture fires

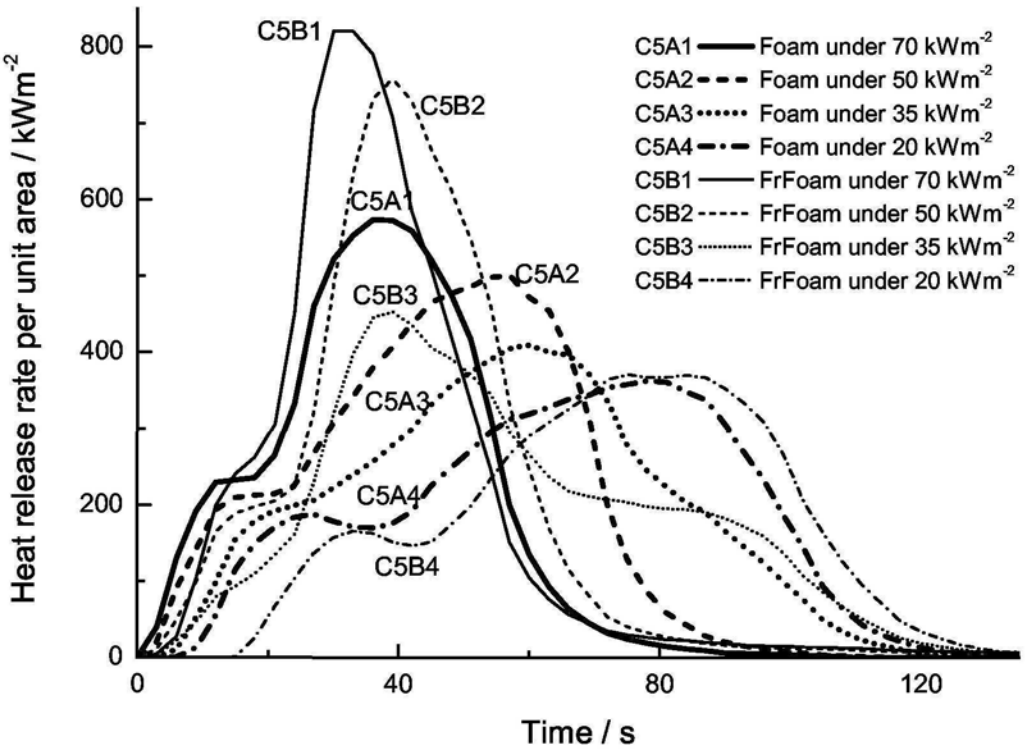

(a) Furniture foam

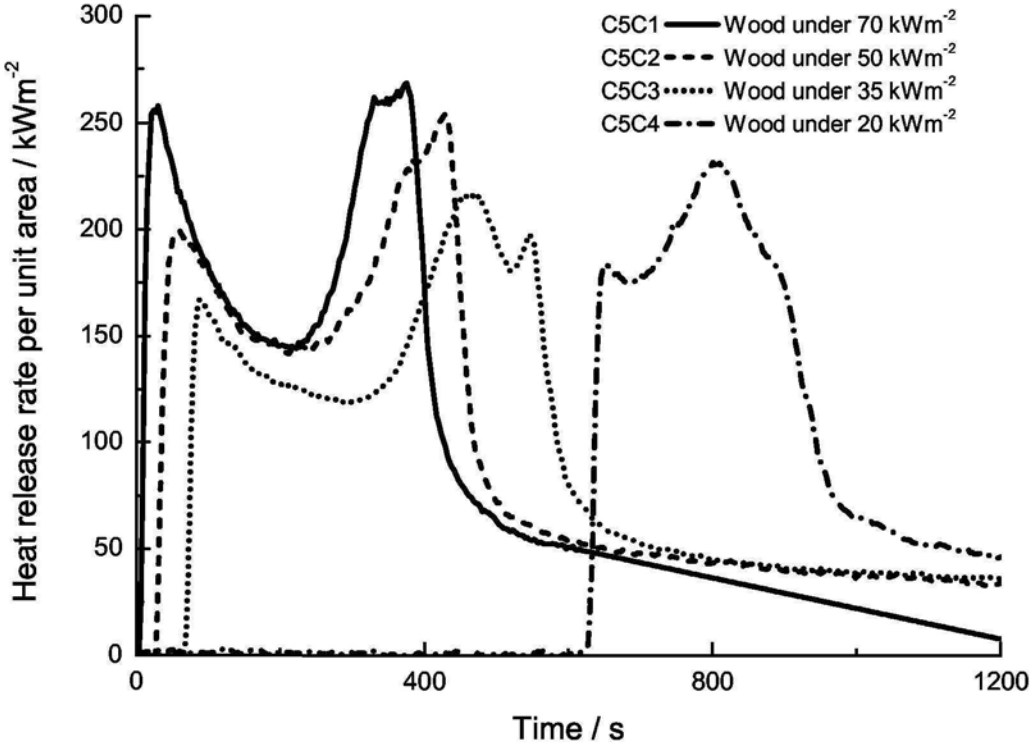

(b) Furniture wood

Figure 5.14: Heat release rate per unit area for furniture wood and foam

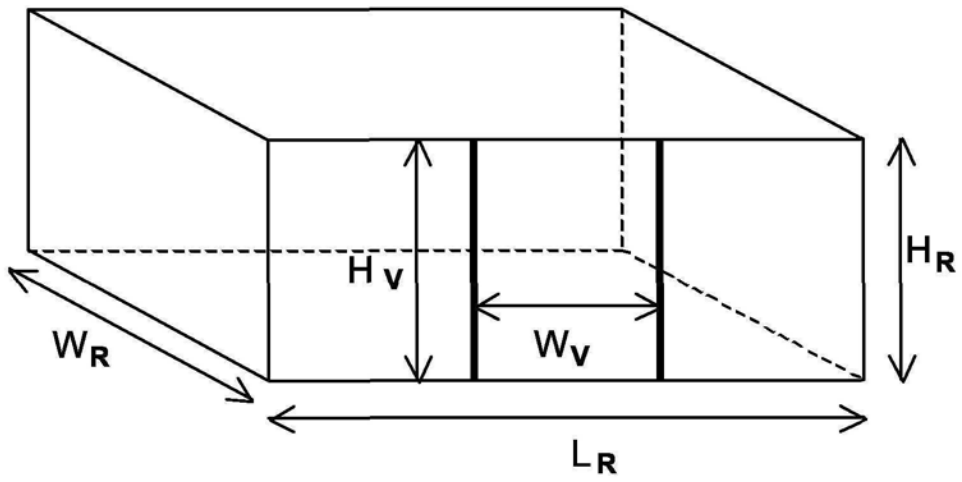

Figure 7.1: Geometry and dimensions of the compartment

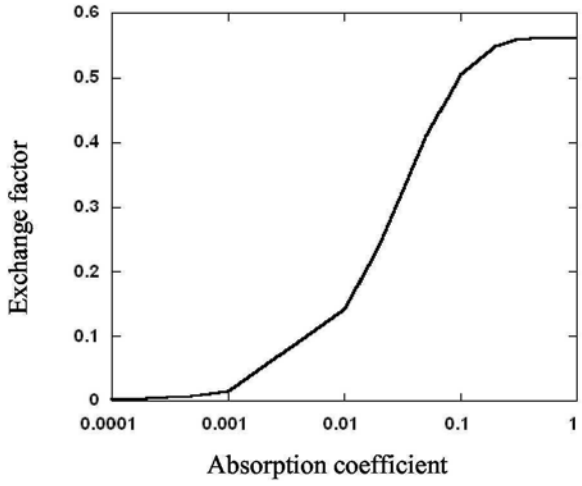

(a) Fire base to hot gas layer

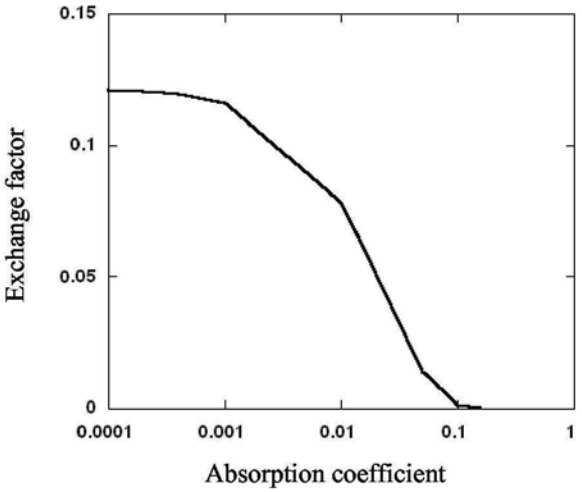

(b) Fire base to ceiling

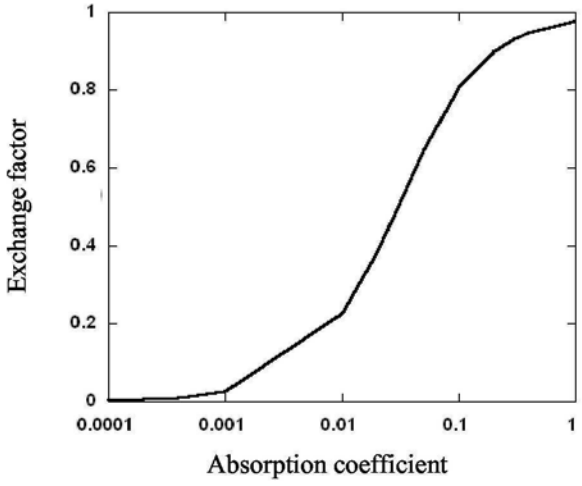

(c) Hot gas layer to ceiling

Figure 7.2: Exchange factors for radiation heat transfer

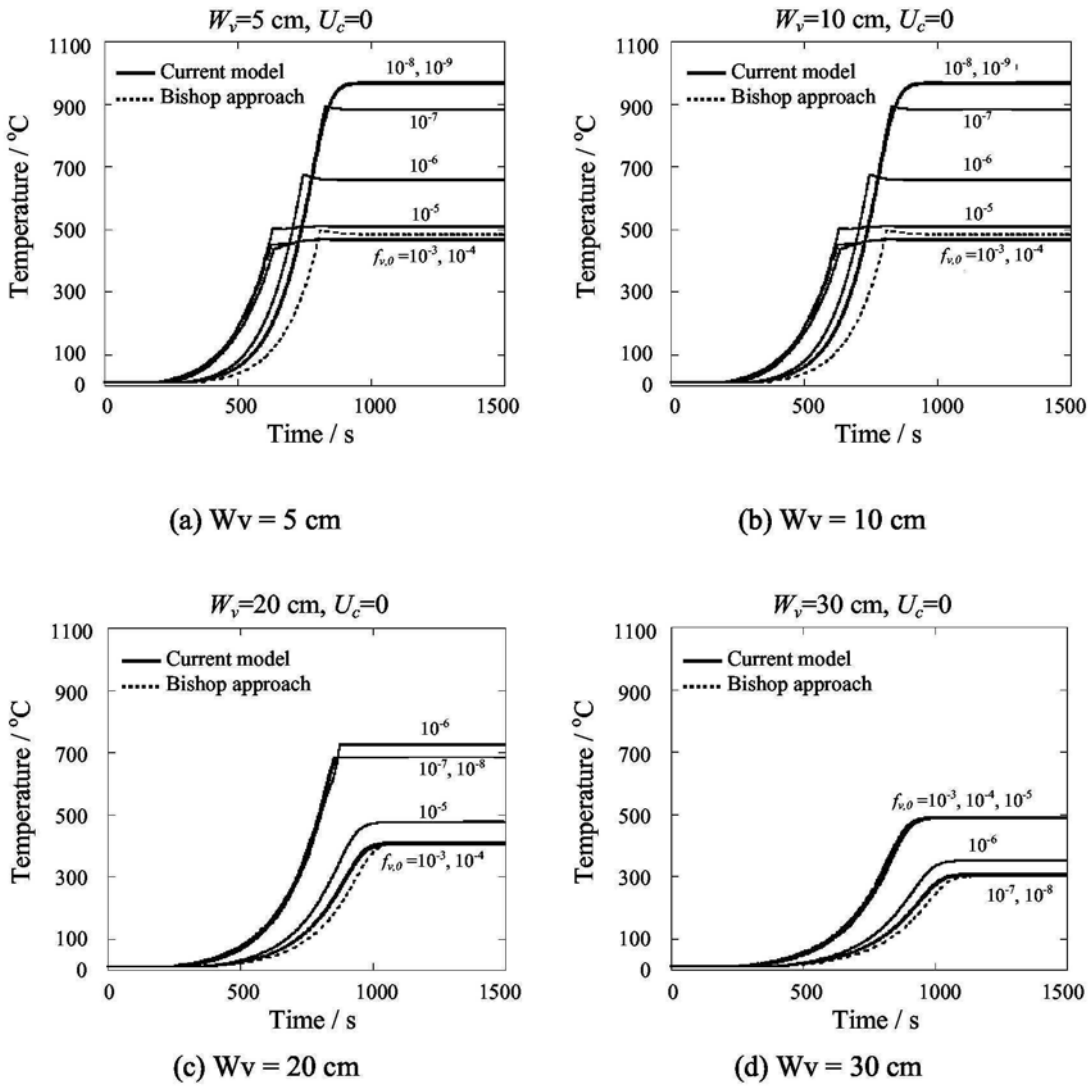

Figure 7.3: Temperature of the hot gas layer for $U_c = 0$

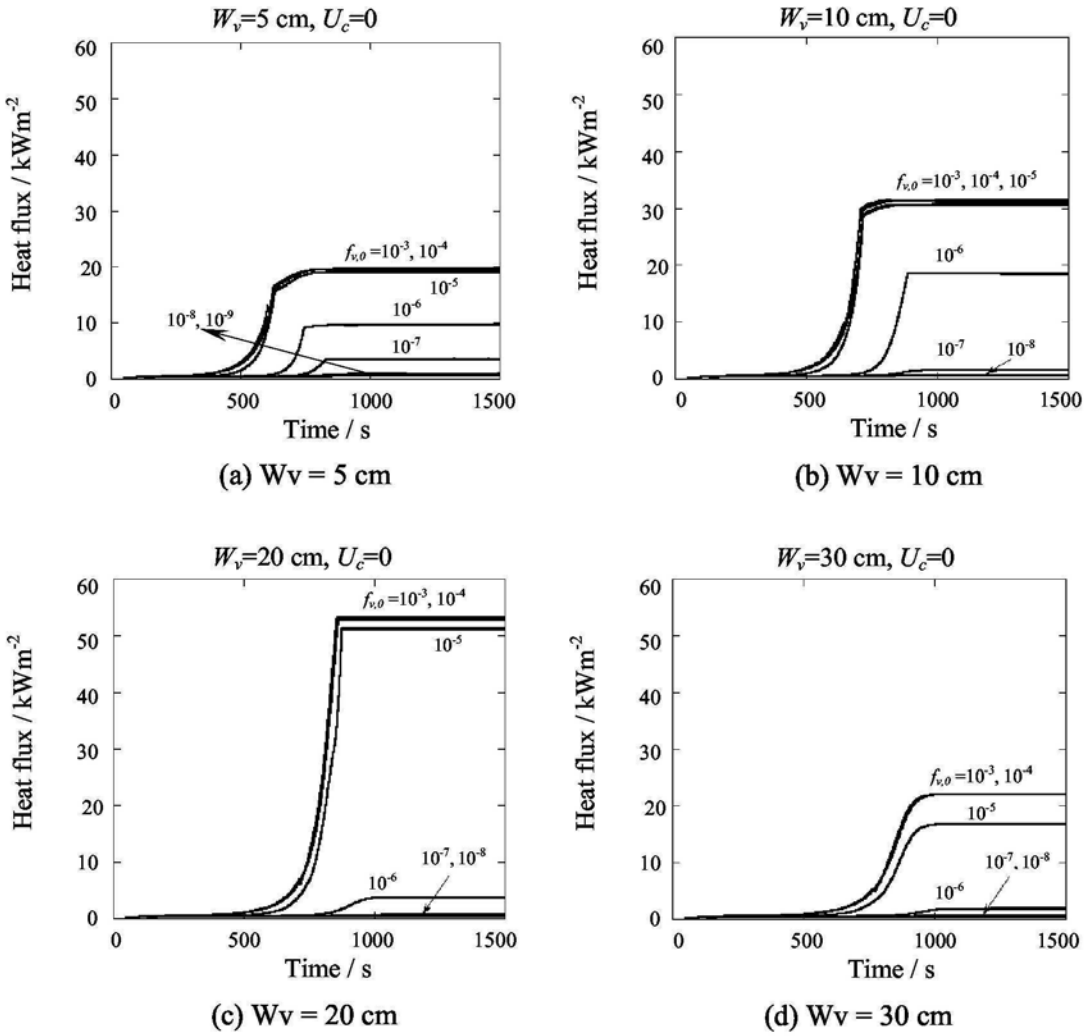

Figure 7.4: Radiative heat flux to the floor for $U_c = 0$

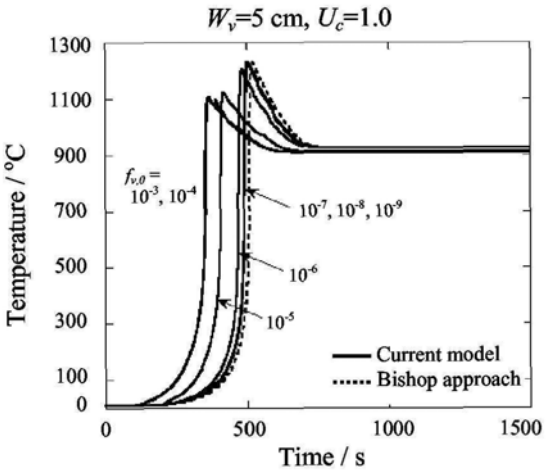

(a) Wv = 5 cm

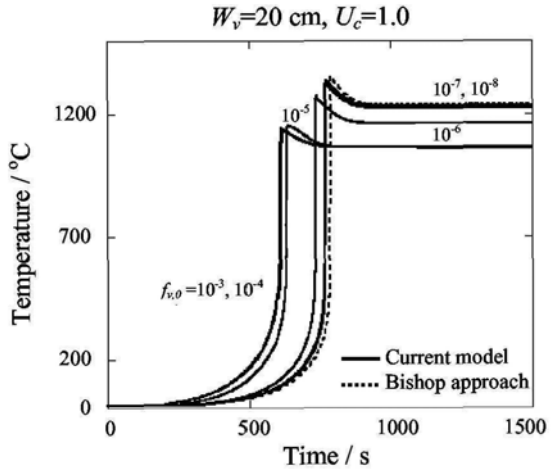

(b) Wv = 20 cm

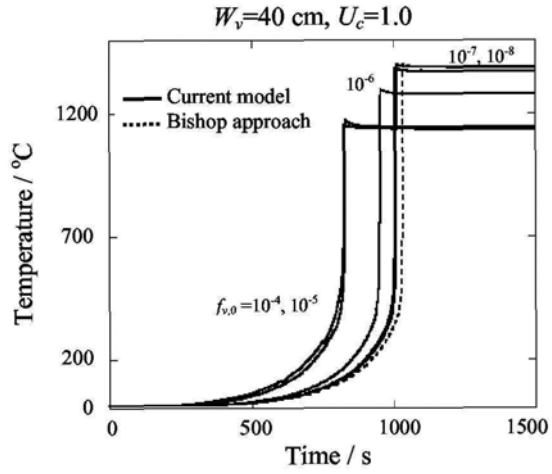

(c) Wv = 40 cm

Figure 7.5: Temperature of the hot gas layer for $U_c = 1.0$

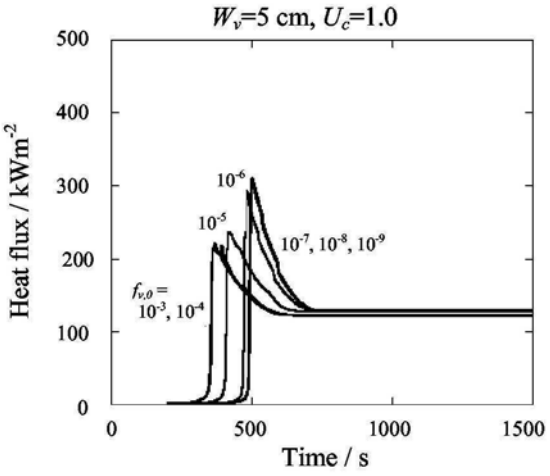

(a) Wv = 5 cm

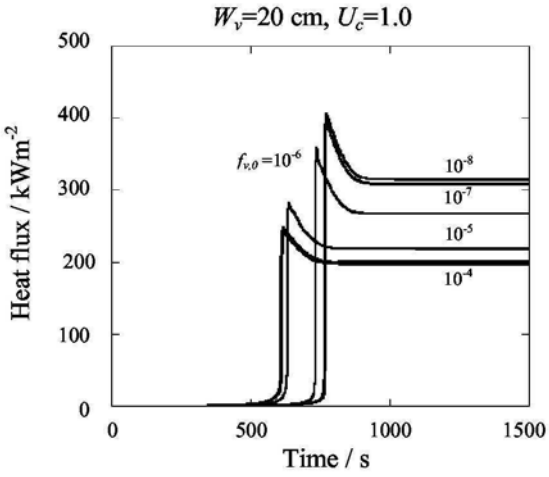

(b) Wv = 20 cm

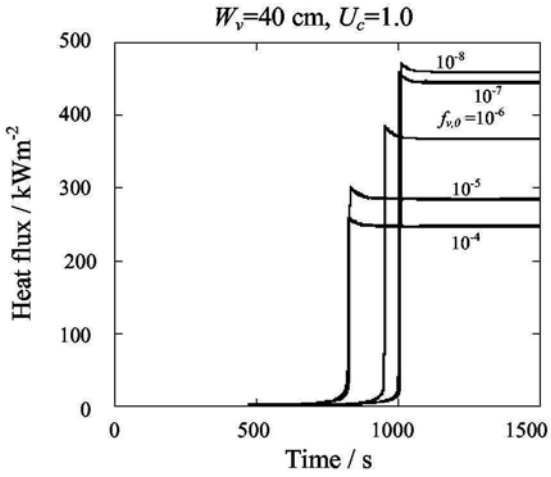

(c) Wv = 40 cm

Figure 7.6: Radiative heat flux to the compartment floor for $U_c = 1.0$

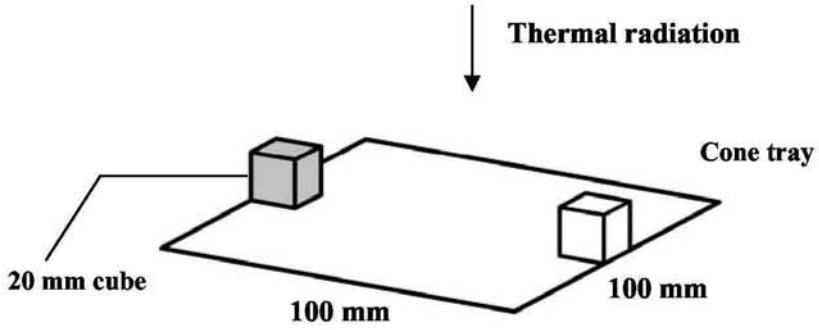

(a) Test C8A

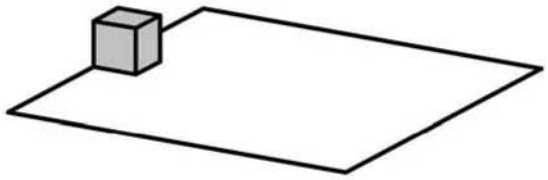

(b) Tests C8B, C8C, C8D, C8E

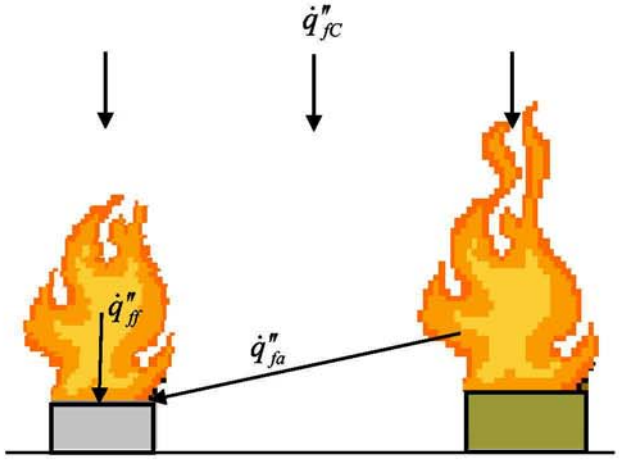

(c) Schematic view of heat fluxes

Figure 8.1: Schematic view of samples tested with cone calorimeter

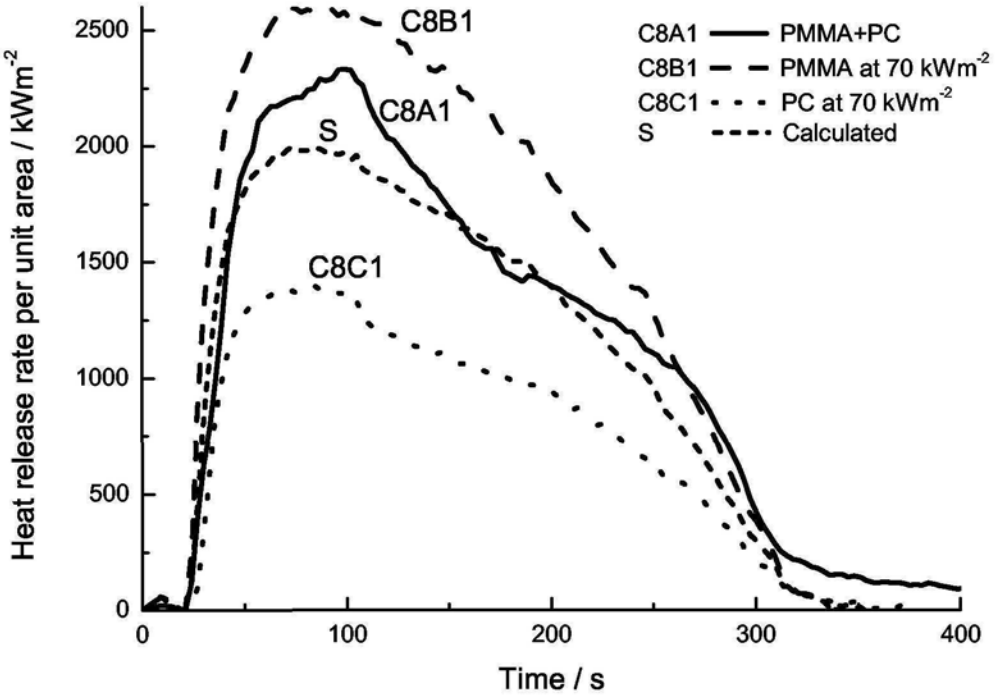

(a) Heat release rate per unit area

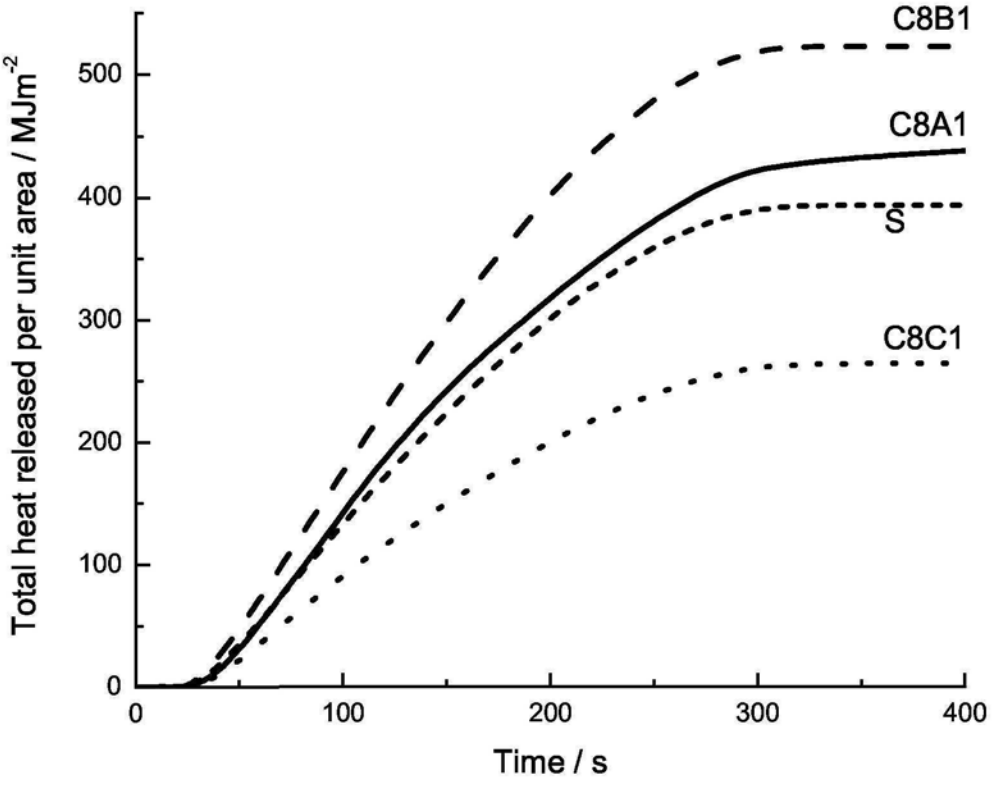

(b) Total heat released per unit area

Figure 8.2: Superposition results for cone test C8A1

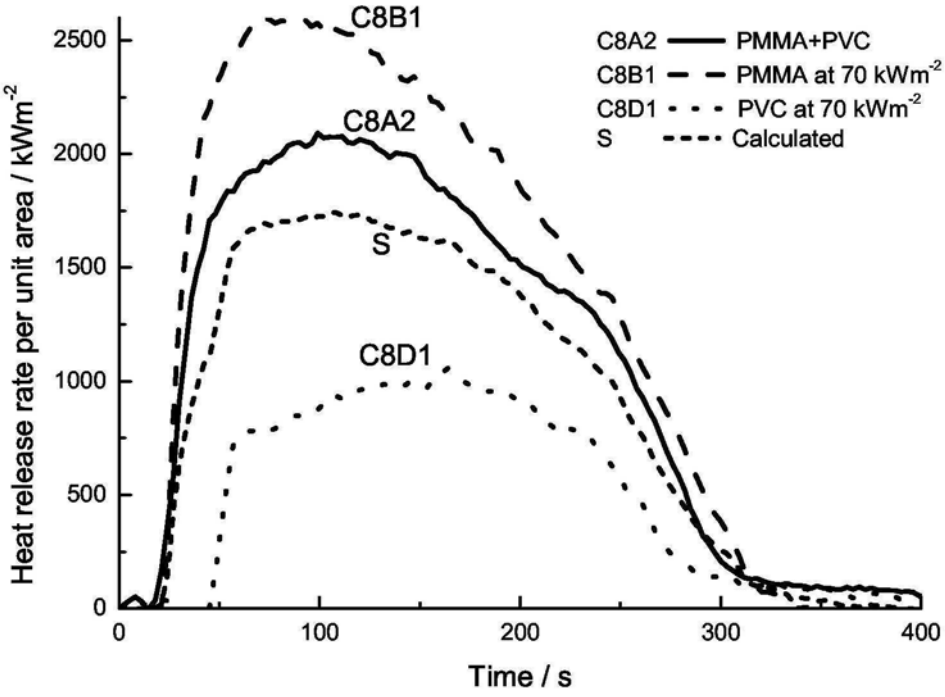

(a) Heat release rate per unit area

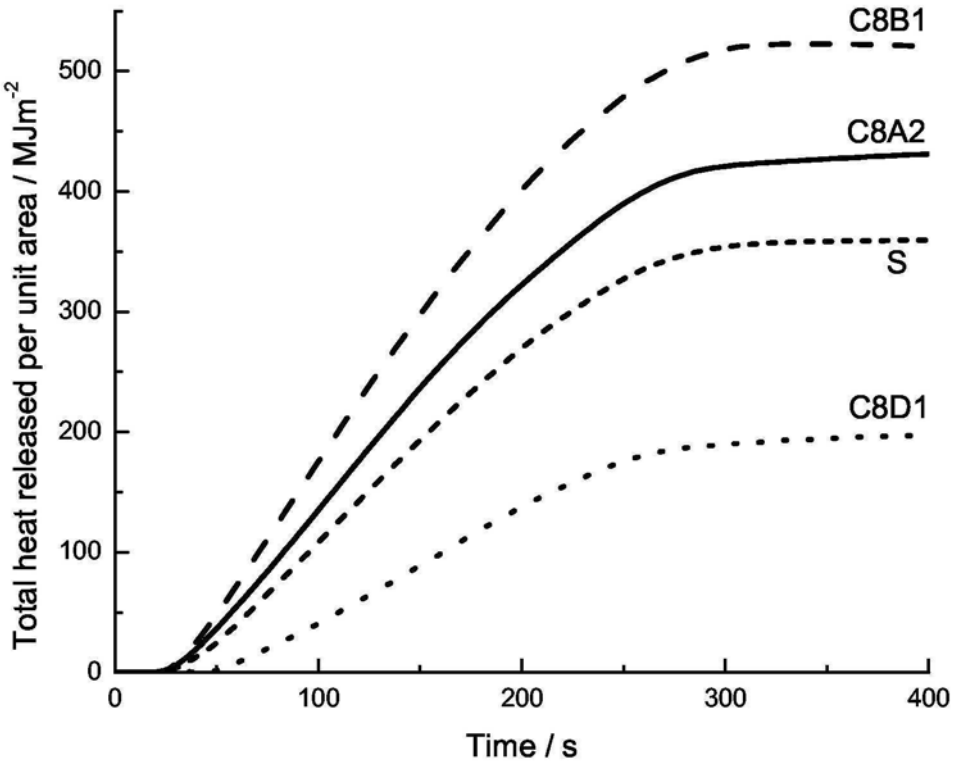

(b) Total heat released per unit area

Figure 8.3: Superposition results for cone test C8A2

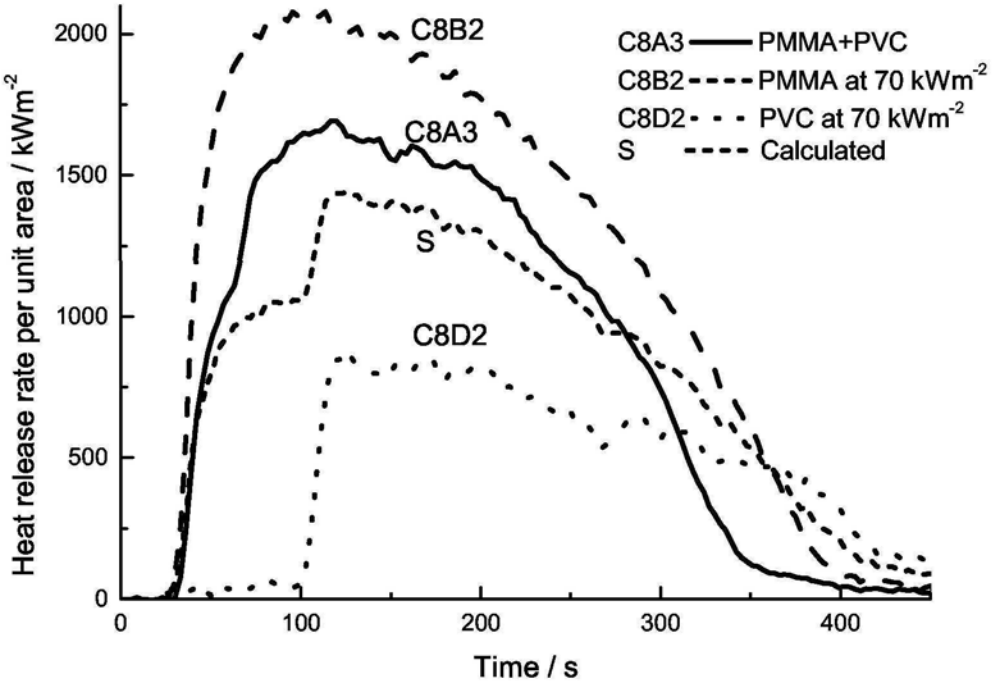

(a) Heat release rate per unit area

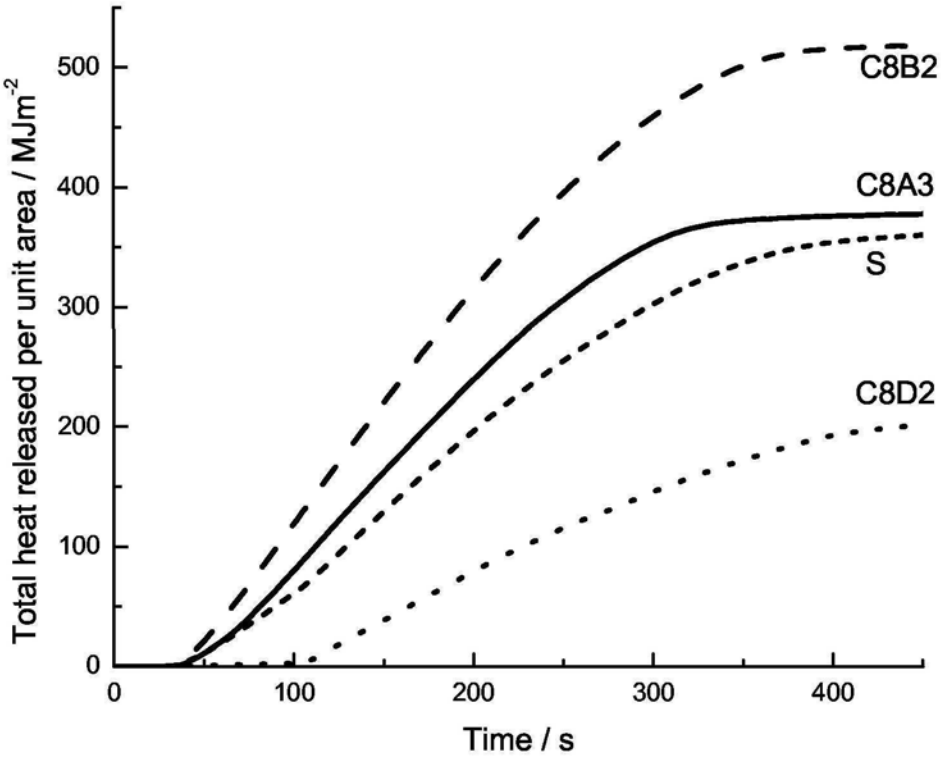

(b) Total heat released per unit area

Figure 8.4: Superposition results for cone test C8A3

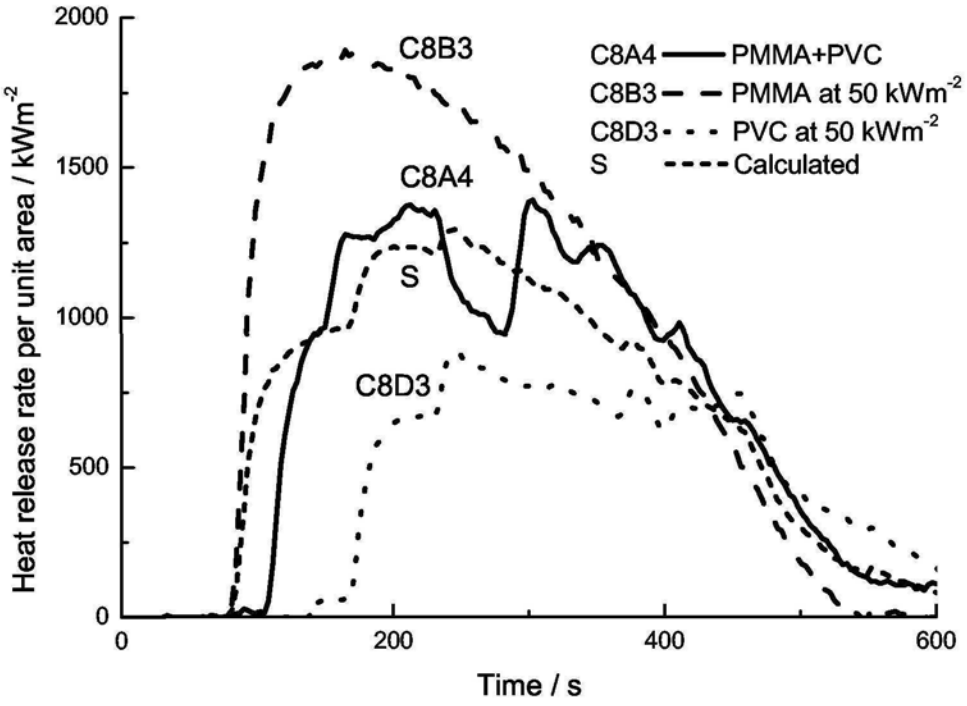

(a) Heat release rate per unit area

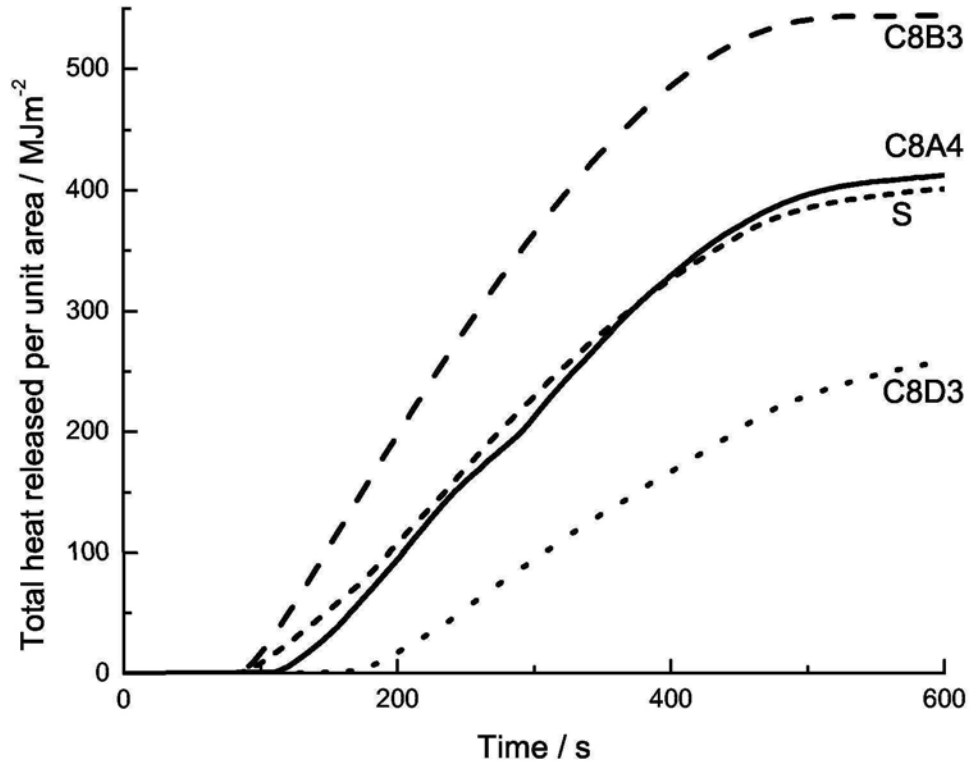

(b) Total heat released per unit area

Figure 8.5: Superposition results for cone test C8A4

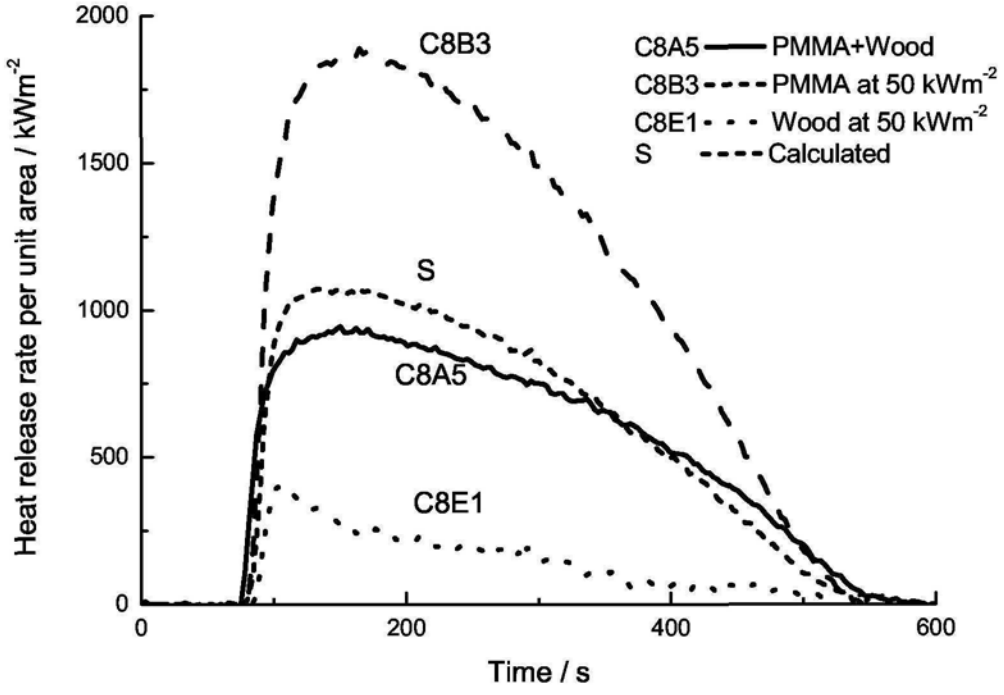

(a) Heat release rate per unit area

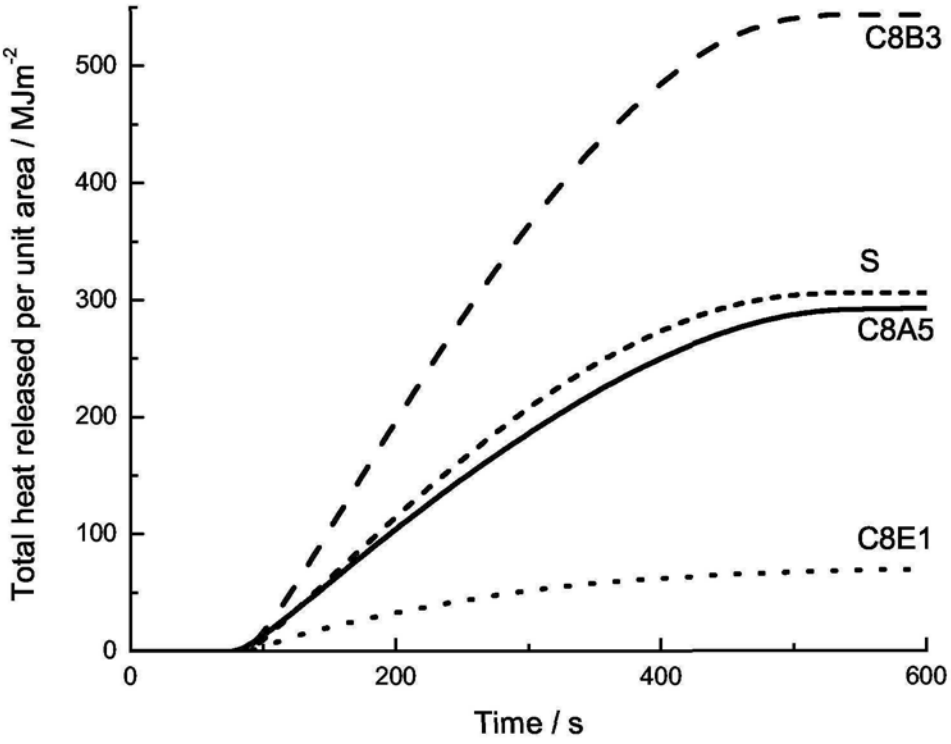

(b) Total heat released per unit area

Figure 8.6: Superposition results for cone test C8A5

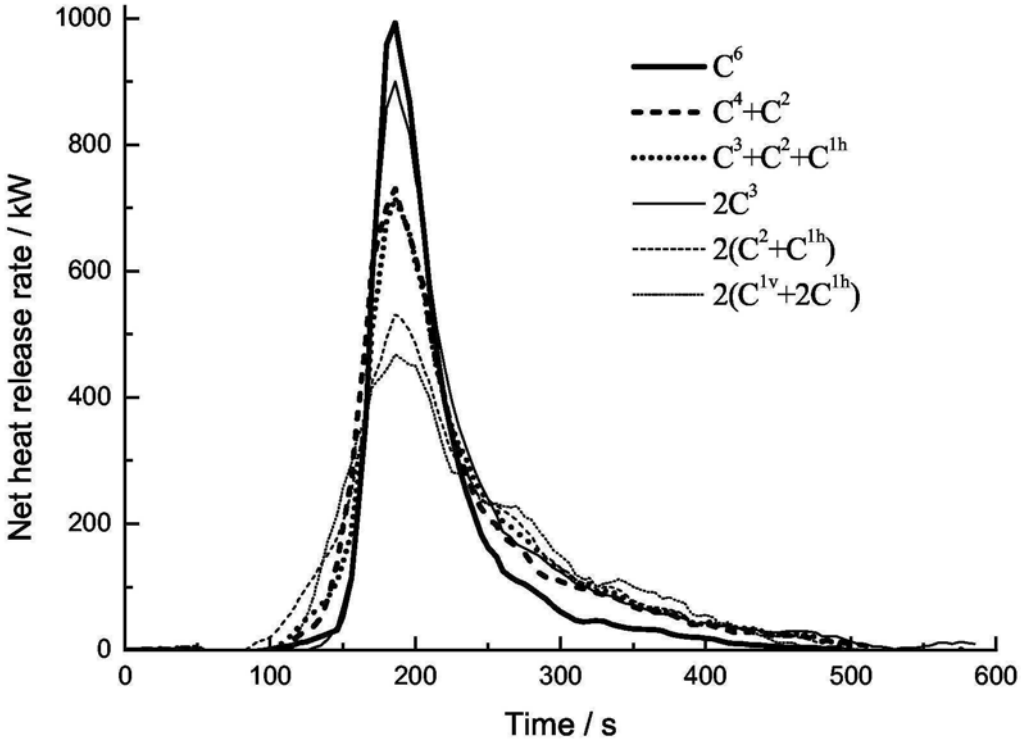

(a) Net heat release rate

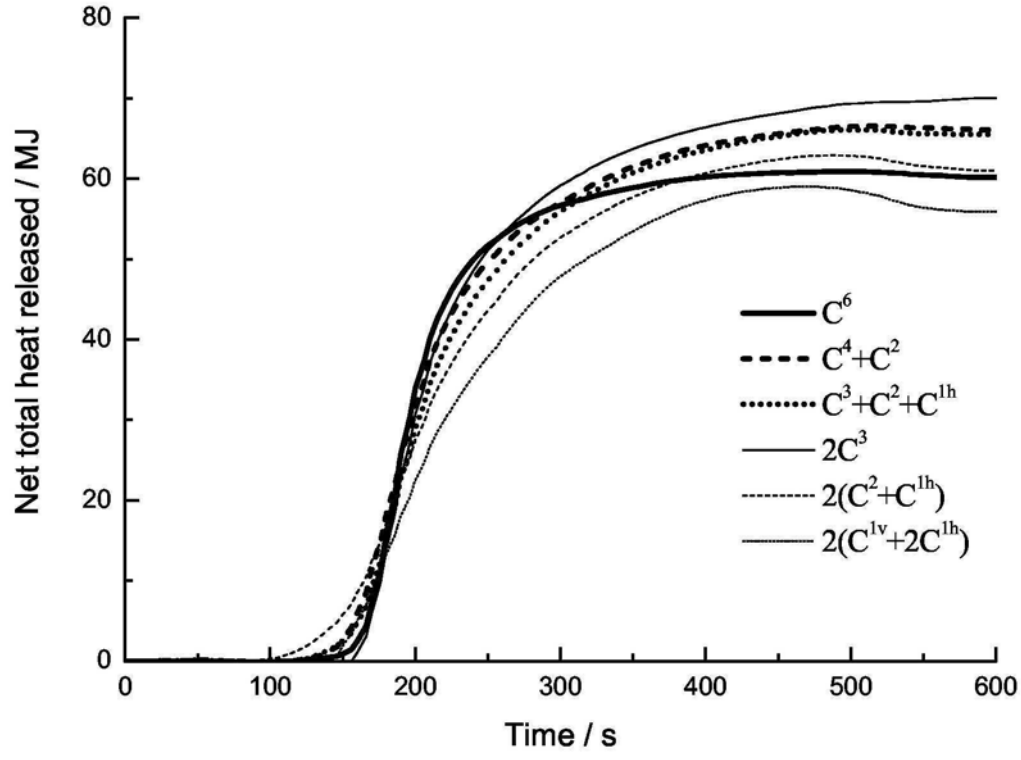

(b) Net total heat released

Figure 8.7: Superposition for full-scale burning tests on cushions

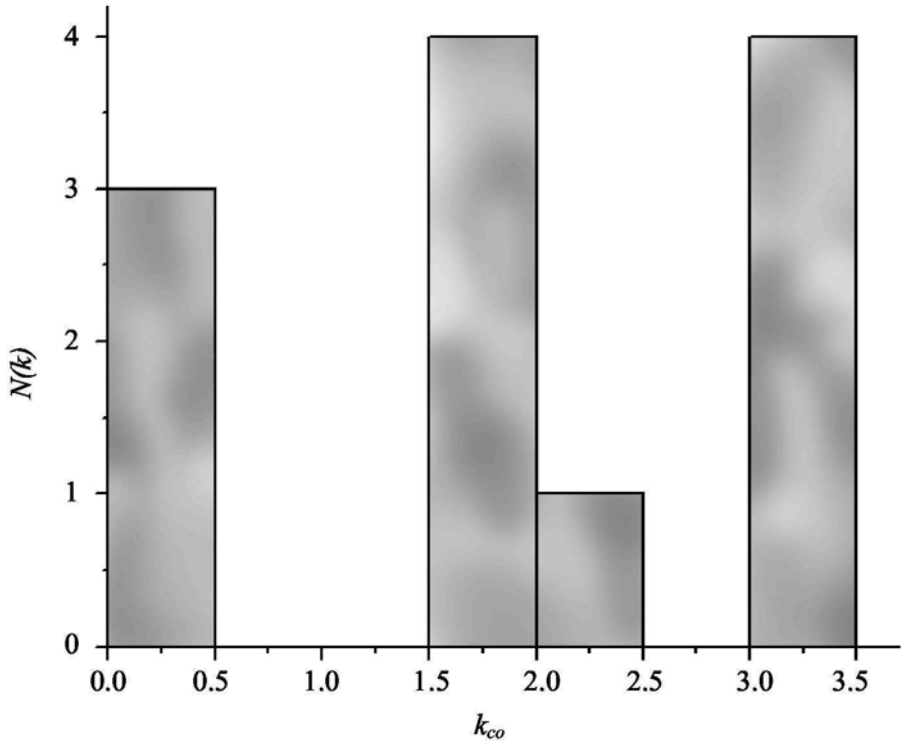

(a) Number distribution

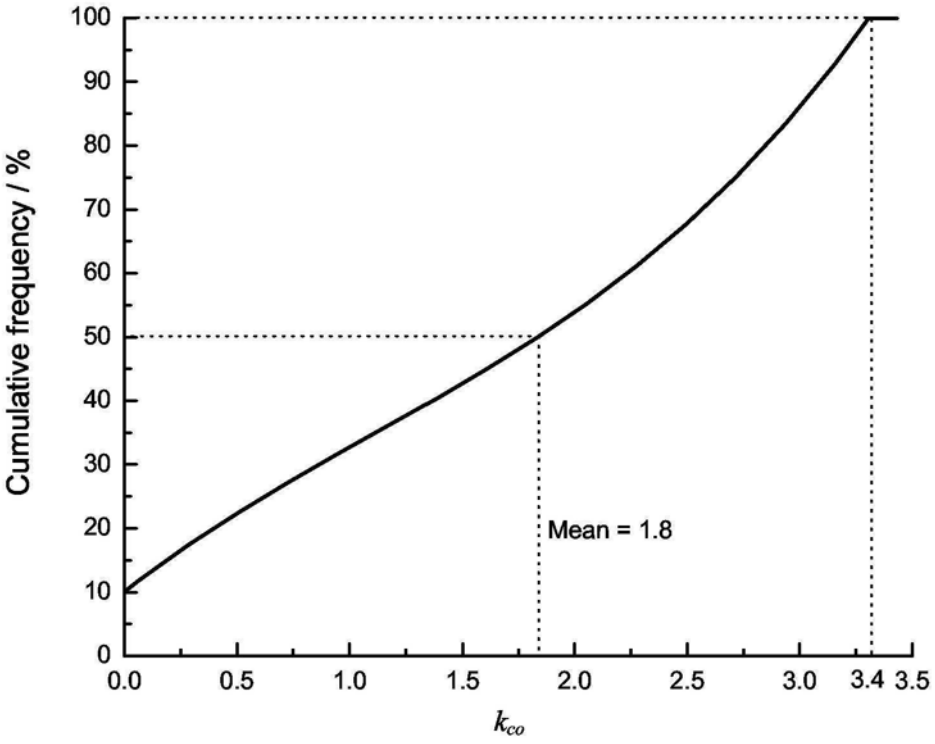

(b) Cumulative frequency

Figure 9.1: Number distribution of the correction factor for [CO]

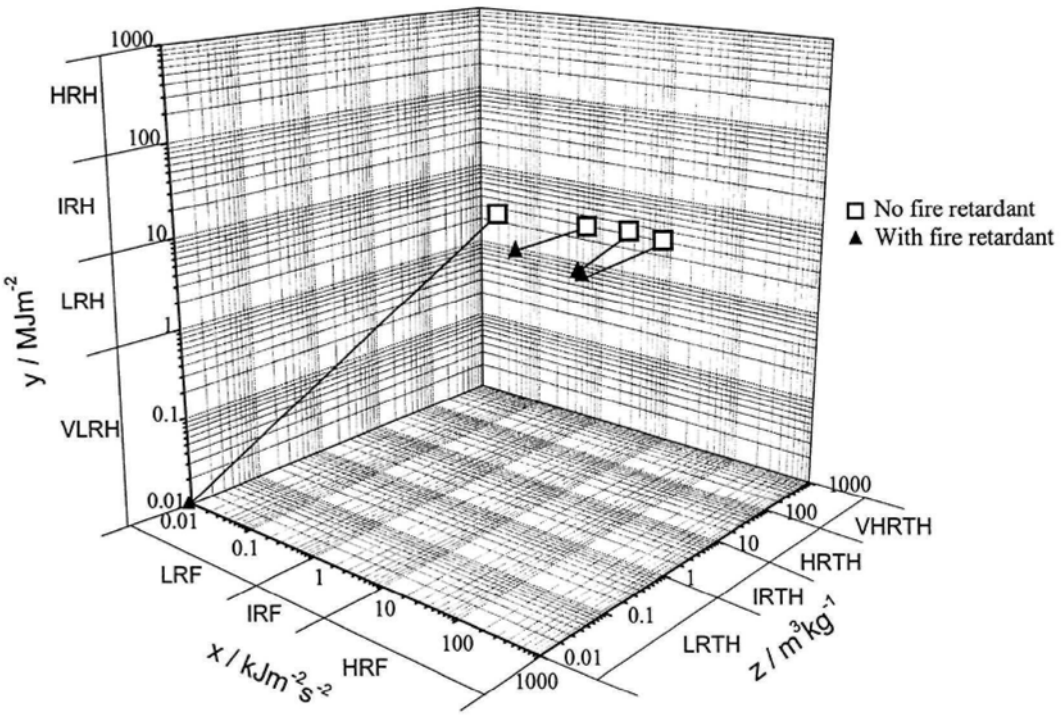

Figure 10.1: Risk diagram for burning furniture foam

APPENDIX A: ESTIMATION OF MOLECULAR WEIGHT OF THE EXHAUST GAS

Average molecular weight of exhaust gas is:

$$M_e = \sum_i X_i M_i \qquad (A1)$$

Normally, most of the combustion products are carbon dioxide or water, or both of them. Carbon dioxide might have the maximum values of $X_i M_i$ and water might have the minimum one, though molecular weights of some nitrogen oxides are higher than that of carbon dioxide and hydrogen is 'lighter' than water. Therefore, carbon dioxide can further increase the value of M_e while water can just reverse this effect.

Note that hydrogen is not a common fuel that satisfies the oxygen consumption theory with constant 13.1 MJ/kg oxygen consumed. The heat generated by hydrogen combustion is 16.35 MJ/kg oxygen consumed [Babrauskas and Grayson 1992]. Corrections should be considered if hydrogen is a fuel, but it can be neglected in the combustion products under normal conditions. Hydrogen fuel is not included herein as an uncommon fuel. Hydrocarbon and carbon are taken as the main parts of fuels in this analysis.

Consider two fuels under limiting conditions with a volumetric ratio of oxygen to air of 1 to 5.

In all the combustion products of hydrocarbon fuels, the ratio of water to carbon dioxide for methane combustion is the highest, and so it might have the smallest value of M_e. Carbon fuel can produce most carbon dioxide. Therefore, these two fuels can be taken as limiting fuels.

- Reaction 1: methane combustion

$$CH_4 + 2O_2 \rightarrow CO_2 + 2H_2O$$

2 moles of oxygen in 10 moles of air to give 1 mole of carbon dioxide and 2 moles of water vapour, leaving 8 moles of air unused.

Assuming all the oxygen will be consumed, the molecular weight of exhaust gas is:

$$M_e = \frac{M_{CO_2} + 2M_{H_2O} + 8M_a}{11} \qquad (A2)$$

Putting in numerical values, M_e is 28.4.

- Reaction 2: carbon combustion

$$C + O_2 \rightarrow CO_2$$

1 mole of oxygen in 5 moles of air is changed into 1 mole of carbon dioxide, leaving 4 moles of air unused.

$$M_e = \frac{M_{CO_2} + 4M_a}{5} \qquad (A3)$$

Putting in numerical values, M_e is 32.

Average molecular weight of the exhaust gas would be decreased with the water content increased:

$$M_e = X_{H_2O} M_{H_2O} + (1 - X_{H_2O}) M_e^d \qquad (A4)$$

Taking a higher value of the water content in the exhaust gas, say 30%, and a lower value of the average molecular weight of other mixed dry gas M_e^d, say 29 would give M_e of 25.7.

In summary, the limiting range of M_e varies from 25.7 to 32 if water content is less than 30% in the exhaust gas.

However, the range of M_e is lying from 28.4 to 32 if there is no additional water except that formed as combustion product.

APPENDIX B: EXPANSION FACTOR UNDER WATER SUPPRESSION

Assuming there are β moles of products generated by consuming 1 mole of oxygen:

Fuel + $O_2 \rightarrow \beta$. Products including H_2O and CO_2

The expansion factor α is defined in the literature by Parker [1982, 1984] as:

$$\alpha = 1 + X^o_{O_2}(\beta - 1) \qquad (B1)$$

Values of α are 1, 1.21 and 1.105 for the fuel being carbon $(\beta = 1)$, hydrogen $(\beta = 2)$ and methane $(\beta = 1.5)$ respectively when $X^o_{O_2}$ is 21%, as the reactions are:

$$C + O_2 \rightarrow CO_2$$

$$2H_2 + O_2 \rightarrow 2H_2O$$

$$CH_4 + 2O_2 \rightarrow 2H_2O + CO_2$$

Assuming the total mole flow rate is not changed, concentration of oxygen will be diluted by water vapour:

$$X^o_{O_2} = X^{A^o}_{O_2}\left(1 - X^o_{H_2O}\right) \qquad (B2)$$

where $X_{O_2}^{A^o}$ is the oxygen concentration of the incoming gas with water removed; and $X_{H_2O}^{o}$ is the mole fraction of water vapour in the incoming gas.

Defining the expansion factor under water suppression as α^w, it is given by putting equation (B2) in (B1):

$$\alpha^w = 1 + X_{O_2}^{A^o}\left(1 - X_{H_2O}^{o}\right)(\beta - 1) \qquad (B3)$$

Rearranging:

$$\alpha^w = 1 + X_{O_2}^{A^o}(\beta - 1) - X_{O_2}^{A^o} X_{H_2O}^{o}(\beta - 1) \qquad (B3a)$$

Note that incoming gas is assumed to be dry in α. $X_{O_2}^{o}$ in equation (B1) is in fact $X_{O_2}^{A^o}$ with water removed before measurement by the analyzer. Substituting equation (B1) into (B3a):

$$\alpha^w = \alpha - X_{O_2}^{A^o} X_{H_2O}^{o}(\beta - 1) \qquad (B4)$$

Taking $X_{O_2}^{A^o}$ as 21% if the incoming air is fresh, equation (B4) is given by:

$$\alpha^w = \alpha - 0.21 X_{H_2O}^{o}(\beta - 1) \qquad (B5)$$

The range of α^w varies from $\left(\alpha - 0.21X^o_{H_2O}\right)$ to α.

The relation between incoming gas and exhaust gas can be expressed as:

$$\frac{\dot{m}_e}{M_e} = (1-\phi)\frac{\dot{m}_a}{M_a} + \alpha^w \phi \frac{\dot{m}_a}{M_a} \qquad (B6a)$$

Or rewriting the above equation by assuming M_e is the same as M_a:

$$\dot{m}_a = \frac{\dot{m}_e}{1+\phi(\alpha^w - 1)} \qquad (B6b)$$

Substituting equation (B5) into equations (B6a) and (B6b), the corrected relation of total exhaust gas $\dot{m}_e$ and incoming gas $\dot{m}_a$ upon discharging water is:

$$\begin{cases} \dfrac{\dot{m}_e}{M_e} = (1-\phi)\dfrac{\dot{m}_a}{M_a} + \left[\alpha - 0.21X^o_{H_2O}(\beta - 1)\right]\phi\dfrac{\dot{m}_a}{M_a} & (B7a) \\ \dot{m}_a = \dfrac{\dot{m}_e}{1+\phi\left[\alpha - 1 - 0.21X^o_{H_2O}(\beta - 1)\right]} & (B7b) \end{cases}$$

As α is commonly taken as 1.105 (based on $\beta = 1.5$), equation (B7) becomes:

$$\begin{cases} \dfrac{\dot{m}_e}{M_e} = (1-\phi)\dfrac{\dot{m}_a}{M_a} + \left[\alpha - 0.105X^o_{H_2O}\right]\phi\dfrac{\dot{m}_a}{M_a} & (B8a) \\ \dot{m}_a = \dfrac{\dot{m}_e}{1+\phi\left[\alpha - 1 - 0.105X^o_{H_2O}\right]} & (B8b) \end{cases}$$

APPENDIX C: BASIC CONCEPTS OF RADIATION

Thermal radiation in terms of electromagnetic wave would be emitted from objects at non-zero temperature [e.g. Hottel and Sarofim 1967; Edwards 1985; Modest 1993; Mbiock and Weber 2000]. The radiation flux E_∞ radiated from an object per unit time per unit area is proportional to the fourth power of its temperature T t hrough the emissivity ε, radiation flux for a black body E_b and the Stefan-Boltzman constant σ:

$$E = \varepsilon E_b = \varepsilon \sigma T^4 \qquad (C1)$$

The fundamental quantity of radiation transport is the spectral intensity I_λ, which is defined as the radiant energy per unit time per unit wavelength interval passing per unit surface area normal to the direction Ω into a solid angle $d\Omega(\theta, \omega)$ centered around Ω. The intensity $I_{\lambda,\theta}$ across a surface of an arbitrary orientation θ is:

$$I_{\lambda,\theta} = I_\lambda \cos\theta \qquad (C2)$$

The total net radiative energy flux E is:

$$E = \int_0^{4\pi} I_\lambda \cos\theta \, d\Omega \qquad (C3)$$

Planck's Law can be applied to a perfect emitter or absorber to calculate the energy spectrum of the radiation emitted from a surface using quantum theory. For a

blackbody radiator with a small opening from an enclosed cavity, the spectral intensity of blackbody radiation, $I_{b\lambda}$, also known as the Planck function, is given by [Tien et al. 2002]:

$$I_{b\lambda} = \frac{2hc^2}{n^2\lambda^5\left(e^{\frac{hc}{n\lambda kT}} - 1\right)} \qquad (C4)$$

In the above equation, c is the speed of light, n is the index of refraction for the medium and k is the constant.

The total radiant intensity for a blackbody, I_b, can be obtained by integrating over all wavelengths according to Stefan-Boltzman law, giving

$$I_b = \int_0^\infty I_{b\lambda} d\lambda = \frac{n^2\sigma T^4}{\pi} \qquad (C5)$$

The variation of radiation intensity for a real object will not follow the Planck's Law. The Krichhoff's Law can be applied to study the emissivity and absorption of a real object:

$$\varepsilon_{\lambda,\theta,T} = \alpha_{\lambda,\theta,T} \qquad (C6)$$

Under steady temperature, the monochromatic emissivity from a certain direction is equal to the absorption from the same direction.

When the incident radiation is independent of the incident angle (diffuse reflect) and has the same spectral proportions as a blackbody radiator (gray body), the Krichhoff's law can be revised as:

$$\varepsilon_T = \alpha_T \qquad (C7)$$

REFERENCES

Adiga K.C., Ramaker D.E., Tatem P.A. and Williams F.W., 1990
Numerical Predictions for a Simulated Methane Fire
Fire Safety Journal, Vol. 16, No. 6, pp. 443-458

ASTM E 1537-02a, 2002
Standard Test Method for Fire Testing of Upholstered Furniture
American Society for Testing and Materials (ASTM), USA

ASTM E 1678-02, 2002
Standard Test Method for Measuring Smoke Toxicity for Use in Fire Hazard Analysis
American Society for Testing and Materials (ASTM), USA

ASTM E 1354 – 04a, 2004
Standard Test Method for Heat and Visible Smoke Release Rates for Materials and Products Using an Oxygen Consumption Calorimeter
American Society for Testing and Materials (ASTM), USA

ASTM E 1474 – 04, 2004
Standard Test Method for Determining the Heat Release Rate of Upholstered Furniture and Mattress Components or Composites Using a Bench Scale Oxygen Consumption Calorimeter
American Society for Testing and Materials (ASTM), USA

Au Yeung H.W. and Chow W.K., 2002
Necessity of Testing Furniture Materials with a Cone Calorimeter
International Journal on Engineering Performance-based Fire Codes, Vol. 4, No. 3, pp. 60-67

Babraukas V., 1979
Full Scale Burning Behaviour of Upholstered Chairs
NBS-TN 1103, National Bureau of Standards, Gaithersburg, Maryland

Babrauskas V., 1981.
Will the Second Item Ignite?
Fire Safety Journal, Vol. 4, pp. 281-292.

Babrauskas V., Lawson J., Walton W. and Twilley W., 1982
Upholstered Furniture Heat Release Rates Measured with the Furniture Calorimeter
NBSIR 82-2604, National Bureau of Standards, Gaithersburg, MD, USA

Babrauskas V., 1984
Development of the Cone Calorimeter-A Bench-scale Heat Release Rate Apparatus Based on Oxygen Consumption
Fire and Materials, Vol. 8, No. 2, pp. 81-94

Babrauskas V. and Grayson S.J., 1992
Heat Release in Fires
Elsevier Applied Science, London and New York

Babrauskas V., 1992
A Cone Calorimeter for Controlled-atmosphere Studies
Fire and Materials, Vol. 16, pp. 37-43

Babrauskas V., 1996
Toxic Fire Hazard Comparison of Pipe Insulations: The Realism of Full-scale Testing Contrasted with Assessments from Bench-scale Toxic Potency Data Alone
Interflam' 96: Proceedings of the seventh international conference

Babrauskas V., 1997
Sandwich Panel Performance in Full-scale and Bench-scale Fire Tests
Fire and Materials, Vol. 21, pp. 53-65

Babrauskas V., 2000
Fire Safety Improvements in the Combustion Toxicity Area: Is There a Role for LC50 Tests?
Fire and Materials, Vol. 24, pp. 113-119

Babrauskas V., 2002
Heat Release Rates
The SFPE Handbook of Fire Protection Engineering, 3rd Edition, Section 3, Chapter 1, pp. 3-1 to 3-37, The National Fire Protection Association, Quincy, MA, USA.

Babrauskas V., 2003
Ignition Handbook: Principles and Applications to Fire Safety Engineering, Fire Investigation, Risk Management and Forensic science
Issaquah, Wash.: Fire Science Publishers: Society of Fire Protection Engineers

BD Code, 1996a
Codes of Practice for Fire Resistance Construction
Buildings Department, Hong Kong

BD Code, 1996b
Codes of Practice for the Provision of Means of Escape in Case of Fire, Buildings Department, Hong Kong

BD Code, 2004
Codes of Practice for Means of Access for Firefighting and Rescue, Buildings Department, Hong Kong

Beaulieu P.A. and Dembsey N.A., 2005
Enhanced Equations for Oxygen and Carbon Dioxide Calorimetry
Proceedings in Fire and Materials 2005 Conference, 31 January – 1 February, 2005, San Francisco, CA, USA

Birky M.M., Halin B.M., Caplan Y.H., Fisher R.S., McAllister J.M., and Dixon A.M., 1979
Fire Fatality Study
Fire and Materials, Vol. 3, pp. 211-217

Bishop S.R., Holborn P.G., Beard A.N. and Drysdale D.D., 1993
Nonlinear Dynamics of Flashover in Compartment Fires
Fire Safety Journal, Vol. 21, pp. 11-45

Brohez S., Delvosalle C., Marlair G. and Tewarson A., 1998
Accurate Calculations of Heat Release in Fires
13th international congress of chemical and process engineering (2nd symposium on environmental and safety engineering, CHISA'98), Praha, 23-28 August 1998

Brohez S., Delvosalle C., Marlair G. and Tewarson A., 1999
Soot Generation in Fires: An Important Parameter for Accurate Calculation of Heat Release
Fire Safety Science - Proceedings of the Sixth International Symposium, pp. 265-276

Brohez S., Delvosalle C., Marlair G. and Tewarson A., 2000
The Measurement of Heat Release from Oxygen Consumption in Sooty Fires
Journal of Fire Sciences, Vol. 18, pp. 327-353

Brohez S., 2005
Uncertainty Analysis of Heat Release Rate Measurement from Oxygen Consumption Calorimetry
Fire and Materials, Volume 29, Issue 6, pp. 383-394

BS 476, 1972
Fire Tests on Building Materials and Structures – Part 8: Test methods and criteria for the fire resistance of elements of building construction
British Standards Institution (BSI), UK

BS 476, 1979
Fire Tests on Building Materials and Structures – Part 5: Method of Test for Ignitibility
British Standards Institution (BSI), UK

BS 7974, 2001
Application of Fire Safety Engineering Principle to the Design of Buildings
British Standards Institution (BSI), UK

BS EN ISO 4589:2, 1999
Plastics – Determination of Burning Behaviour by Oxygen Index – Part 2: Ambient Temperature Test
British Standard Institute (BSI), UK

BS ISO TR 13387:3, 1999
Fire Safety Engineering – Part 3: Assessment and Verification of Mathematical Fire Models
British Standard Institute (BSI), UK

BS EN 13823: 2002
Reaction to Fire Tests for Building Products - Building Products Excluding Floorings Exposed to the Thermal Attack by a Single Burning Item
British Standard Institute (BSI), UK

Budnick E.K. and Klein D.P., 1979
Mobile Home Fire Studies: Summary and Recommendation
NBSIR 79-1720, National Bureau of Standards, Gaithersburg, Maryland

Bukowski R.W., Clarke III.F.B., Hall Jr.J.R. and Stiefel S.W., 1990
Fire Risk Assessment Method: Case Study 1, Upholstered Furniture in Residences
NFPA, MA, USA

Chow W.K. and Cheung K.C., 1996
Aspect of fires for factories in Hong Kong
Journal of Applied Fire Science, Vol. 5, No. 1, pp. 17-32

Chow W.K., 1998
Building Fire Zone Models
The Hong Kong Polytechnic University, Hong Kong, China

Chow W.K., 1999
Predictability of Flashover by Zone Models
Journal of Fire Sciences, Vol. 16, pp. 335-350

Chow W.K., 2001a
Fire Dynamics
The Hong Kong Polytechnic University, Hong Kong, China

Chow W.K., 2001b
Fire Spread and Control
The Hong Kong Polytechnic University, Hong Kong, China

Chow W.K. and Lui C.H., 2001
A Fire Safety Ranking System for Karaoke Establishments in Hong Kong
Journal of Fire Sciences, Vol. 19, pp. 106-120

Chow W.K., 2002a
Review on Heat Release Rate of Burning Furniture
International Journal on Engineering Performance-based Fire Codes, Vol. 4, No. 2, pp. 54-59

Chow W.K., 2002b
Assessment on heat release rate of furniture foam arrangement by a cone calorimeter
Journal of Fire Sciences. Vol. 20, No. 4, pp. 319-328

Chow W.K. and Au Yeung H.W., 2002
Necessity of testing furniture materials with a cone calorimeter
International Journal on Engineering Performance-based Fire Codes, Vol. 4, No. 3, pp. 60-67

Chow W.K., 2003
Fire Safety in Green or Sustainable Buildings: Application of the Fire Engineering Approach in Hong Kong
Architectural Science Review, Vol. 46, No. 3, pp. 297-303

Chow W.K. and Au Yeung H.W., 2003
On the superposition of heat release rate for polymeric materials,
Architecture Science Review. Vol. 46, No. 2, pp. 145-150

Chow W.K., Zou G.W., Dong H. and Gao Y., 2003
Necessity of Carrying Out Full-scale Burning Tests for Post-flashover Retail Shop Fires
International Journal on Engineering Performance-Based Fire Codes, Vol. 5, No. 1, pp. 20-27

Chow W.K. and Han S.S., 2004
Full-scale Burning Tests on Heat Release Rates of Furniture
International Journal on Engineering Performance-Based Fire Codes, Vol. 6, No. 3, pp. 168-180

Chow W.K., 2004a
Special Issue on Full-scale Burning Tests
International Journal on Engineering Performance-Based Fire Codes, Vol. 6, No. 3

Chow W.K., 2004b
Fire safety in train vehicle: Design based on accidental fire or arson fire?
The Green Cross, March/April, 7 pages

Chow W.K., 2005
Building Fire Safety in the Far East
Architectural Science Review, Vol. 48, No. 4, pp. 285-294

Chow W.K., 2006
Experimental Studies on Fire Engineering Systems for Non-industrial Workplaces poster paper in CIBSE National Conference 2006, 21-22 March, The OCS Stand, Brit Oval Cricket Ground, London

Cleary T.G., Ohlemiller T.J. and Villa K.M., 1994
Influence of Ignition Source on the Flaming Fire Hazard of Upholstered Furniture
Fire Safety Journal, Vol. 23, pp. 79-102

Consumer Protection, 1988
The Furniture and Furnishings (Fire) (Safety) Regulations, No. 1324, UK

Cox G., 1995
Combustion Fundamentals of Fires
Academic Press, UK

CTB 133, 1991
California Technical Bulletin 133: Flammability Test Procedure for Seating Furniture for Use in Public Occupancies
BHFTI, North Highlands, CA, USA

Consumer Protection Circular, 1999
Consumer Goods Safety Ordinance: Mattresses and Upholstered Furniture - Flammability Standards
Customs and Excise Department, Hong Kong

de Ris J., 1979
Fire radiation - a review
17th Symposium (International) on Combustion, Pittsburgh, Pa.: Combustion Institute, pp. 1003-1016

Dlugogorski B.Z., Mawhinney J.R., Duc V.H., 1994
The Measurement of Heat Release Rates by Oxygen Consumption Calorimetry in Fires under Suppression
Fire Safety Science - Proceedings of the Fourth International Symposium, pp. 877-888.

Dowling V.P. and White N., 2004
Fire sizes in railway passenger saloons
Proceedings of the 6th Asia-Oceania Symposium on Fire Science & Technology, 17-20 March 2004, Daegu, Korea, (Eds: E.S. Kim et al.,) Korean Institute of Fire Science and Engineering, pp. 602-611

Drysdale D.D., 1999
An Introduction to Fire Dynamics, 2nd Ed.
Wiley, Chichester, UK

Duggan G.J., 1997
Usage of ISO 5660 data in UK railway standards and fire safety cases, Paper 3, Fire Hazards, Testing, Materials and Products
Proceedings of a One Day Conference, 13 March, 1997, Rapra Technology Ltd, Shawburry, Shrewsbury, Shropshire, U.K.

Edwards D.K., 1985
Handbook of Heat Transfer Fundamentals
McGraw-Hill Book Company, New York

Emmons H.W., 1978
Prediction of Fires in Buildings
Proceeding of the Seventeenth (International) Symposium on Combustion, pp. 1101-1112.

Enright P.A., 1995
A Study of Full-scale Room Fire Experiments", Fire engineering research report 95/2 School of engineering, University of Canterbury, New Zealand

Enright P.A. and Fleischmann C.M., 1999
Uncertainty of the Heat Release Rate Calculation of the ISO5660-1 Cone Calorimeter Standard Test Method
Fire Technology, Vol. 35, pp. 153-169

Fang J.B. and Breese J.N., 1980
Fire Development in Residential Basement Rooms
NBSIR 80-2120, National Bureau of Standards, Gaithersburg, Maryland

Fang J.B., 1975
Measurement of the Behaviour of Incidental Fires in a Compartment
NBSIR 75-679. National Bureau of Standards, Gaithersburg, Maryland

FSD Circular Letter 1/2000
Flammability Standards for Polyurethane (PU) Foam Filled Mattresses and Upholstered Furniture in Licensed Premises and Public Areas
Fire Services Department, Hong Kong

FSD Code, 2005
Codes of Practice for Minimum Fire Service Installations and Equipment and Inspection, Testing and Maintenance of Installations and Equipment
Fire Services Department, Hong Kong

Fletcher D.F., Kent J.H., Apfe V.B. and Green A. R., 1994
Numerical simulations of smoke movement from a pool fire in a ventilation tunnel
Fire Safety Journal, Vol. 23, No. 3, pp. 305-325

Fowell A.J., 1994
Fire and Flammability of Furnishings and Contents of Buildings
ASTM (STP 1233), 1916 Race Street, Philadelphia, PA 19103, USA

Friday P.A. and Mowrer F.W., 2001
Comparison of FDS model predictions with FM/SNL fire test data
NIST GCR 01-810, National Institute of Standards and Technology, US Department of Commerce, USA

Göransson U., 1993
Model, based on cone calorimeter results, for explaining the heat release rate growth of tests in a very large room
Interflam'93–Conference Proceedings of Sixth International Interflam Conference, Interscience Communications Ltd, London, UK, pp. 39-47

Gottuk D.T. and Lattimer B.Y., 2002
Effect of Combustion Conditions on Species Production
The SFPE Handbook of Fire Protection Engineering, 3rd Edition, Section 2, Chapter 5, pp. 2-54 to 2-82, National Fire Protection Association, Quincy, MA, USA

Graham T.L., Makhviladze G.M. and Roberts J.P., 1995
On the Theory of Flashover Development
Fire Safety Journal, Vol. 25, pp. 229-259

Grayson S.J. and Smith D.A., 1986
New Technology to Reduce Fire Losses & Costs
New York: Elsevier Applied Science Publishers

Hagglund B., Jannson R. and Onnermark B., 1974
Fire Development in Residential Rooms after Ignition from Nuclear Explosion
FOA C20016-DG (A3), Forsvarets Forskningsanstalt, Stockholm

Hagglund B., Jannson R. and Onnermark B., 1974
Fire Development in Residential Rooms after Ignition from Nuclear Explosion
FOA C20016-DG (A3), Forsvarets Forskningsanstalt, Stockholm

Han S.S. and Chow W.K., 2004
Review on Equations used in Calculating the Heat Release Rate in an Oxygen Consumption Calorimetry
Proceedings of 3rd Education Symposium on Advanced Fire Research and the Fire Conference 2004 – Total Fire Safety Concept, 6-7 December 2004, Hong Kong, China, Vol. 3, Paper 4

Han S.S. and Chow W.K., 2005
Cone Calorimeter Studies on Fire Behaviour of Polycarbonate Glazing Sheets
Journal of Applied Fire Science, Vol. 12, No. 3, pp. 245-261

Hottel H.C. and Sarofim A.F., 1967
Radiative Transfer
McGraw-Hill Book Company

Huggett C., 1980
Estimation of Rate of Heat Release by Means of Oxygen Consumption Measurements
Fire and Materials, Vol. 4, No. 2, pp. 61-65

ISO 9705: 1993(E)
Fire tests – Full-scale Room Test for Surface Products
International Standards Organization (ISO), Geneva, Switzerland

ISO/TR 9122-4: 1993(E)
Toxicity Testing of Fire Effluents – Part 4: The Fire Model (Furnaces and Combustion Apparatus Used in Small-scale Testing), First edition
International Organization for Standardization, Switzerland

ISO 3534-1: 1993(E/F)
Statistics – Vocabulary and Symbols – Part 1: Probability and General Statistical Terms, First edition
International Organization for Standardization, Switzerland

ISO 13344: 1996(E)
Determination of the Lethal Toxic Potency of Fire Effluents, First edition
International Organization for Standardization, Switzerland

ISO 5660: 2002(E)
Reaction-to-Fire Tests – Heat Release Rate, Smoke Production and Mass Loss Rate
International Organization for Standardization, Switzerland

Janssens M., 1991
Measuring Rate of Heat Release by Oxygen Consumption
Fire Technology, pp. 234-249

Janssens M., 2000
Heat Release Rate (HRR)
Ohlemiller, T.J., Johnsson, E.L., and Gann, R.G., eds., Measurement Needs for Fire Safety: Proceedings of an International Workshop (NISTIR 6527), pp. 186-206, National Institute of Standards and Technology, Gaithersburg, MD, USA

Janssens M., 2002
Calorimetry
The SFPE Handbook of Fire Protection Engineering, 3rd Edition, Section 3, Chapter 2, pp. 3-46 to 3-48, The National Fire Protection Association, Quincy, MA, USA

Kent J.H. and Honnery D.R., 1990
A soot formation rate map for a laminar ethylene diffusion flame
Combustion and Flame, Vol. 79, No. 3-4, pp. 287-299

Krasny J.F., Parker, W.J. and Babrauskas V., 2001
Fire Behaviour of Upholstered Furniture and Mattresses
New York: Noyes Publications

Krause R.F. and Gann R.G., 1980
Rate of Heat Release Measurements Using Oxygen Consumption
Journal of Fire and Flammability, Vol. 12, pp. 117-130

Lattimer B.Y. and Beitel J.J., 1998
Evaluation of Heat Release Rate Equations used in Standard Test Methods
Fire and Materials, Volume 22, Issue 6, pp. 167-173

Lee B.T. and Breese J.N., 1978
Submarine Compartment Fire Study – Fire Performance Evaluation of Hull Insulation
NBSIR 78-1548, National Bureau of Standards, Gaithersburg, MD, USA

Levin B.C., 1987
A summary of the NBS literature Reviews on the Chemical Nature and Toxic of the Pyrolysis and Combustion Products from Seven Plastics: Acrylonitrile-Butadiene-Styrenes (ABS), Nylons, Polyesters, Polyethylenes, Polystyrenes, Poly (Vinyl Chlorides), Rigid Polyurethane Foams
Fire and Materials, Vol. 11, pp. 143-157

Li Y.Z. and Chow W.K, 2004
Review and importance of thermal radiation in room fires
Proceedings of the Fire Conference 2004 – Total Fire Safety Concept, 6-7 December 2004, Hong Kong, China, Vol. 2, Paper 6

Liang F.M., Chow W.K. and Liu S.D., 2002
Preliminary Study on Flashover Mechanism in Compartment Fires
Journal of Fire Sciences, Vol. 20, pp. 87-112

Mbiock A., Weber R., 2000
Radiation in Enclosures
Springer-Verlag Berlin Heidelberg, New York

McCaffrey B.J., Quintiere J.D. and Harkleroad M.F., 1981
Esitmating Room Temperatures and the Likelihood of Flashover using Fire Test Data Correlation
Fire Technology, Vol. 17, pp. 98-119

McCaffrey B.J. and Harkleroad M., 1988
Combustion Efficiency, Radiation, CO and Soot Yield from a Variety of Gaseous, Liquid, and Solid Fueled Buoyant Diffusion Flames
Twenty-Second Symposium (international) on Combustion, pp. 1251-1261

Modest M.F., 1993
Radiative Heat Transfer
McGraw-Hill, New York

Mowrer F.W. and Williamson R.B., 1990
Methods to characterize heat release rate data
Fire Safety Journal. 16, pp. 367-387

Newman J.S., 2005
Application of Building-scale Calorimetry
Proceedings of the Eighth International Symposium on Fire Safety Science, Beijing, China, 18-23 September 2005

NFPA 101, 2000
Life Safety Code 2000
Ed. Quincy, MA: National Fire Protection Association, USA

NFPA 269, 2000
Standard Test Method for Developing Toxic Potency Data for Use in Fire Hazard Modeling
NFPA, USA

NFPA 272, 2003
Standard Method of Test for Heat and Visible Smoke Release Rates for Materials and Products Using an Oxygen Consumption Calorimeter
NFPA, USA

Novozhilov V., 2001
Computational fluid dynamics modeling of compartment fire
Progress in Energy and Combustion Science, Vol. 27, No. 6, pp. 611-666

Ogle R.A. and Schumacher J.L., 1998
Fire Patterns on Upholstered Furniture: Smoldering versus Flaming Combustion
Fire Technology, Vol. 34, No. 3, pp. 247-265

Paabo M. and Levin B.C., 1998
Review of the Literature on the Gaseous Products and Toxicity Generated from the Pyrolysis and Combustion of Rigid Polyurethane Foams
Elsevier Engineering Information, Inc

Parker W.J. and Lee B.T., 1974
Fire Build-up in Reduced Size Enclosures
A Symposium on Fire Safety Research, NBS SP-411, National Bureau of Standards, pp. 139-153

Parker W.J., 1982
Calculations of the Heat Release Rate by Oxygen Consumption for Various Applications
NBSIR 81-2427, National Bureau of Standards, Gaithersburg, MD, USA

Parker W.J., 1984
Calculations of the Heat Release Rate by Oxygen Consumption for Various Applications
Journal of Fire Sciences, Vol. 2, pp. 380-395

Peacock R.D., Bukowski R.W., Jones W.W., Reneke P.A., Babrauskas V. and Brown J.E.,1994
Fire safety of passenger trains: A review of current approaches and of new concepts
NIST Technical Note 1406, NIST, MD, USA

Peacock R.D., Reneke P.A., Bukowski R.W. and Babrauskas V., 1999
Defining Flashover for Fire Hazard Calculations
Fire Safety Journal, Vol. 32, pp. 331-345

Peacock R.D., Reneke P.A., Bukowski R.W. and Babrauskas V., 1999
Defining Flashover for Fire Hazard Calculations
Fire Safety Journal, Vol. 32, pp. 331-345

Peacock R.D., Reneke P.A., Davis W.D. and Jones W.W., 1999
Quantifying fire model evaluation using functional analysis
Fire Safety Journal, Vol. 33, pp. 167-184

Petrella R.V., 1994
The assessment of full-scale fire hazards from cone calorimeter data
Journal of Fire Sciences, Vol. 12, No. 1, pp. 14-43

Purser D.A., 2002
Toxicity Assessment of Combustion Products
The SFPE Handbook of Fire Protection Engineering. 3rd edition. Quincy: Society of Fire Protection Engineers, Chapter 2, pp. 83-172

Quintiere J.D., 1989
Fundamentals of Enclosure Fire Zone Models
Journal of Fire Protection Engineering, Vol. 1, No. 2, pp. 99-119

Rasbash D.J., 1991
Major Fire Disasters Involving Flashover
Fire Safety Journal, Vol. 17, pp. 85-93

Ravigururajan T.S. and Beltran M.R., 1989
A model for attenuation of fire radiation through water droplets
Fire Safety Journal, Vol. 15, No. 2, pp. 171-181

Rockett A.J., 1976
Fire Induced Gas Flow in an Enclosure
Combustion Science and Technology, Vol. 12, pp. 165-175

South China Morning Post (SCMP), 21 November 1996

South China Morning Post (SCMP), 17 April 1997

South China Morning Post (SCMP), 19 February 2003

South China Morning Post (SCMP), 6 January 2004

Sensenig D.L., 1980
An Oxygen Consumption Technique for Determining the Contribution of Interior Wall Finishes to Room Fires
NBS Tech Note 1128, NBS, Gaithersburg, MD, USA

Siegel R. and Howell J.R., 2002
Thermal Radiation Heat Transfer, 4th Ed.
Taylor and Francis, New York

Smith D.A. and Shaw K., 1999
The single burning item (SBI) test, the Euro classes and transitional arrangement
Proceedings of Interflam '99, 29 June – 1 July, 1999, Edinburgh, UK, Interscience, Comm., London, UK (1999), pp. 1-9

Snegirev A.Y., 2004
Statistical modeling of thermal radiation transfer in buoyant turbulent diffusion flames
Combustion and Flame, Vol. 136, No. 1-2, pp. 51-71

Sundstöm B., 1996
Fire Safety of Upholstered Furniture - The Final Report on the CBUF Research Programmes
London: Interscience Communication Ltd

Takeda H., 1987
Transient Model of Early Stages of Fire Growth
Mathematical Modelling of Fires, Ed. Mehaffey J.R., ASTM, Philadelphia, pp. 21-34

Tewarson A., 2002
Generation of Heat and Chemical Components in Fires
The SFPE Handbook of Fire Protection Engineering, 3rd Edition, Section 3, Chapter 4, pp. 3-82 to 3-161, The National Fire Protection Association, Quincy, MA, USA

Thomas P.H., Bullen M. L., Quintiere J.D. and McCaffrey B.J., 1980
Flashover and Instabilities in Fire Behaviour
Combustion and Flame, Vol. 39, pp. 159-171

Thompson J.M.T. and Steward H.B., 1986
Non-linear Dynamics and Chaos
Wiley, Chichester

Thornton W.M., 1917
The Relation of Oxygen to the Heat of Combustion of Organic Compounds
Philosophical Magazine and J. of Science, Vol. 33, No. 196, pp. 196-203

Tien C.L., Lee K.Y. and Stretton A.J., 2002
Radiation Heat Transfer
The SFPE Handbook of Fire Protection Engineering, 3rd Edition, Quincy, Mass.: National Fire Protection Association, Boston, Mass.: Society of Fire Protection Engineers, pp. 1-73 - 1-89

UL 1056, 2000
Standard for Fire Test of Upholstered Furniture, 3rd Edition
Underwriters Laboratories Inc. USA

Vanspeybroeck R., Hees P. Van and Vandevelde P., 1993
Combustion behaviour of polyurethane flexible foams under cone calorimeter test conditions
Fire and Materials. 17, pp. 155-166

White N. and Dowling V.P., 2004
Conducting a full-scale experiment on a railway passenger car
Proceedings of the 6th Asia-Oceania Symposium on Fire Science & Technology, 17-20 March 2004, Daegu, Korea, (Eds: E.S. Kim et al.,) Korean Institute of Fire Science and Engineering, pp. 591-601

Wickström U and Göransson U, 1992
Full-scale/Bench-scale Correlations of Wall and Ceiling Linings
Fire and Materials, Vol. 16, No. 1, pp. 15-22

Yuen W.W. and Tien C.L., 1976
A Simplified Calculation Scheme for the Luminous Flame Emissivity
Proceeding of the 16th Symposium of Combustion, pp. 1481-1487

Yuen W.W. and Takara E.E., 1997
The Zonal Method, a Practical Solution Method for Radiative Transfer in Non-Isothermal Inhomogeneous Media
Annual Review of Heat Transfer, Vol. 8, pp. 153-215

Yuen W.W., Han S.S. and Chow W.K., 2003
The Effect of Thermal Radiation on the Dynamics of Flashover in a Compartment Fire
JSME International Journal, Series B: Fluids and Thermal Engineering, Vol. 46, No. 4, pp. 528-538

Yuen W.W. and Chow W.K, 2004
The role of thermal radiation on the initiation of flashover in a compartment fire
International Journal of Heat and Mass Transfer, Vol. 47, No. 19-20, pp. 4265-4276

PUBLICATIONS RELATED TO THIS THESIS

Refereed Journal Papers:

J1 Yuen W.W., Han S.S., Chow W.K.
The effect of thermal radiation on the dynamics of flashover in a compartment fire.
JSME International Journal, Series B: Fluids and Thermal Engineering, Vol. 46, No. 4, pp. 528-538 (2003).

J2 Han S.S.
Fire safety and furniture.
International Journal on Engineering Performance-Based Fire Codes, Vol. 5, No. 4, pp. 158-162 (2003).

J3 Han S.S., Chow W.K.
Cone calorimeter studies on fire behaviour of polycarbonate glazing sheets.
Journal of Applied Fire Science, Vol. 12, No. 3, pp. 245-261 (2003-2004).

J4 Chow W.K., Han S.S., Dong H., Gao Y., Zou G.W.
Full-scale burning tests on heat release rates of furniture.
International Journal on Engineering Performance-Based Fire Codes, Vol. 6, No. 3, pp. 168-180 (2004).

J5 Han S.S., Chow W.K.
Review on key equations in the two-layer zone model CFAST.
International Journal on Engineering Performance-Based Fire Codes, Vol. 6, No. 4, pp. 277-283 (2004).

J6 Han S.S., Chow W.K.
Calculating FED and LC50 for testing toxicity of materials in bench-scale tests with a cone calorimeter.
Polymer Testing, Vol. 24, No. 7, pp. 920-924 (2005).

J7 Chow W.K., Han S.S.
Superposition of heat release rate curves for combustibles with bench scale tests.
Polymer Testing, Vol. 25, No. 1, pp. 75-82 (2006).

J8 Chow W.K., Han S.S.

A study on heat release rates of furniture under well-developed fire. Experimental Heat Transfer, Vol. 19, No. 3, pp. 209-226 (2006).

Refereed Conference Papers:

C1 Yuen W.W., Han S.S., Chow W.K.

The effect of thermal radiation on the dynamics of flashover in a compartment fire.

Proceedings of the 6th ASME-JSME Thermal Engineering Joint Conference, 16-20 March 2003, Hapuna Bench Prince Hotel, Kohala Coast, Hawaii Island, Hawaii, USA, Paper TED-AJ03-127 (2003).

C2 Han S.S., Chow W.K.

Brief review on meanings of fire safe furniture.

Proceedings of the International Symposium on Fire Science and Fire-protection Engineering (2003 ISFSFE), 12-15 October 2003, Beijing, China, pp. 404-409 (2003).

C3 Han S.S.

Common problems encountered in bench-scale burning tests with a cone calorimeter.

Proceedings of 2nd Education Symposium on Advanced Fire Research, University of Science and Technology of China, Hefei, China, May (2004).

C4 Han S.S., Chow W.K.

Review on the equations used in calculating the heat release rate in an oxygen consumption calorimetry.

Proceedings of the Fire Conference 2004 – Total Fire Safety Concept, 6-7 December 2004, Hong Kong, China, Vol. 3, Paper 4 (2004).

C5 Han S.S., Chow W.K.

Assessing fire behaviour of polycarbonate materials by a cone calorimeter.

Proceedings of the 7th Asia-Pacific International Symposium on Combustion and Energy Utilization (7th APISCEU), 15-17 December 2004, Hong Kong, Paper A5-307 (2004).